ORIGIN AND MODULATION OF ACTION POTENTIAL EVOKED CALCIUM SIGNALS IN HIPPOCAMPAL CA1 PYRAMIDAL NEURONS

by

VLADISLAV M. SANDLER

B.Sc., The Rostov State University, 1990
M.Sc., The University of British Columbia, 1996

A THESIS SUBMITTED IN PARTIAL FULFILLMENT OF THE REQUIREMENTS FOR THE DEGREE OF

DOCTOR OF PHILOSOPHY

in

THE FACULTY OF GRADUATE STUDIES

(Neuroscience Programme)

We accept this thesis as conforming to the required standard

THE UNIVERSITY OF BRITISH COLUMBIA

February 1999

In presenting this thesis in partial fulfilment of the requirements for an advanced degree at the University of British Columbia, I agree that the Library shall make it freely available for reference and study. I further agree that permission for extensive copying of this thesis for scholarly purposes may be granted by the head of my department or by his or her representatives. It is understood that copying or publication of this thesis for financial gain shall not be allowed without my written permission.

Department of Graduate Studies, Neuroscience Programme

The University of British Columbia
Vancouver, Canada

Date Feb. 15, 1999

ABSTRACT

ORIGIN AND MODULATION OF ACTION POTENTIAL EVOKED CALCIUM SIGNALS IN HIPPOCAMPAL CA1 PYRAMIDAL NEURONS

by Vladislav M. Sandler

Calcium is an important second messenger that participates in triggering and regulating numerous neuronal processes. Action potentials (APs or AP) initiate rapid changes of intracellular Ca^{2+}-concentration ($[Ca^{2+}]_i$) in both soma and dendrites of central neurons. We addressed two major questions about the origin and modulation of these changes in $[Ca^{2+}]_i$. Firstly, how does a neurotransmitter, serotonin (5-HT), modulate the backpropagation of APs and associated changes in the $[Ca^{2+}]_i$ in CA1 hippocampal pyramidal neurons? Secondly, do APs trigger Ca^{2+}-induced Ca^{2+}-release (CICR) from internal stores in these neurons?

We used whole-cell somatic or dendritic patch-clamp recordings combined with high-speed imaging of $[Ca^{2+}]_i$ and analyses of the responses to applications of pharmacological agents, studying the changes in electrical membrane properties and $[Ca^{2+}]_i$. The experiments were conducted in the

CA1 pyramidal neurons of *in vitro* slices from the rat hippocampus (11 day- to 5 week-old). Changes in $[Ca^{2+}]_i$ were measured in neurons filled with bis-fura-2, Calcium Green-1 or fura-2-AM.

Bath applications of 5-HT increased membrane conductance and hyperpolarized both soma and apical dendrites. They also lowered peak potentials of antidromically-activated, backpropagating APs in the dendrites. In the soma, 5-HT applications increased the absolute AP-amplitude while slightly decreasing peak potentials. 5-HT reduced the amplitude of the AP-evoked changes in $[Ca^{2+}]_i$ at all locations along the apical dendrites and soma.

The application of 5-HT and antidromically evoked APs generated, through synergistic actions, increases in $[Ca^{2+}]_i$ that propagated along dendrites (Ca^{2+} waves). Such waves originated in the proximal or middle apical dendrites and were not accompanied by a significant change in somatic membrane potential. A minimum of five APs was required to evoke the waves. According to these new observations and supporting literature, the waves are a likely consequence of Ca^{2+}-induced Ca^{2+}-release (CICR) from internal stores through (inositol-1,4,5-triphosphate) IP_3-sensitive channels.

In the absence of 5-HT, APs evoked CICR. Caffeine application increased the amplitude of AP-induced changes in $[Ca^{2+}]_i$. During simultaneous calcium imaging, the whole-cell recordings showed that caffeine

application did not significantly change either the resting membrane potential or amplitude and shape of APs. The enhancement of AP-evoked Ca^{2+}-transients due to caffeine application could not be attributed to protein phosphorylation or modulation of high-threshold Ca^{2+}-channels. Applications of IBMX, a non-specific inhibitor of phosphodiesterases, forskolin, an activator of adenylyl cyclase, H-89, an inhibitor of PKA and PKG, or nifedipine, a blocker of high-threshold Ca^{2+} channels, did not mimic or prevent the caffeine effect. Pretreatment of neurons with thapsigargin or cyclopiazonic acid (CPA) -- substances that facilitate depletion of intracellular Ca^{2+}-stores by blocking endoplasmic reticulum specific Ca^{2+}-ATPases -- precluded this effect. Similar pretreatment with ryanodine, a blocker of 'ryanodine-sensitive' channels, also precluded the caffeine effect. Despite a presence or absence of caffeine, applications of thapsigargin, ryanodine or CPA reduced the AP-evoked changes in $[Ca^{2+}]_i$.

From these new experimental observations, we can conclude that the CICR through ryanodine-sensitive channels contributes to the AP-induced changes of $[Ca^{2+}]_i$ in hippocampal CA1 pyramidal neurons.

Table of Contents

List of figures

Number *Page*

LIST OF ABBREVIATIONS

5-HT	Serotonin, 5-hydroxitryptamine
ACSF	Artificial cerebro-spinal fluid
ALV	Alveus
AP	Action potential
APV	D-2-amino-5-phosphonovalerate
$[Ca^{2+}]_i$	Intracellular calcium concentration
CCD	Charged coupled device
CICR	Calcium induced calcium release
CNS	Central nervous system
CNQX	6-cyano-7-nitroquinoxaline-2,3-dione
CPA	Cyclopiazonic acid
DIC	Differential interference contrast
EPSP	Excitatory post-synaptic potential
ER	Endoplasmic reticulum
I_h	Hyperpolarization-activated cation current
IPSP	Inhibitory post-synaptic potential
IP_3	Inositol-1,4,5-triphosphate
K_d	Constant of dissociation
LM	Stratum lacunosum moleculare
RyR	Ryanodine-sensitive channels
S.D.	Standard deviation
SERCA	(Sarco)endoplasmic reticulum Ca^{2+} ATPase
SO	Stratum oriens
SP	Stratum pyramidale
SR	Sarcoplasmic reticulum

Acknowledgments

I would like to express my gratitude to Dr. Dietrich W. F. Schwarz without whose support and encouragement this work would not have been possible.

I would like to thank Dr. William. N. Ross for the opportunity to conduct experiments in his laboratory, for scientific expertise he generously shared with me and for his compassion that elevated my spirit and helped me to move ahead.

I would also like to thank Dr. Ernest Puil for his invaluable advice and his endless time invested in me.

I also thank Dr. Paul Finlayson for helpful discussions.

I would like to thank Jean-Gaël Barbara for helpful discussions and collaboration in conducting some experiments.

Dedication

To the best friend, lover and wife Anna.

INTRODUCTION

The scope of the studies

Calcium in its free form (Ca^{2+}) is an important second messenger that participates in the triggering and regulating many neuronal processes. Some of these processes are neurotransmitter release (Mulkey and Zucker 1991; Borst and Sakmann 1996), synaptic plasticity (Malenka 1994; Bear and Malenka, 1994), and transcription control (Hardingham et al. 1997). In neurons of the central nervous system (CNS), Na^+-dependent action potentials trigger a rapid change in intracellular Ca^{2+} concentration ($[Ca^{2+}]_i$) in the soma. Backpropagating sodium action potentials evoke similar changes in $[Ca^{2+}]_i$ in the dendrites (Jaffe et al., 1992; Spruston et al., 1995). Therefore, understanding the origin and modulation of action potential-evoked $[Ca^{2+}]_i$ changes is fundamentally important.

It is generally agreed that action potentials cause elevations in $[Ca^{2+}]_i$ by opening voltage-gated Ca^{2+} channels in both soma and dendrites (Christie et al., 1995). The activation of ionotropic and metabotropic receptors for neurotransmitters on the dendrites can influence action potential backpropagation as well as action potential-evoked dendritic increases in $[Ca^{2+}]_i$. Inhibitory postsynaptic potentials (IPSPs) in dendrites can decrease the amplitude of backpropagating action potentials and, consequently, action potential-evoked dendritic Ca^{2+} transients (Tsubokawa and Ross, 1996; Buzsáki et al., 1996). Muscarinic receptor activation has been shown to inhibit the activity-dependent reduction of backpropagating action potential amplitude, ultimately resulting in an increase of

dendritic $[Ca^{2+}]_i$ (Tsubokawa and Ross, 1997). Both effects are related to a change in dendritic membrane conductance (e.g. K^+ conductance) that control the propagation of action potentials (Tsubokawa and Ross, 1996; Buzsáki et al., 1996; Tsubokawa and Ross, 1997). These results imply that other neurotransmitters, acting on K^+ or other conductances, such as serotonin (5-hydroxytryptamine or 5-HT), might affect dendritic action potential backpropagation and associated $[Ca^{2+}]_i$ changes.

In the investigations presented here we explore how serotonin modulates action potential backpropagation and the associated changes in the $[Ca^{2+}]_i$ in CA1 hippocampal pyramidal neurons. We hypothesized that an increased membrane conductance, due to the activation of a certain type of receptors for 5-HT, can inhibit the backpropagation of the action potentials, leading to a decrease of $[Ca^{2+}]_i$ transients evoked by action potentials.

Action potentials depolarize the neuronal membrane, leading to a Ca^{2+} influx through voltage-controlled Ca^{2+} channels. However, it remains unclear whether this influx is the only source of Ca^{2+} in the action potential-evoked Ca^{2+} signals. Here, we have hypothesized that there is an additional component in an action potential-induced Ca^{2+} transient in neurons. This additional component is calcium induced calcium release (CICR), a process of Ca^{2+} mobilization from intracellular Ca^{2+}stores through ryanodine-sensitive channels (RyR) opened by an elevation of $[Ca^{2+}]_i$.

CICR through RyRs is not the only theoretically feasible action potential-evoked Ca^{2+} release in neurons. Activation of metabotropic receptors for several neurotransmitters, that are coupled to a second messenger pathway leading to the

production of inositol-1,4,5-triphosphate (IP_3), could create the situation when an action potential-evoked increase of $[Ca^{2+}]_i$ might trigger Ca^{2+} mobilization from intracellular Ca^{2+} stores through IP_3-sensitive channels. In the experiments described below we provide the first experimental evidence that a train of action potentials and the neurotransmitter serotonin can cause a synergistic calcium induced calcium release through IP_3 sensitive channels in CNS neurons.

The purpose of the study

In the presented study we itend to demonstrate that 5-HT modulates action potential backpropagation and the associated changes in the $[Ca^{2+}]_i$ in CA1 hippocampal pyramidal neurons. We will also try to prove that a single or a few action potentials can trigger CICR through ryanodine sensitive channels in CA1 hippocampal pyramidal neurons.

Choice of the preparation

We chose CA1 (from the Latin *cornu Ammonis*, or Ammon's horn) pyramidal neurons in the hippocampus (from the Greek *hippokampos* = sea horse) as the object for our studies because of the following reasons.

1. The hippocampus is one of the best-characterized cortical structures in the brain. It has highly regular organization, which makes it an ideal object for physiological investigations.
2. A bulk of knowledge has been accumulated about synaptic organization, structure and origin of the main projections from other parts of the brain, including serotonergic projections from the raphe nuclei. Functional characteristics of hippocampal neurons,

including properties of somatic and backpropagating action potentials, as well as action potential evoked $[Ca^{2+}]_i$ transients, are also well studied.

3. The effects of 5-HT application and mechanisms of its action on membrane conductance, including K^+ conductance, were extensively studied on hippocampal CA1 pyramidal neurons (reviewed in Nicoll 1988 and Nicoll et al. 1990). Existence of detailed information on this subject was important because it allowed us to make the initial assumption on the role of the membrane conductance change in regulation of the action potential backpropagation and associated $[Ca^{2+}]_i$ change.
4. The questions of the origin of action potential-evoked $[Ca^{2+}]_i$ change and the function of intracellular stores were also previously addressed in CA1 hippocampal pyramidal neurons (e.g. Garaschuk et al. 1997, Jacobs and Meyer 1997). Thus, we were able to compare directly our results with the data reported earlier. Earlier observations have also helped us in the choice of the methods we utilized in our studies (see methods section bellow).

Modulation of action potential backpropagation in CA1 pyramidal neurons

The effects of neuromodulators on CNS neurons have generally been evaluated with recordings from the cell body. From this position the most interesting results concern changes in firing rate induced by changes in conductance close to the soma. For example, serotonin (5-HT) applied to hippocampal pyramidal neurons causes changes in several K^+-conductances (Andrade and Nicoll 1987; Colino and Halliwell 1987; reviewed in Nicoll 1988 and Nicoll et al. 1990), usually leading to a suppression of tonic firing rates.

It has been shown in electrophysiological and imaging experiments that dendrites in cortical and hippocampal pyramidal neurons have both sodium and calcium channels (Stuart and Sakmann 1994; Magee and Johnston 1995). Confirmation of the existence of calcium channels in the dendrites of CA1 pyramidal neurons came from imaging experiments using cooled charge-coupled device cameras (Jaffe et al. 1992). Later, two new methods have enabled high resolution imaging of dendritic calcium. The first one utilized confocal microscopy (Fine et al., 1988), where a pinhole is used to exclude light coming from the out of focus parts of a specimen. The second method, multi-photon (two-photon) microscopy (Denk et al., 1994), took advantage of a spatially restricted multi-photon (two-photon) absorption to excite only a fluorophore that is located at the focal point. The later method allowed to image changes of $[Ca^{2+}]_i$ localized in dendritic shafts and spine heads both *in vitro* and *in vivo* (Svoboda et al. 1996; Svoboda et al. 1997).

Control of spike propagation and associated $[Ca^{2+}]_i$ changes may be additional targets for neuromodulatory effects. In pyramidal neurons action potentials usually are initiated in the axon hillock region. From this position they propagate orthodromically along the axon as well as up into the dendritic tree (Turner et al. 1991; Spruston et al. 1995; Colbert and Johnston 1996). Voltage-dependent Na^+ and Ca^{2+} channels, that are distributed all over the dendrites, sustain action potential propagation in the apical arbor (Magee and Johnston 1995). Not all spikes actively spread to the tips of the dendrites (Andreasen and Lambert 1995; Callaway and Ross 1995; Spruston et al. 1995), suggesting that propagation in this region is labile. Therefore, mechanisms that change dendritic conductances and potentials could affect the extent of active propagation. This

kind of regulation could be important since backpropagating action potentials have been implicated in the induction of some forms of long-term potentiation (Magee and Johnston 1997; Markram et al. 1997) and modulate dendritic conductances (Cook and Johnston 1997).

It has been shown previously that synaptic inhibition could block backpropagating action potentials (Tsubokawa and Ross 1996; Buzsaki et al. 1996) and that cholinergic agonists could enhance backpropagation (Tsubokawa and Ross 1997). Inhibition also decreased dramatically the associated $[Ca^{2+}]_i$ changes in the dendrites, while carbachol enhanced the $[Ca^{2+}]_i$ changes. These results suggest that other modulatory mechanisms might affect dendritic propagation. In this study, we examine the effects of bath applied serotonin (5-HT). We report that 5-HT reduces the peak spike potential in the dendrites but not in the soma. However, the action potential-evoked $[Ca^{2+}]_i$ increase was reduced by 5-HT in all locations. The smaller increase occurred at the soma, where the peak spike potential did not change significantly. This implies that 5-HT also reduces Ca^{2+} entry by directly modulating the Ca^{2+} channels that are opened by the action potentials.

Serotonin

Serotonin was first discovered in the mammalian CNS in 1953 (Twarog, 1953) and is now thought to play an important role in a variety of physiological functions and behavior including sleep, appetite, pain perception, locomotion and sexual activity. The study of serotonin in the CNS rapidly developed after the discovery of 5-HT in specific brain structures and pathways. The unique anatomical distribution of 5-HT in the CNS

became perhaps the strongest argument for a role of serotonin as a neurotransmitter (Nicoll et al. 1990).

The complexity of the 5-HT actions in the CNS is explained by the presence of multitude of receptors for this biogenic amine. Several types of 5-HT receptors have been identified in pharmacological, physiological and immunohistochemical studies, as well as in cloning experiments (Saudou and Hen 1994). There are seven types of serotonin receptors according to the latest classification as agreed by the International Union of Pharmacology Committee on Drug Classification and Receptor Nomenclature (NC-IUPHAR). Most of them are subdivided into subclasses. These are 5-HT_{1A}, 5-HT_{1B}, 5-HT_{1D}, 5-HT_{1E}, 5-HT_{1F}, 5-HT_{2A}, 5-HT_{2B}, 5-HT_{2C}, 5-HT_3, 5-HT_4, 5-HT_{5A}, 5-HT_{5B}, 5-HT_6, 5-HT_7. This classification of serotonin receptors is based mainly on different pharmacological profiles of the 5-HT receptors. Their primary structures, as well as the type of intracellular effector are also taken into account. Most 5-HT receptors, except for 5-HT_3, are coupled to G proteins (Saudou and Hen 1994); coupling of 5-HT_{5A} and 5-HT_{5B} receptors to a specific effector pathway has yet to be demonstrated.

5-HT_1 type receptors

The 5-HT_{1A} type receptors are negatively coupled to adenylate cyclase through $G_{i/o}$ (pertussis toxin-sensitive) family of G-proteins. Similar to the other G-protein coupled receptors, the 5-HT_{1A} receptor subtype has seven hydrophobic presumably transmembrane domains. 5-HT_{1A} receptors have high affinity for the selective agonist 8-OH-DPAT (8-hydroxy-2-(di-n-propyl-amino)tetralin). Spiperon, [^{125}I]iodo-cyanopindolol and WAY100635 are antagonists (Andrade and Nicoll 1987; Saudou and

Hen 1994). 5-HT_{1A} receptor activation has been shown to evoke a hyperpolarizing response by opening K^+ channels in hippocampal neurons (Andrade and Nicoll 1987).

5-HT_{1B} and 5-HT_{1D} (human homolog of the 5-HT_{1B} receptor) are coupled to pertussis toxin-sensitive G proteins. Activation of 5-HT_{1B} and 5-HT_{1D} receptors have been shown to inhibit adenylate cyclase (Saudou and Hen 1994). Spiperone and 8-OH-DPAT have low affinities for 5-HT_{1B} and 5-HT_{1D} receptors. Methiothepin (non-selective antagonist for both types), SDZ21009 (for 5-HT_{1B}) and GR127935 (for 5-HT_{1D}) are antagonists.

Similar to the other 5-HT_1 receptors, 5-HT_{1E} and 5-HT_{1F} are negatively coupled to adenylate cyclase through pertussis toxin-sensitive G proteins. It has been shown that stimulation of the 5-HT_{1E} receptors does not activate phospholipase C and, hence, does not change intracellular Ca^{2+} concentration (Saudou and Hen 1994). Selective agonists and antagonists for these receptors are not known.

5-HT_2 type receptors

All 5-HT receptors from the 5-HT_2 receptor family are coupled to the same intracellular effector, phospholipase C. When activated, all members of this family, including 5-HT_{2A}, 5-HT_{2B} and 5-HT_{2C}, stimulate phospolipase C which causes an increase in IP_3 production. An increased IP_3 background in cytoplasm triggers release of Ca^{2+} from IP_3 sensitive internal calcium stores through IP_3 sensitive channels (Lubbert et al. 1987; Lubbert et al. 1987; Julius et al. 1988; Pritchett et al. 1988). 5-HT_2 receptors have similar pharmacological profiles although they can be distinguished on the basis of their affinity to such antagonists as spiperone, ketanserine and yohimbine. Ketanserine

and spiperone have higher affinities for the 5-HT_{2A} receptors than for the 5-HT_{2B} receptors and mianserine has a high affinity for 5-HT_{2A} and 5-HT_{2C} receptors and low affinity for the 5-HT_{2B} receptors. When expressed in *Xenopus* oocytes, the activation of the 5-HT_2 receptors causes an increase in the intracellular Ca^{2+} level and subsequent activation of Ca^{2+}-sensitive chloride channels (Lubbert et al. 1987; Julius, et al. 1988).

5-HT_4, 5-HT_6 and 5-HT_7 type receptors

5-HT_4, 5-HT_6 and 5-HT_7 receptors have a common intracellular effector. They are positively coupled to adenylate cyclase (Saudou and Hen 1994). It has been shown that stimulation of 5-HT_4, 5-HT_6 and 5-HT_7 receptors activate adenylate cyclase. This activation causes an increase in intracellular cAMP, leading to protein kinase A (PKA) activation. Agonists of the 5-HT_4 receptors belong to the benzamide family (e.g. cisapride, renzapride, zacopride), or the benzimidazolones (BIMU8). There are neither selective agonists nor antagonists for 5-HT_6 receptors although some antipsychotic drugs such as clozapine and loxapine, as well as tricyclic antidepressants like amoxapine and clomipramine show comparatively high degree of affinities for 5-HT_6 receptors (Saudou and Hen 1994). Compounds that have a relatively high affinity for 5-HT_7 receptors such as (+)butaclamol and clozapine (antagonists), as well as methiothepin, methysergide and ergotamine have neuroleptic properties. Due to high affinity of this receptor for 8-OH-DPAT, it has been suggested that 5-HT_7 receptor might represent a 5-HT_{1A}-like receptor that is positively coupled to adenylate cyclase (Saudou and Hen 1994).

5-HT_3 type receptor

In contrast to the serotonin receptors that are coupled to G proteins, 5-HT_3 receptors are ligand-gated membrane ion channels (Derkach et al. 1989). These channels are cation-specific with approximately the same permeability for both Na^+ and K^+. 5-HT_3 receptors have a distinct pharmacological profile. ICS 205-930, granisetron, ondansetron and tropisetron are selective antagonists for these receptors. 2-methyl-5-HT and m-chlorphenyl-biguanide are thought to be selective agonists of the 5-HT_3 receptors.

5-HT actions in the CNS neurons

The amount of information on serotonin actions in the CNS neurons is overwhelming (for reviews see Nicoll, et al. 1990; Saudou and Hen 1994). 5-HT actions in CNS neurons were initially studied in hippocampus and later confirmed in many other structures (Nicoll et al. 1990). Only few of them, relevant to this study, are described.

It has been shown, for example, that 5-HT application causes an increase in resting K^+ conductance and a hyperpolarization in the CA1 neurons. However, it decreases the K^+ current, which is responsible for the long afterhyperpolarization (I_{AHP}) (Andrade and Nicoll 1987; Colino and Halliwell 1987). The hyperpolarization, explained to be the result of K^+ channel opening, was mediated by 5-HT_1 receptor activation (Andrade and Nicoll 1987; Colino and Halliwell 1987). However, in the nucleus accumbens, a decrease in the resting K^+ current in response to the 5-HT application has been proven to be the result of 5-HT_2 receptor activation.

It has also been reported that serotonin enhances a hyperpolarization-activated cation current (I_h) in the thalamic neurons and that this effect is connected to an increase in intracellular cyclic AMP concentration (Pape and McCormick 1989; McCormick and Pape 1990). 5-HT also shifts the I_h activation range towards more positive values. It appeared to be impossible to attribute this 5-HT action to either the activation of 5-HT_{1A} or 5-HT_2 receptors at the time the studies were conducted. Today one can make an assumption that either 5-HT_4, 5-HT_6 or 5-HT_7 receptors, that are thought to be positively coupled to adenylate cyclase, could be responsible for the described effect.

Components of the system of calcium homeostasis

Ca^{2+} is an important second messenger that participates in the triggering and regulating many neuronal processes. Precise control over localization and concentration of Ca^{2+} as a second messenger is crucial for its function. A special transport system has been developed in neurons to control cellular homeostasis of calcium. This system moves Ca^{2+} between four different pools: extracellular milieu, cytoplasm, mitochondria and endoplasmic or sarcoplasmic reticulum (ER or SR respectively).

It is certain that the free form of Ca^{2+} in the cytoplasm acts as second messenger. Two major mechanisms are utilized in regulation of free $[Ca^{2+}]_i$ in cytoplasm: a passive and an active one (Thastrup 1990).

There are two components of passive $[Ca^{2+}]_i$ regulation. The first one includes a variety of cytosolic and membrane bound proteins that bind Ca^{2+} (Baimbridge et al. 1992). Such proteins as calmodulin, troponin C, parvalbumin, calbindin-D28K and calretinin are among them. These and other proteins are considered to be the major component of

endogenous Ca^{2+} buffering system. The second one is a gradient dependent non-gated Ca^{2+} flux across both plasmalemma and membranes of endoplasmic and sarcoplasmic reticulum (e.g., Garaschuk et al. 1997). Existence of a similar leak across mitochondria membrane has yet to be demonstrated.

The active mechanism of $[Ca^{2+}]_i$ regulation is carried out by a variety of voltage-operated (e.g., L-type channel) and ligand-gated channels (e.g. NMDA-type receptor), pumps (e.g., Ca^{2+}-ATPases), exchangers (e.g. Na^+-Ca^{2+} exchanger) and uniporters (e.g. Ca^{2+} uniporter in mitochondria; Thastrup 1990). They play different roles in Ca^{2+} homeostasis. For instance, ATP-dependent calcium pumps (Ca^{2+}-ATPases) are considered to be a part of a cellular defense system that brings $[Ca^{2+}]_i$ to a basal level after a Ca^{2+} signaling event has occurred. On the other hand, voltage operated and ligand-gated channels including ryanodine-(caffeine)-sensitive receptors/channels (RyR) and Inositol-1,4,5-triphosphate (IP_3)-gated channels are the main sources of $[Ca^{2+}]_i$ increase, which is often a beginning of a Ca^{2+} dependent signaling pathway. Na^+-Ca^{2+} exchangers can work as 'double agents': they either increase or decrease $[Ca^{2+}]_i$. The mode of their action depends on their position in the cell. Na^+-Ca^{2+} exchangers positioned in the plasmalemma exchange Ca^{2+} for Na^+ lowering $[Ca^{2+}]_i$, while those positioned in the membrane of organelles (e.g., mitochondria) pump Ca^{2+} to the cytoplasm.

Figure 1 shows the components of the Ca^{2+} homeostasis, which are of relevance to the experiments described bellow. Among these components are RyR, IP_3-gated channels and Ca^{2+}-ATPase.

Endoplasmic reticulum calcium pump

The Ca^{2+}-ATPase belongs to the phosphorylating class of ion transport ATPases. Among other members of this class are Na^+ - K^+- and H^+ - K^+ -ATPases. All pumps in this class are phosphorylated during the catalytic cycle. They can exist in three main forms. E1 form pumps have their transport sites accessible to transported ions on the cytoplasmic side of a membrane. Transport sites of E2 form pumps are on the extracellular face of a membrane. Pumps with slowly available transport sites to ions in solution have a 'hidden' form of the cation-binding domain. These are $E2(X^+)$ or $E2P(X^+)$ pumps (Sachs and Munson 1991).

The main emphasis of the present study is on (sarco)endoplasmic reticulum Ca^{2+} ATPase (SERCA). This pump participates in the sequestration of calcium in the ER/SR. It is classified as E1 form (Sachs and Munson 1991).

Structure and location of (sarco)endoplasmic reticulum Ca^{2+} ATPases (SERCAs)

SERCA is a single peptide chain protein with a molecular mass of 110 kDa (MacLennan et al. 1985; Brandl et al. 1986). It forms homodimer in the membrane. However, it is unknown whether there is cooperative interaction between the monomers.

Figure 1 Schematic diagram showing cellular components contributing to calcium signaling and $[Ca^{2+}]_i$ regulation in the cytoplasm of the neuron.

Blue arrows across oval symbols show the direction of calcium flow. The outer shell is the plasmalemma, the inner shell is the endoplasmic reticulum. Two different shades of blue symbolize two different levels of $[Ca^{2+}]$ (deep blue corresponds to a higher $[Ca^{2+}]$. Small symbols next to oval symbols show minimal requirements for activation of the components depicted in the figure. Only components that have relevance to our study are shown.

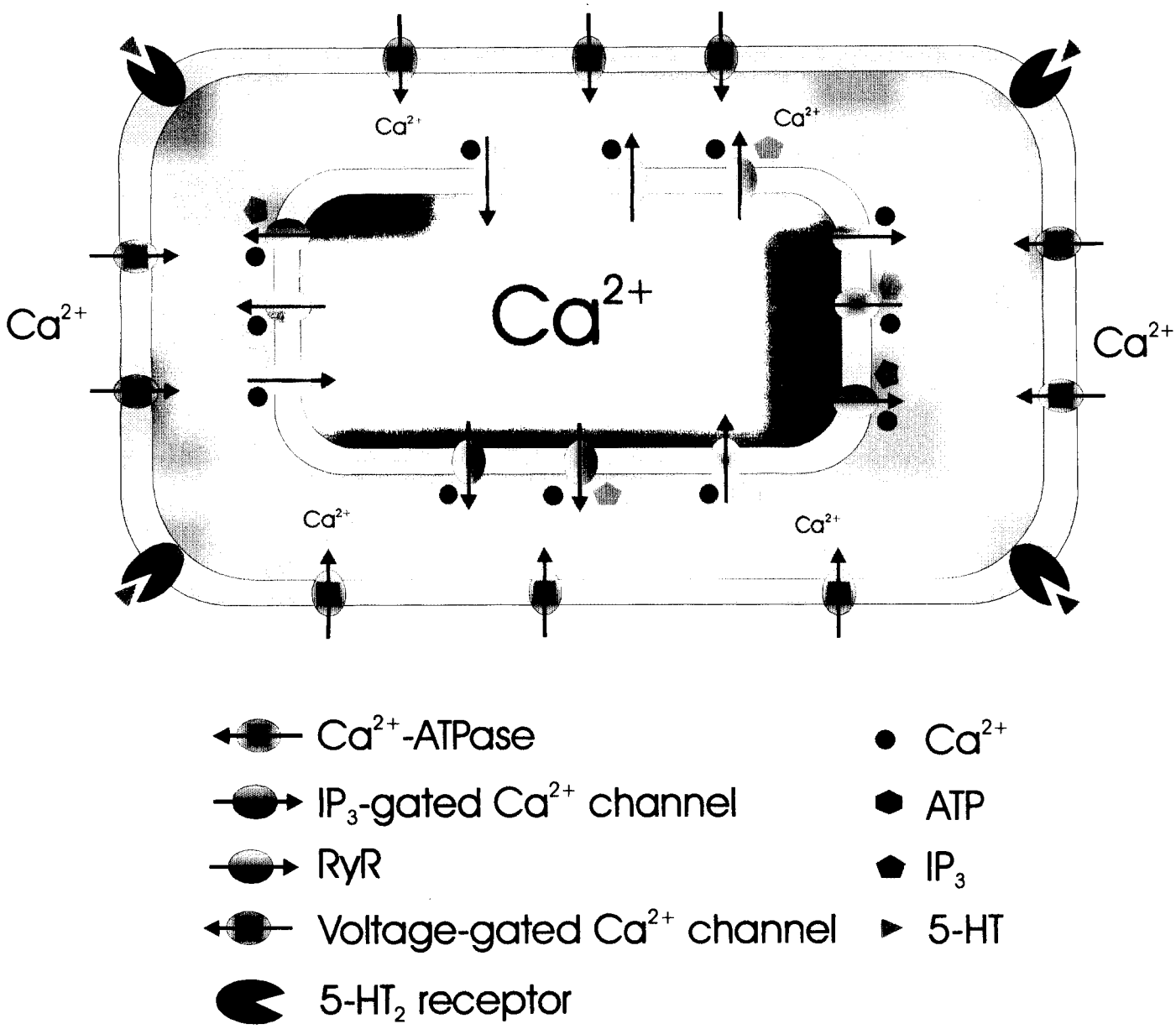
Ca2+
Ca2+
Ca2+
Ca2+
Ca2+
Ca2+
Ca2+-ATPase
IP3-gated Ca2+ channel
RyR
Voltage-gated Ca2+ channel
5-HT2 receptor
Ca2+
ATP
IP3
5-HT

Figure 1.

It appears that Ca^{2+}-ATPase has three isoforms coded by three different genes. The first gene, encoding SERCA1, is expressed in fast-twitch skeletal muscle. Two developmentally regulated alternatively spliced species are transcribed from this gene. They are translated into SERCA1a and SERCA1b proteins with different carboxyl termini (Brandl et al. 1987). A functional difference between SERCA1a and SERCA1b has not been shown.

Two tissue dependent alternatively spliced species are transcribed from the second gene: SERCA2a and SERCA2b. These proteins differ in their carboxyl termini. Four amino acids of the SERCA2a carboxyl-terminal are replaced by hydrophobic sequence of 49 or 50 amino acids in the SERCA2b (Brandl et al. 1987). SERCA2a is expressed in slow-twitch skeletal, smooth and cardiac muscles. SERCA2b is ubiquitous in smooth- and non-muscle tissues including neurons (Sachs and Munson 1991).

SERCA2b mRNA expression was documented in many brain regions (Miller et al. 1991; Baba-Aissa et al. 1996). Using *in situ* hybridization, the highest levels of SERCA2b mRNA expression have been found in cerebellar cortex, pyramidal cell layer of hippocampus and in thalamus. Heavy labeling was also observed in cortex, thalamus, pontine nuclei and the mitral cell layer of the olfactory bulb (Miller et al. 1991). Visualization of radioactive ^{45}Ca uptake revealed a similar pattern with heaviest accumulation in cerebellum, hippocampus, cortex, thalamus and olfactory bulb (Miller, et al. 1991).

The third gene, encoding SERCA3, is less well documented. While SERCA2b is found in all brain regions, SERCA3 is specifically expressed in both soma and dendrites of

the Purkinje neurons in cerebellum and poorly expressed or absent in brainstem and cerebral cortex. The total level of SERCA3 expression in the Purkinje neurons is 3-fold lower than expression of SERCA2 in the same neurons (Baba-Aissa et al. 1996).

Functional comparison of SERCA isoforms

Both plasmalemma and membranes of ER/SR form barriers to an approximately 20,000-fold $[Ca^{2+}]_i$ gradient between extracellular and ER/SR space and the cytoplasm. An increase in permeability to Ca^{2+} of either barrier leads to an elevation of $[Ca^{2+}]_i$ while active pumping leads to a $[Ca^{2+}]_i$ decrease (van Breemen and Saida 1989). The ER/SR act as a site of Ca^{2+} accumulation for subsequent release and as a sink for removal of Ca^{2+} from the cytoplasm. The SERCA carries out active pumping, replenishing Ca^{2+} in the SR/ER.

As a result of their conservative primary structure, SERCA isoforms have almost identical trans-membrane topologies and tertiary structures. Site-directed mutagenesis studies revealed that all residues critical for normal functioning of the pump are conserved among different SERCA isoforms (MacLennan 1990). Each isoform has been demonstrated to pump Ca^{2+} in an ATP-dependent fashion. All isoforms display similar enzymatic properties and are activated by calcium and ATP in a cooperative manner. Quantitatively, SERCA1 and SERCA2a are virtually identical (Lytton et al. 1992).

Thapsigargin, a tumor-promoting naturally occurring sesquiterpene lactone (Thastrup et al. 1990; Thastrup 1990) inhibits all of the SERCA isoforms equally well (Lytton et al. 1991). The interaction of thapsigargin with the SERCA isoforms is rapid and irreversible. Doses of thapsigargin that effectively inhibit SERCAs have no influence

on either plasma membrane Ca^{2+}-ATPase families, or Na^{+}- K^{+}-ATPase (Lytton, et al. 1991). Specifically, all SERCA isoforms are irreversibly inhibited by 25 nM of thapsigargin, whereas 2000 nM of this substance does not block plasmalemma Ca^{2+}-ATPase activity. The same dose reduces Na^{+}- K^{+}-ATPase (kidney, brainstem) activity by less than 10-15%. Inhibition of SERCA by thapsigargin is rapid and is unaffected by varying the concentration of either ATP or Ca^{2+} (Lytton et al. 1991).

Certain functional differences exist among SERCA isoforms. Calcium affinity of the relative rate of calcium uptake of SERCA2b, $K_{1/2} \approx 0.27$ μM (half activation coefficient), is slightly higher compared to SERCA1 and SERCA2a isoforms with $K_{1/2} \approx 0.44$ μM and $K_{1/2} \approx 0.39$ μM respectively; SERCA3 shows reduced calcium affinity with $K_{1/2} \approx 1.1$ μM. An almost identical situation is observed for the calcium dependence of Ca^{2+}-ATPase activity of SERCA isoforms. $K_{1/2}$ of SERCA3 is significantly higher than $K_{1/2}$ of SERCA1 and SERCA2 isoforms (Lytton et al. 1992; Baba-Aissa, et al. 1996). In addition to lower calcium affinity and higher affinity to vanadate, a universal inhibitor of enzymes with phosphorylated intermediates, SERCA3 demonstrates altered pH dependence. While optimum pH for SERCA1, SERCA2a and SERCA2b is about 6.8-7.0, SERCA3 displays the maximum rate of calcium uptake at pH ≈ 7.2 - 7.4 (Lytton et al. 1992; Baba-Aissa, et al. 1996). Due to the tissue- or cell-specific expression of SERCAs, these differences might be important for calcium homeostasis in the given tissue or cell type.

Functional properties of IP_3-gated channels

Calcium release from ER/SR through calcium-gated RyR channels is one of the two major pathways of calcium fluxes from the ER/SR. The second pathway depends on IP_3-gated channels (IP_3 receptor). Functional properties of both RyRs and IP_3-gated channels, as well as their modulation, have been extensively studied with numerous radio-isotopic and other techniques. (Streb et al. 1983; Berridge and Irvine 1984; Prentki et al. 1984; Bezprozvanny et al. 1991; Bezprozvanny and Ehrlich 1994; Ehrlich et al. 1994).

The major known physiological activator of IP_3 receptor is inositol 1,4,5-triphosphate. Activation of the channel by IP_3 is concentration-dependent and reversible. Single-channel current recordings of IP_3 receptors fused with a planar lipid bilayer revealed that IP_3 receptors are completely inhibited when IP_3 is washed out and return to their control level of activity after readdition of IP_3 (Ehrlich et al. 1994; Bezprozvanny et al. 1991).

Cytoplasmic Ca^{2+} inhibits IP_3 sensitive channels at high concentrations. It has been demonstrated that cytoplasmic concentrations of calcium above 0.3 μM decrease activity of IP_3-gated channels from cerebellum, reduce binding of IP_3 to its receptor, and diminish Ca^{2+} release from SR of smooth muscle cells and brain synaptosome-derived microsomal vesicles (Finch et al. 1991). The open probability of IP_3 sensitive channels displays bell-shape curve of dependence on free Ca^{2+}, with a maximum probability of opening at ≈0.2 μM of Ca^{2+} in the presence of 2 μM of IP_3 (Bezprozvanny et al. 1991). Similar optimal $[Ca^{2+}]$ and role of calcium as co-agonist of IP_3 for IP_3 induced Ca^{2+} release have been demonstrated elsewhere (Finch et al. 1991).

It has also been shown that [Ca^{2+}]-dependent change of the Ca^{2+} release rate has very fast kinetics. For instance, when brain synaptosome-derived microsomal vesicles were superfused with a solution containing 10 μM Ca^{2+} in the presence of 1 μM of IP_3, the rate of Ca^{2+} release reached its maximum in just 70ms. In reality, Ca^{2+}-dependent modulation of Ca^{2+} release kinetics through IP_3 receptor might have been even faster because 70 ms was the maximal speed of perfusion solution change in the described experiment (Finch et al. 1991). Moreover, the change of Ca^{2+} release rate has a non-linear dependence on the [Ca^{2+}] in the presence of a constant background IP_3 level. The shape of this dependence curve is somewhat similar to the bell-shaped response curve of IP_3-sensitive channels (Bezprozvanny et al. 1991) with maximal release rate at [Ca^{2+}] ≈ 0.3 μM (Finch et al. 1991).

Ca^{2+} and ATP are thought to be allosteric modulators or cofactors for IP_3 receptors. They cannot open IP_3-sensitive channel in the absence of IP_3 (Bezprozvanny et al. 1991). However, in the presence of IP_3 both Ca^{2+} and ATP can increase the frequency and average duration of channel openings (Bezprozvanny and Ehrlich 1993). Based on these observations, it has been proposed that, in the presence of resting levels of IP_3, Ca^{2+} is the actual messenger that opens IP_3 sensitive channels. Heparin inhibits IP_3 binding to the purified IP_3 receptor.

Structure and location of ryanodine sensitive receptors

Three different genes encoding RyRs have been found in mammals, *ryr*-1, *ryr*-2 and *ryr*-3. In addition to the three mammalian RyR genes, a part of a homologous gene, called the *dry* gene, has been identified in *Drosophila*. The *dry* and *ryr* type genes are highly

conserved. The *dry* gene encodes an ~15 kilobase mRNA. It is expressed both in muscles and, at a lower level, in the nervous system of *Drosophila* (Hasan and Rosbash 1992). All three mammalian *ryr* genes encode mRNA of ~16 kilobases and proteins of ~5000 amino acids. It has been shown that skeletal RyR from humans has 5032 amino acid residues (Zorzato et al. 1990).

Two hypothetical models of the RyR structure have been proposed (Coronado et al. 1994). According to the first one, there are four putative transmembrane segments in the carboxy-terminal part of the protein. 12 transmembrane segments are identified in the second model. Ten of them are located close to the carboxy-terminal part of the molecule, and two segments are found near the center of the protein. A hydrophilic center and the amino terminus of the molecule, which consists of 656 amino acid residues, are believed to form so-called RyR cytoplasmic foot (Takeshima et al. 1993).

Tissue specificity of the three proteins encoded by *ryr* genes is not strict. For example, RyR-1 is found in fast- and slow-twitch skeletal muscles (rabbit) and in the cerebellum (mouse). RyR-2 is found in heart (rabbit, cow), hippocampus and forebrain (cow), and the brain of the rabbit; The RyR-3 has been identified in corpus striatum, thalamus, hippocampus, midbrain, pons, medulla, as well as in aorta, urinary bladder, urethra, and uterus (rabbit). Based on the level of expression, and for the sake of simplicity, *ryr*-1, *ryr*-2, and *ryr*-3 genes are designated as skeletal, cardiac and brain *ryr* genes respectively (Coronado et al. 1994).

Functional properties of RyRs

Functionally, RyRs are similar to the IP_3 gated channels. They can be activated by a rise of $[Ca^{2+}]$ in the cytoplasm. Activation of RyRs by calcium is concentration-dependent and reversible. Single-channel recordings of these channels incorporated into a planar lipid bilayer revealed that they have a bell-shaped curve of dependence on $[Ca^{2+}]$. Contrary to the behavior of the IP_3-sensitive channels, RyRs reach their maximal level of activation at 10 μM of calcium. Calcium concentrations above 100 μM inhibit RyRs (Bezprozvanny et al. 1991).

In the presence of low levels of calcium RyRs can be activated by the xanthine derivative caffeine. It has been shown that caffeine activates RyRs by increasing the frequency and duration of opening events without change in the unit conductance. It has also been shown that ATP can further increase activation of RyRs, whereas Mg^{2+}, ruthenium red, and calmodulin significantly inhibit them (Rousseau and Meissner 1989; Sitsapesan & Williams, 1990). Mg^{2+} probably inhibits RyRs by competing with Ca^{2+} binding on the cytoplasmic side of the ER membrane (Ashley and Williams 1990). In addition, a novel second messenger, cADP ribose, has been shown as a physiological agonist of RyRs (Galione 1994; Lee 1997; Lee 1998).

As the name implies, ryanodine receptors are able to bind ryanodine, a plant alkaloid. It has been shown that ryanodine activates RyRs when applied at relatively low concentration, e.g., <10 μM. When ryanodine binds to the RyR, it locks a receptor in a subconductance state and slows the kinetics of transition between open and closed states of the channel. Ryanodine binding to the RyR is use-dependent. Thus, binding occurs

when the channel is in open state or in a process of transition from the one state to the other (Smith et al. 1988).

Minimal requirements for existence of calcium induced calcium release in neurons

Ca^{2+}-induced Ca^{2+} release (CICR), a process of Ca^{2+} mobilization from intracellular Ca^{2+} stores through RyR channels in response to an elevation of $[Ca^{2+}]_i$, has been described as a major contributor to the action potential-evoked Ca^{2+} signals in skeletal and cardiac muscles (Nabauer et al. 1989; Cannell, et al. 1995; Lopez-Lopez et al. 1995) and in peripheral sensory neurons (Usachev and Thayer 1997). Depolarization-induced Ca^{2+} influx has also been suggested to cause CICR in cerebellar Purkinje cells (Llano et al. 1994) and cultured hippocampal neurons (Jacobs and Meyer 1997). In addition to RyRs, endoplasmic reticulum Ca^{2+}-ATPase (SERCA), co-expressed with RyRs, is necessary for CICR. A close proximity of RyRs to voltage-gated Ca^{2+} channels is probably important, given that high concentrations of Ca^{2+}, reached only in the vicinity of voltage-gated Ca^{2+} channels, are required to open RyR channels. Single-channel recordings of RyRs isolated from the brain and incorporated into planar lipid bilayers have shown that their maximal activity is maintained in the presence of 1 to 100 μM of calcium (Bezprozvanny et al. 1991). Theoretical calculations predict that $[Ca^{2+}]$ can reach hundreds of μM in several μs at distances of tens of nanometers from the mouth of a voltage-gated Ca^{2+} channel in neuroendocrine and cardiac muscle cells (Chow et al. 1994; Klingauf 1997; Soeller and Cannell 1997; Cannell and Soeller 1997).

CA1 hippocampal pyramidal neurons have the highest levels of expression of the brain-type RyR2 (Furuichi et al. 1994), expressed in the soma, dendrites and axon. Similarly, the highest expression levels of the SERCA-2 found in the brain, cardiac and slow-twitch muscle are shown in the hippocampus, as well as in the cerebellum, cortex and thalamus (Miller et al. 1991). In addition, it has been shown that RyRs in central neurons are mostly located in the close vicinity to the plasmalemma (for reviews: Berridge 1997; Berridge 1998). Moreover, they are co-localized with the SERCA in the smooth ER (Sah and McLachlan 1991; Sah et al. 1993). Both, the speed of $[Ca^{2+}]$ build up underneath plasmalemma in response to voltage-sensitive channel activation and the location of RyRs inside the cell, lead to a prediction that a possible action potential-evoked CICR might have a very fast onset (<1ms). Hence, it might be almost indistinguishable from the Ca^{2+} influx. Equally important is that ER in the CA1 pyramidal neurons is filled with Ca^{2+} at rest (Garaschuk et al. 1997).

Here we reiterate the above stated hypothesis: calcium influx evoked by either a single action potential or a few action potentials, generated at physiologically feasible frequencies, triggers CICR. This type of CICR is bound to significantly influence the overall magnitude of action potential-induced $[Ca^{2+}]_i$ change. Using fast optical imaging (Lasser-Ross et al. 1991) in fura-2-AM loaded hippocampal slices of the rat (Grynkiewicz et al. 1985; Garaschuk et al. 1997) and whole-cell patch-clamp recordings we provide evidence in favor of this hypothesis.

MATERIALS AND METHODS

Slice preparation

Transverse hippocampal slices (300 μm thick) were prepared from 3- to 5 week old (10 to 17-days old for fura-2-AM experiments) Sprague Dawley rats as previously described (Tsubokawa and Ross 1997). The cutting solution was composed of (in mM) : 120 choline-Cl, 3 KCl, 8 $MgCl_2$, 1.25 NaH_2PO4, 26 $NaHCO_3$ and 10 glucose. Special attention was paid to the preservation of structural integrity of both stratum pyramidale (SP) and stratum radiatum (SR) in the CA1 region of hippocampus. For this purpose, a tissue block was positioned on a vibratome so that a cutting blade would move in the direction parallel to the CA1 pyramidal neuron dendrites: from the alveus to the stratum lacunosum moleculare. After cutting, the slices were warmed to 30-32^{0}C for 30 min, then cooled and maintained at room temperature in normal artificial cerebro-spinal fluid (ACSF). ACSF was composed of (in mM): 124 NaCl, 2.5 KCl, 2 $CaCl_2$, 2 $MgCl_2$, 1.25 NaH_2PO_4, 26 $NaHCO_3$, and 10 glucose, pH 7.4 when bubbled with 95% O_2/5% CO_2.

Fura-2 AM loading procedure

CA1 pyramidal neurons were loaded with cell-permeant acetoxymethyl ester of fura-2 (fura-2 AM, Molecular Probes, Eugene, OR) similar to the procedure described by Garaschuk et al. (1997). A generalized scheme of the loading procedure is shown in the Figure 3B. For these experiments, fura-2-AM was dissolved in DMSO (3.3 mM stock solution), diluted to 15 μM with normal ACSF and sonicated. Hippocampal slices were incubated individually in 1 ml of 15 μM fura-2-AM at 35-36^{0}C for 13-15 min. Upon

diffusion into the cell, the lipophilic fura-2-AM is hydrolyzed into the membrane impermeable fura-2 and trapped inside the neuron.

Special attention was paid to the level of oxygenation and pH of the loading solution. In order to insure constant values of both of these parameters the loading procedures were performed under the excessive pressure (>1 atmosphere) of 95% O_2/5% CO_2 gas mixture. Brain slices were flipped over at least twice during loading or placed onto a nylon mesh submerged into the loading solution to assure equal loading of both sides of the slice. After loading, slices were transferred to the recording chamber where they were washed for at least 30 min with ACSF. Two groups of neurons were loaded especially well, pyramidal neurons and granule cells in the stratum lacunosum moleculare (LM, Fig. 5).

In addition, cells, that looked like interneurons, were loaded in both stratum oriens (SO) and stratum radiatum (SR). Most were located in SO.

The location of the trapped dye inside the cell was of special interest and importance. The conclusions made upon results obtained in the experiments with fura-2-AM loaded slices were dependent on it. The interpretation of the modulation of action potential-evoked calcium transients would be drastically different if the dye were mainly trapped inside organelles. In order to check location of the dye inside the neuron we conducted an experiment as described elsewhere (Golovina and Blaustein 1997).

Fura-2-AM loaded slices were subjected to the application of saponin, a mild detergent that permeabililizes cellular membrane. Upon application of saponin (30 μg/ml) fura-2 fluorescence measured at 600nm was washed out from the cells within 2-3 min.

This result is consistent with the assumption that loading of neurons was restricted to the cytoplasm (Golovina and Blaustein 1997).

Figure 2 CA1 hippocampal pyramidal neurons are loaded with calcium sensitive fluorescent indicators, *bis*-fura-2 and fura-2-AM.

A. A neuron is loaded through a patch pipette. A dye is allowed to diffuse into the neuron for at least 15 minutes (in many instances diffusion took up to half an hour) to ensure its propagation into the dendritic tree and equilibration of the dye concentration in the pipette and the neuron. **B.** A neuron in a hippocampal slice is loaded with fura-2-AM. The slice is submerged into the solution of fura-2-AM. The dye diffuses into the neuron. In the cell, it is hydrolyzed and trapped as the membrane impermeable form (fura-2). The green color indicates the presence of fura-2-AM in the ACSF. **C.** The main parameters of *bis*-fura-2 and fura-2, relevant to imaging and data interpretation.

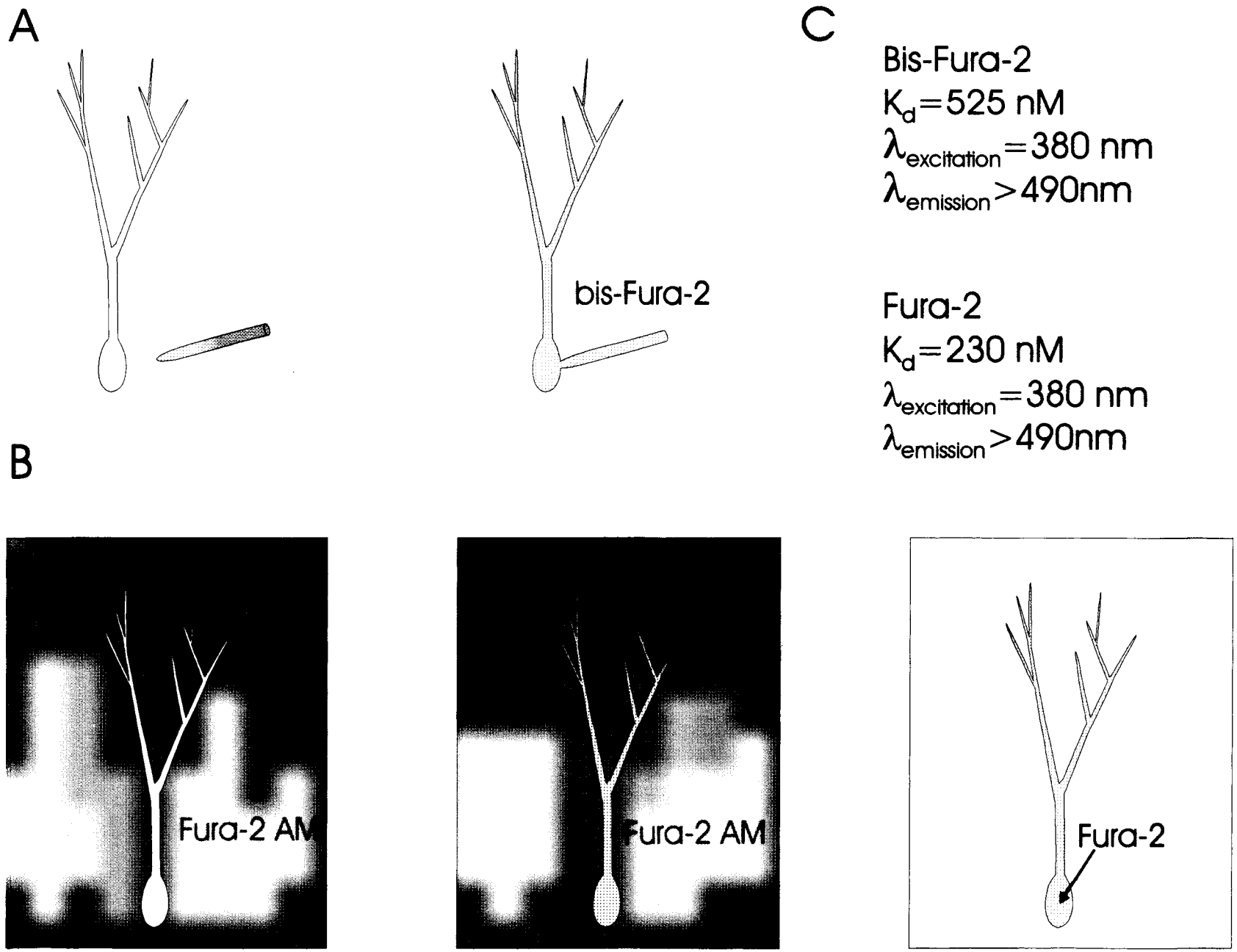
A
bis-Fura-2
C
Bis-Fura-2
K_d=525 nM
$\lambda_{excitation}$=380 nm
$\lambda_{emission}$>490nm
Fura-2
K_d=230 nM
$\lambda_{excitation}$=380 nm
$\lambda_{emission}$>490nm
B
Fura-2 AM
Fura-2 AM
Fura-2

Figure 2.

Recording of Ca^{2+} transients

$[Ca^{2+}]_i$ measurements were made on hippocampal pyramidal neurons from the CA1 region loaded either with fura-2-AM (K_d ~ 230nM) or *bis*-fura-2 (K_d ~ 525nM) through a patch pipette. The Ca^{2+}-sensitive dye *bis*-fura-2, a conjugate of two molecules of fura-2, was chosen because it gave better signal to noise ratio compared to the fura-2. High-speed digital fluorescence image sequences (25-30 ms frame intervals) were recorded with a cooled CCD camera (Lasser-Ross et al. 1991) on an upright Olympus BX50WI microscope equipped with a 40x water immersion objective, N.A. 0.8).

A schematic diagram of the system for synchronous optical and electrical recordings is shown in the Figure 4. The major component of this system is a cooled CCD camera (Photometrics, Tucson, AZ) controlled, through a GPIB interface, by a personal computer (PC) with custom-written software. The configuration used consisted of a camera control unit with 4 Mbytes of image buffer memory, a camera electronics unit with a 500 kHz, 12-bit analog-to-digital converter, and a thermo-electrically cooled camera head with a Thompson 7882 CCD chip capable of working in the frame-transfer mode. This chip has 384 x 576 pixels, half of which are masked and used as a frame transfer buffer area, leaving 384 x 288 pixels for simultaneous image acquisition. Commands specifying parameters of the image acquisition were downloaded, through the GPIB interface, from the computer to the camera control unit. The computer also controlled a programmable 8-channel stimulator (Master-8, AMPI, Jerusalem, Israel) through its serial port. The stimulator controlled a shutter, triggered A/D converter acquiring electrical

signals from the cell, sent trigger pulses to the camera controller initiating each frame acquisition, and triggered extracellular stimulation.

Figure 3 The schematic diagram of the system used for synchronous optical and electrical recording.

Arrows show the data flow (thick arrows), command instructions (thin arrows) and synchronized commands (dotted arrows). All instruments were synchronized using TTL pulses. The same custom-written program (N. Lasser-Ross and J. Callaway, unpublished) handled both, electrical and optical recordings. The figure is adapted from Lasser-Ross et al. (1991).

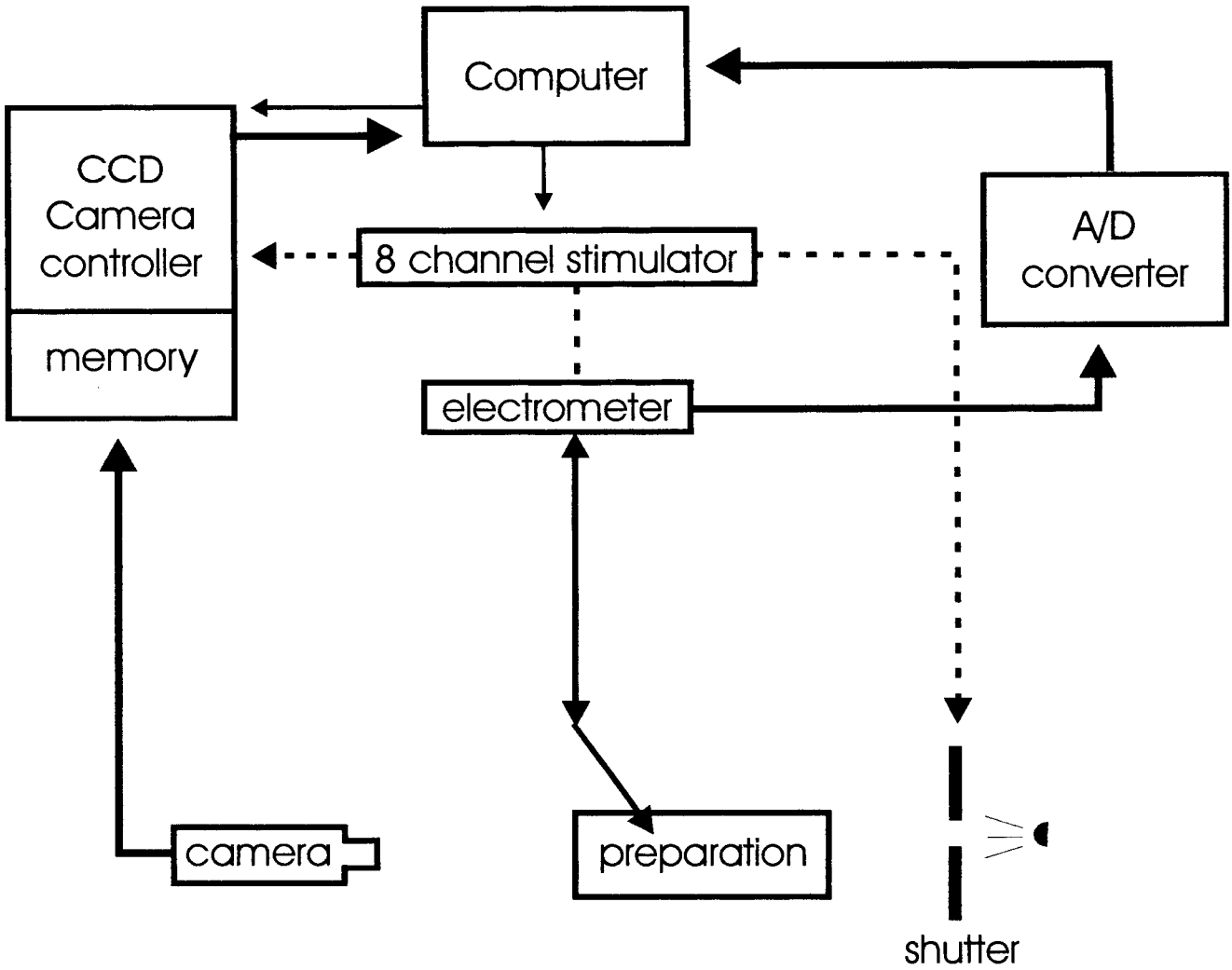
Computer
CCD
Camera
controller
memory
8 channel stimulator
A/D
converter
electrometer
camera
preparation
shutter

Figure 3.

Fura-2 fluorescence (F) was measured using excitation of 382±6 nm and emission of > 455 nm. Changes in $[Ca^{2+}]_i$ were presented as the spatial average of ΔF/F (in %) over cell bodies, in which F is the fluorescence intensity at resting $[Ca^{2+}]_i$ and ΔF is the time-dependent change in fluorescence corrected for bleaching. To correct for bleaching, we recorded change of fluorescence (ΔF/F) in the cell without stimulation. This optical trace was subtracted from the optical recording obtained from the same neuron when it was stimulated. We calculated maximal ΔF/F when antidromic action potentials were evoked. Then we used this maximal ΔF/F to construct pseudo-color images. Regions of high ΔF/F matched the position of loaded neurons. Spatial averages over individual neurons were used for calculation of the time course of Ca^{2+} signals. We chose boxes of 5x5 pixels (~200 μm^2) that matched the area in which ΔF/F values for a single neuron was maximal. The center of each box was defined using ΔF/F pseudo-color images. Position of the maximal ΔF/F regions was monitored throughout the experiments and used as an indicator of the spatial stability of a neuron in the field of view. To determine which box size was optimal to measure signals from a single cell, ΔF/F values were calculated in the box containing the cell and in all surrounding it boxes. ΔF/F values in the box containing the cell were 3.17±0.5 times larger than in surrounding boxes for 5x5 pixels boxes (n=4 cells). This value was 2.6 and 2.5 for box sizes of 3x3 and 7x7 pixels respectively. All recordings were performed at 30^0C, in the presence of D-2-amino-5-phosphonovalerate (APV; 50-100 μM) and 6-cyano-7-nitroquinoxaline-2,3-dione (CNQX; 5-20 μM).

In several instances a single photodiode was used instead of a cooled CCD camera. A general electric scheme of the photodiode controlling circuitry is shown in the Figure

4A. We used the photodiode to increase dramatically the speed of optical recordings (up to 10 kHz). The speed of optical data acquisition was limited by the time constant of the photodiode circuitry (τ~2.5 ms; Fig. 4B).

In these experiments a different calcium sensitive indicator, Calcium Green-1, was loaded into neurons through the patch-pipette. We chose this dye because it has an excellent signal to noise ratio. Fluorescence was measured using excitation of 488 nm and emission > 515 nm with the emission peak at 530 nm. At these wavelengths calcium green-1, spilled from a patch pipette, created high level of background fluorescence around the soma. Thus we could not utilize this dye in the experiments where we measured Ca^{2+} in the soma. The photodiode responded to the light from an area with a radius of about 5 μm when a x40 objective was used. In every experiment we measured calcium transients from 1-5 different regions in the dendritic tree and soma. For every new measurement, the photodiode was moved and refocused to a new position without interruption of electrical recording.

Two methods were employed to define the timing of a calcium transient: 1) visual identification of the point where the signal starts and 2) calculation of the maximal first derivative of the signal. Although the simple inspection gave fairly good results consistent with those obtained with the help of the other method, it was not used for quantification because of the difficulty to justify the choice of the starting point of a signal. Instead, an absolute value of the maximum of the first derivative (MFD) of the calcium signal was used to define the timing of a calcium transient. This was done with the help of custom-written software. Theoretically, the position of a MFD would have been right in the

starting point of a signal if the photodiode had infinitely small response time. Instead, MFD was always found on the shoulder of the signal (Fig. 4).

Background fluorescence and background signals in fura-2 AM loaded slices.

The quality of optical recording from the fura-2-AM loaded brain slices depends on the discrimination between fluorescence of loaded neurons and background fluorescence. In order to estimate its contribution to the overall calcium signals background fluorescence was sampled in regions within stratum radiatum, 50-120 μm away from the CA1 layer, where no loaded neurons were visible. The major source of background fluorescence was attributed to the autofluorescence of the tissue. Autofluorescence, measured from slices that were not loaded with fura-2-AM, contributed 60.7±2.3% (n=7) to the total background fluorescence, measured after the slices were loaded with fura-2-AM.

Figure 4 A single photodiode circuitry and its response characteristics are shown.
A. An electric scheme of the photodiode circuitry is depicted. **B.** A result of a test of a photodiode response time. An emitting photodiode, with response time of less that 10 μs, was used as a source of light. Time constant of the photodiode response was τ~2.6 ms. Note that the signal has a smooth onset despite the fact that the duration of light switching on is practically negligible. This explains the position of the peak of the first derivative on the shoulder. (see Fig. 8).

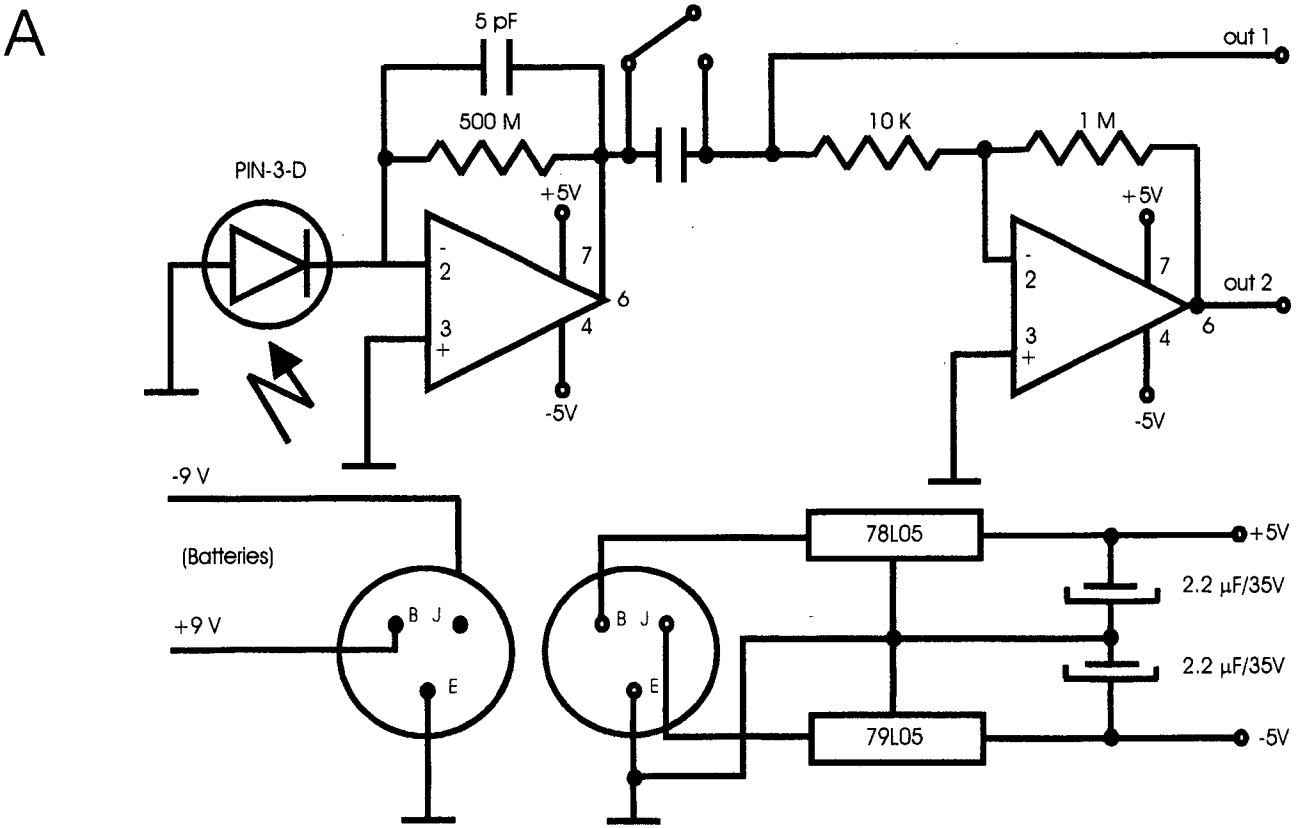
A
5 pF
500 M
PIN-3-D
+5V
-5V
out 1
10 K
1 M
out 2
-9 V
(Batteries)
+9 V
B J
E
78L05
79L05
+5V
2.2 µF/35V
2.2 µF/35V
-5V

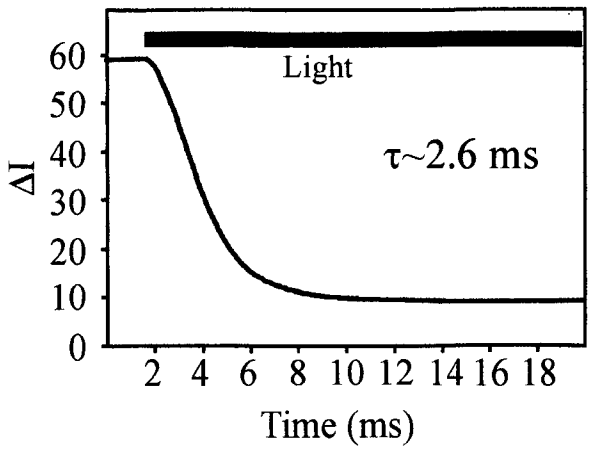
B
Light
τ~2.6 ms
ΔI
60
50
40
30
20
10
0
2 4 6 8 10 12 14 16 18
Time (ms)

Figure 4.

The remaining part was probably due to the residual fura-2-AM that could not be washed out from the slice and from stained cellular elements, which could not be visually resolved. Background fluorescence was typically 40-60 % of the fluorescence in loaded neurons (average 58.5±2.6 %, n=7 slices).

Background fluorescence in the fura-2-AM loaded slices was compared with the background fluorescence in the whole-cell experiments when a neuron was loaded with bis-fura-2 (100-200 μM). In the latter case, background fluorescence accounted for only 10.8±3.4%. In these experiments the background fluorescence originated predominantly from the autofluorescence of the tissue because at ~380 nm excitation fluorescence of the residual (spilled) dye in the presence of 2 mM of Ca^{2+} may be considered negligible (Grynkiewicz et al. 1985).

Since the purpose of the experiments was to compare the $[Ca^{2+}]_i$ changes in response to the application of different pharmacological agents, rather than to calculate absolute calcium concentrations, no correction was made for background fluorescence.

When antidromic action potentials were evoked, ΔF/F signals were measured both in loaded cells and in surrounding regions where background fluorescence was detected. These background signals contributed to 18.5±2.8 % (n=5 slices) of signals in CA1 neurons. They probably originated, in part, from loaded fibers or fine dendrites. Background signals recorded far from loaded cells were insensitive to treatments with caffeine, ryanodine, thapsigargin or CPA.

Stability of fluorescence and ΔF/F signals in fura-2-AM loaded neurons.

Fluorescence with no stimulation was recorded in all experiments. Assuming that the concentration of the indicator remained constant, F was taken as a measure of the relative resting $[Ca^{2+}]_i$. We noticed a small decrease in F with time occurring over all areas of slices, probably because of bleaching. However, since this decrease of F was gradual and linearly dependent on time, changes of resting $[Ca^{2+}]_i$ could be detected as abrupt changes in F during drug applications. In our experiments only CPA (20 μM) affected the resting $[Ca^{2+}]_i$ in some cells. Moreover, bleaching did not significantly affect measurements of ΔF/F values. ΔF/F, recorded every 5 min in antidromically stimulated loaded cells, was stable over one hour. The ratio between amplitudes of two Ca^{2+} signals evoked by 5 action potentials and separated by 5 min was 99.9±1.0% (n=66 cells). For each slice 2-4 controls of ΔF/F were recorded at the beginning of each experiment. Experiments were discarded if ΔF/F values varied by more than 20 %.

Electrical stimulation

Bipolar stimulating electrodes (tip diameter 10μm, resistance 1 MOhm) were placed either on the alveus for stimulating antidromic spikes (500-700 μm away from the pyramidal cell layer) or on the stratum oriens (SO) for generating EPSPs (Fig. 5). 1-10 stimulation pulses (100-500 μA, 200 μs, at 20 Hz) were delivered from an isolated stimulator (World Precision Instrument, Sarasota, FL). The quality of antidromic stimulation was assessed based on the sharpness of the threshold for the evoked action potential and associated Ca^{2+} transient. An action potential was considered to be antidromic when it had a constant latency without evidence for an EPSP, showed all-or-

none type behavior and had a threshold below 500 μA. Antidromically evoked action potentials had drastically different prepotential shapes compared to synaptically evoked action potentials, as well as precise delays between the artifact signifying electrical stimulation and the beginning of an action potential. For fura-2-AM loaded slices stimulus intensity was set so that 1-10 neurons could be reproducibly stimulated in the field of view. Supra-threshold stimulation evoked calcium signals from regions in the slice where no loaded neurons were visible. The stimulus strength was adjusted to keep such "background" signals low (below 20% of the signal measured from a visible loaded neuron).

Electrical Recordings

Experiments were performed in two different recording stations. In one (Callaway and Ross 1995) the chamber was set on the stage of an Olympus IMT-2F inverted microscope. The recording electrode was positioned with a dissecting microscope mounted over the preparation, but the dendrites were approached blindly (Blanton et al. 1989; Sandler et al. 1998).

Figure 5 Schematic representation of a hippocampal CA1 pyramidal neuron is shown. Electrical recordings were made from either soma or dendrites in stratum radiatum (SR). Stimulating electrodes (arrows) were placed either in alveus (ALV) or stratum oriens (SO). LM- stratum lacunosum moleculare.

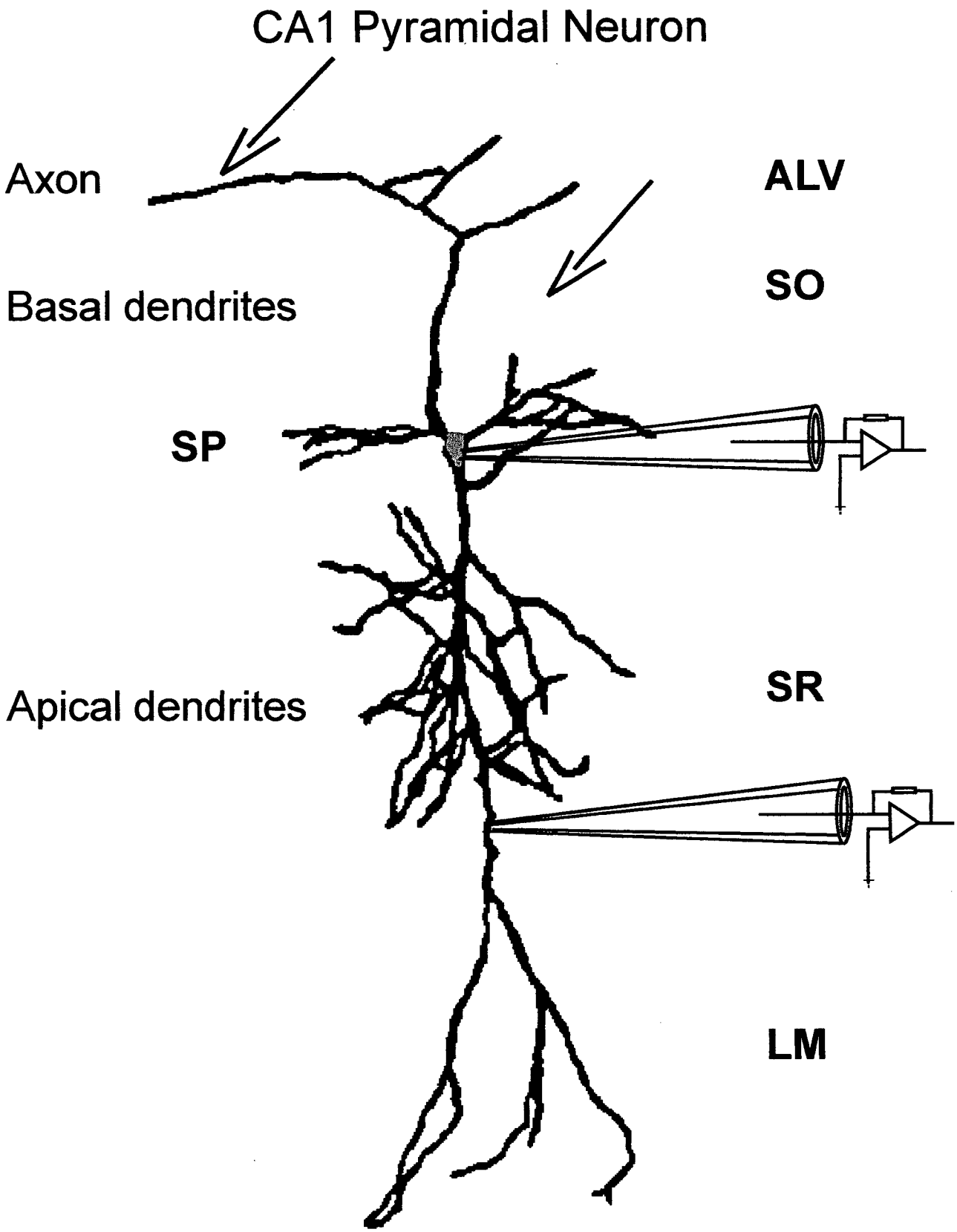
CA1 Pyramidal Neuron
Axon
ALV
Basal dendrites
SO
SP
Apical dendrites
SR
LM

Figure 5.

In the other station the chamber was set on the custom made stage of an upright Olympus BX50WI microscope. Simultaneous measurements of membrane potential and changes of $[Ca^{2+}]_i$ were performed on individual neurons in that setup. Whole-cell tight seals were made on the cell bodies using video-enhanced differential interference contrast (DIC) optics (Stuart and Sakmann 1994). Both dendritic and somatic recordings were made with pipettes containing (in mM): 130 K-gluconate, 10 Na-gluconate, 4 NaCl, 2 Mg-ATP, 0.3 Na-GTP, and 10 HEPES, pH-adjusted to 7.2 with KOH, osmotic pressure 300 mOsmoles. In some experiments K-gluconate was replaced with K-methylsulphate. For simultaneous electrical and $[Ca^{2+}]_i$ measurements, 100 μM bis-fura-2 was added to the patch-solution. This concentration of indicator (also a Ca^{2+} buffer) appears to be well below the concentration that modulates the effect of some transmitters in other preparations (Beech et al. 1991). No additional Ca^{2+} buffers were used. Similar spike potentials and responses to 5-HT were recorded with electrodes containing 100-200 μM bis-fura-2 or no indicator.

Bis-fura-2 was allowed to diffuse into the cell for at least 15 min before Ca^{2+} transient recording. Patch pipettes were pulled from 1.5 mm outer diameter thick-walled glass tubing (No. 1511-M, Friderick and Dimmock, Millville, NJ). Open resistance of the pipettes was 5-7 MΩ for somatic recording and 6-10 MΩ for dendritic recording. After breaking into the cell, the holding current was always < 50 pA and usually zero. No correction was made for the junction potential between the bath and the pipette. Full correction for this potential would make the resting potentials ~11 mV more negative than indicated for the electrodes and solutions applied (Neher 1992).

Chemicals and drugs

Fura-2-AM and bis-fura-2 were obtained from Molecular Probes (Eugene, OR). Thapsigargin and CPA were purchased from Calbiochem (La Jolla, CA). CNQX and APV were from Research Biochemicals International (Natik, MA). Other chemicals were obtained from Sigma (St. Louis, MO).

Perfusion system

All drugs were bath applied through the perfusion system of the recording chamber. Solutions were exchanged at a rate of 1 ml/min using a peristaltic pump (Rainin Instruments, Woburn, MA). The recording chamber had a volume of 2.4 ml.

Special attention was devoted to the precise timing of drug application. For this purpose we measured the dynamics of solution exchange in the recording chamber. When a drug entered the chamber its concentration rose by approximately 10% of its maximal concentration every 9 s, as assayed by measuring the fluorescence intensity of a 0.4 μM fluorescein solution. Thus, a solution exchange of 98% could be achieved within 1.5 min. This allowed a slow rise in drug concentration. Complete wash of fluorescein fluorescence required 10-15 min.

Statistical analysis

Quantitative data are presented as averages ± S.D., unless stated otherwise. Responses under different conditions were compared using Student's t-test. Differences were considered significant for $p<5\%$ (0.05).

RESULTS

We would like, first, to describe basic properties of backpropagating action potentials and associated $[Ca^{2+}]_i$ change in CA1 pyramidal neurons. The knowledge of these properties will help us to better understand and interpret observations obtained in the experiments where action potential backpropagation and associated $[Ca^{2+}]_i$ change are modulated. Among these properties are the spatial distribution of action potential-induced $[Ca^{2+}]_i$ changes in apical dendrites of CA1 pyramidal neurons, the dependencies of the (1) action potential-evoked Ca^{2+} transient amplitude on the number of action potentials and (2) time delay for action potential-evoked Ca^{2+} transient backpropagation on the distance from the soma.

A train of antidromic action potentials back-propagates into the apical dendrites and induces $[Ca]_i$ transients in both soma and apical dendrites in CA1 pyramidal neurons.

A train of antidromically evoked action potentials (20 Hz) recorded in the soma of a CA1 pyramidal neuron showed little attenuation, (n=170; cf. Callaway and Ross 1995; Spruston et al. 1995; Fig. 7D). When a train of antidromically evoked backpropagating action potentials was recorded in the dendrites of the CA1 pyramidal neurons at a distance of 200-300 μm from the soma, a characteristic attenuation of these action potentials was observed (n=75; cf. Callaway and Ross 1995; Spruston et al. 1995; Fig. 6E). The further away from the soma a recording was made, the larger was the observed attenuation. In

addition, the amplitude of the first spike in the train was always smaller than the amplitude of the spikes recorded in the soma (Fig 6 D,E). This is also consistent with previous reports (Callaway and Ross 1995; Spruston et al. 1995).

It has been shown (Jaffe et al. 1992) that backpropagating action potentials determine the pattern of dendritic Ca^{2+} transients in CA1 neurons. In order to check how the profile of backpropagating action potentials was reflected in the evoked calcium signals in the dendrites, we performed synchronous electrical and fast optical recordings of $[Ca^{2+}]_i$ changes in CA1 pyramidal neurons (n=15).

A neuron was filled with a calcium sensitive dye, bis-fura-2, through a patch pipette. The dye was allowed to diffuse through the apical dendrites (Fig. 6A). Simultaneous electrical and optical recordings of $[Ca^{2+}]_i$ changes were made when the neuron was stimulated antidromically. A train of antidromic action potentials evoked $[Ca^{2+}]$ change in the soma of CA1 pyramidal neurons. A typical attenuating profile of a train of antidromic action potentials recorded in dendrites evoked calcium changes in dendrites in CA1 pyramidal neurons (Fig. 6B, C).

Figure 6 A train of antidromically evoked action potentials back-propagates into the apical dendrites and evokes a Ca^{2+} transient in both soma and apical dendrites in CA1 pyramidal neurons.

A. Fluorescent image of a cell filled with *bis*-fura-2. **B.** A change of $[Ca^{2+}]_i$ (% $\Delta F/F$) shown simultaneously in space and time in response to a train of 10 action potentials. **C.** Selected traces of a $[Ca^{2+}]_i$ change (% $\Delta F/F$) measured in the dendrite of the cell in A. Colors of the traces correspond to the colors of the rectangles in the fluorescent image, indicating the places of recordings. **D.** A train of action potentials recorded in the soma. **E.** A train of action potentials recorded in a dendrite (225 μm from the soma).

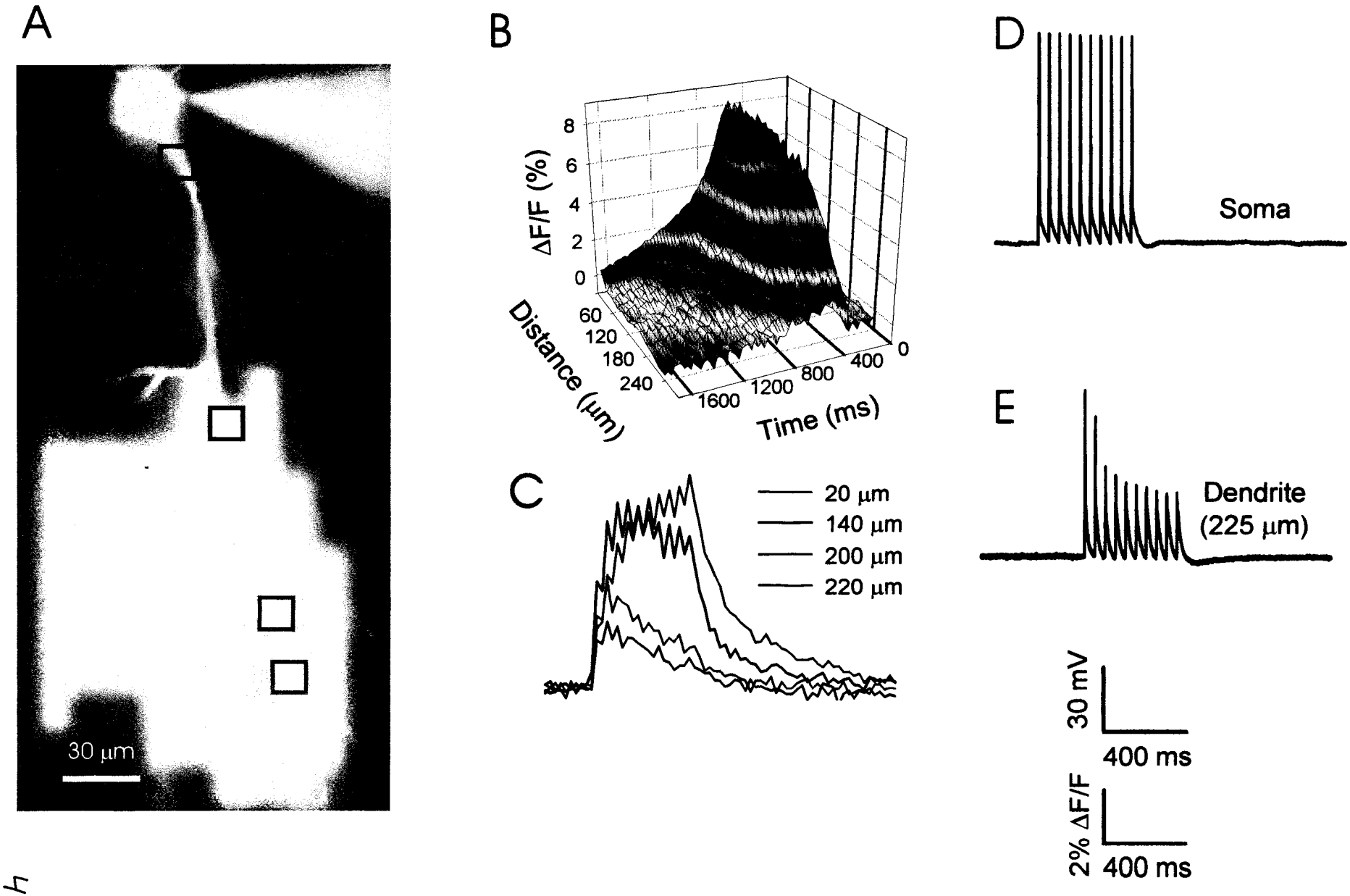
A
30 μm
B
ΔF/F (%)
8
6
4
2
0
60
120
180
240
Distance (μm)
1600
1200
800
400
0
Time (ms)
C
20 μm
140 μm
200 μm
220 μm
D
Soma
E
Dendrite
(225 μm)
30 mV
400 ms
2% ΔF/F
400 ms

Figure 6.

This attenuation was consistent with attenuation in a train of spikes propagating back into the dendrites (Fig. 6E; Jaffe et al. 1992; Callaway and Ross 1995; Spruston et al. 1995).

A train of antidromically evoked action potentials causes linear increase of maximal $[Ca^{2+}]_i$ in the soma and a saturating change of $[Ca^{2+}]_i$ in the apical dendrites in CA1 pyramidal neurons.

When a neuron was filled with 100-200 μM of bis-fura-2, a train of antidromically evoked action potentials (1-10 action potentials at 20 Hz) induced Ca^{2+} transients in the soma. Their maximal amplitudes grew as a linear function of the number of evoked spikes (n=7; Fig. 7C). Such linear dependence corresponds to almost an absence of action potential accommodation in the soma. Moreover, these data indicated that the amount of calcium sensitive dye used in our experiments was low and did not alter endogenous calcium buffering in the CA1 pyramidal neurons (Helmchen et al. 1996).

Figure 7 $[Ca^{2+}]_i$ increase evoked by a train of action potentials is linear in the soma and non-linear in the dendrites.

A. A change of Ca^{2+} transient amplitude (% ΔF/F) shown simultaneously in space and time in response to a train of 1-10 action potentials. **B.** Dependence of Ca^{2+} transient amplitude change (% ΔF/F) on the number of action potentials in the train and the distance from the soma. **C.** Selected traces that show dependence of a Ca^{2+} transient amplitude change (% ΔF/F) on the number of action potentials in the train for the three different locations along the dendritic tree.

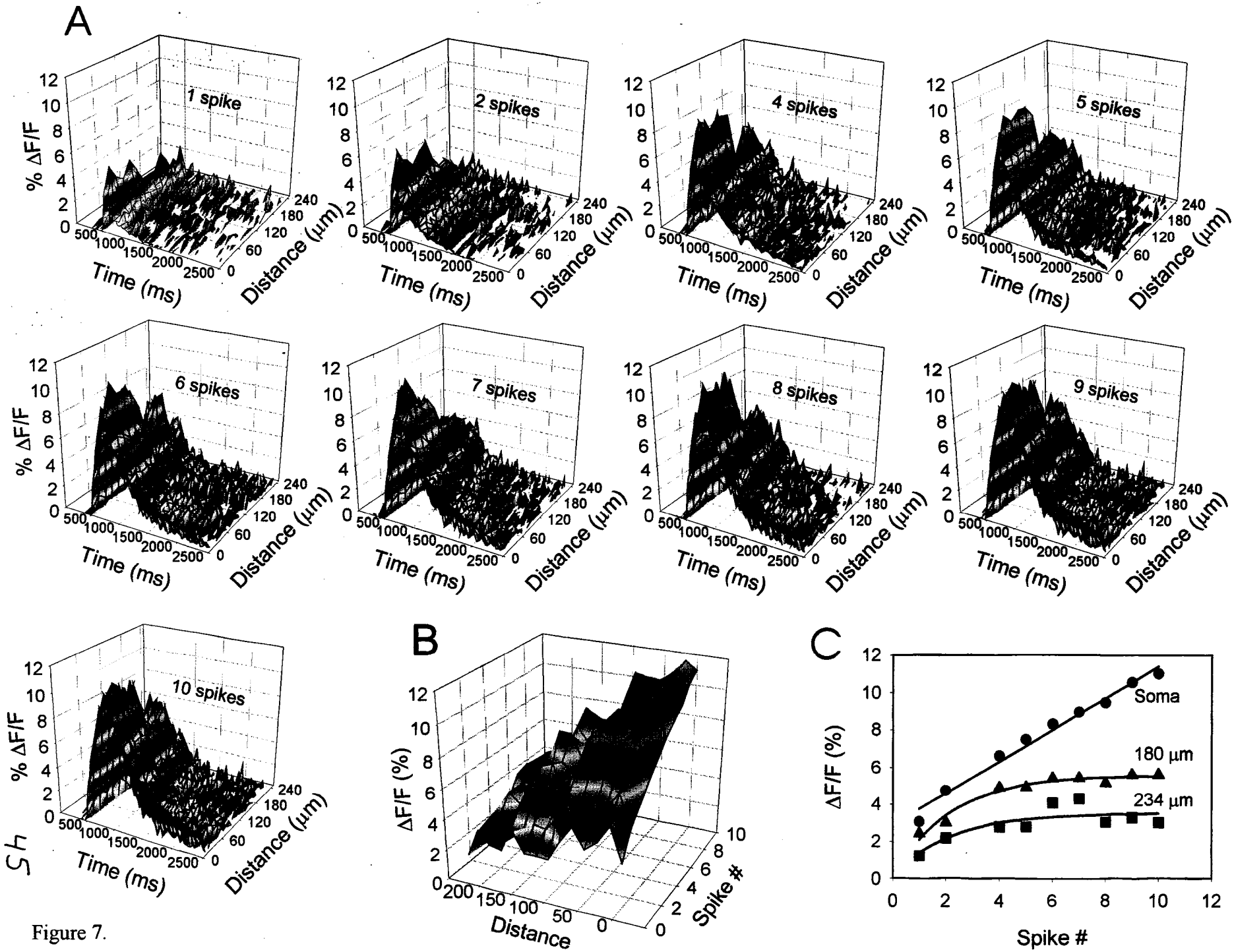
A
1 spike
2 spikes
4 spikes
5 spikes
6 spikes
7 spikes
8 spikes
9 spikes
10 spikes
% ΔF/F
Time (ms)
Distance (μm)
B
ΔF/F (%)
Distance
Spike #
C
Soma
180 μm
234 μm
ΔF/F (%)
Spike #

Figure 7.

A confirmation of a low artificial calcium buffering introduced by 100-200 μM of bis-fura-2 was of special importance for the latter experiments in which calcium transients were used to measure drug actions on the cell.

Moving away from the soma, the action potential-induced maximal $[Ca^{2+}]_i$ changes saturated at progressively lower levels (Fig. 7B,C). Such non-linearity was probably a reflection of the failure of action potentials to invade more distal parts of the dendritic tree. Similar observations have been reported elsewhere (Callaway and Ross 1995; Spruston et al. 1995; Schiller et al. 1995).

Figure 8 Linear dependence of time delay between an action potential in the soma and a calcium transient evoked by a backpropagating action potential in apical dendrites.

A. Schematic representation of a CA1 pyramidal neuron. 1,2,3,4 are the points in the dendritic tree of the neuron where measurements of backpropagating action potential evoked calcium transients were made. **B.** A result of an experiment shown in A. The delay of a maximum of the first derivative of the calcium transient in a soma (S) was taken as a reference point. Ordinate numbers mark corresponding points in the dendrite shown in A. **C.** An example of a measurement of a maximum of the derivative of a calcium transient and its temporal position relative to the electrical signal recorded in the soma. Red dotted line shows approximate position chosen by the eye examination of the beginning of the optical signal. Green dotted line shows the position of the maximum of the first derivative. **D**. Dependence of the delay of a maximum of the first derivative of an action potential evoked Ca^{2+} transient on the distance from the soma (n=11).

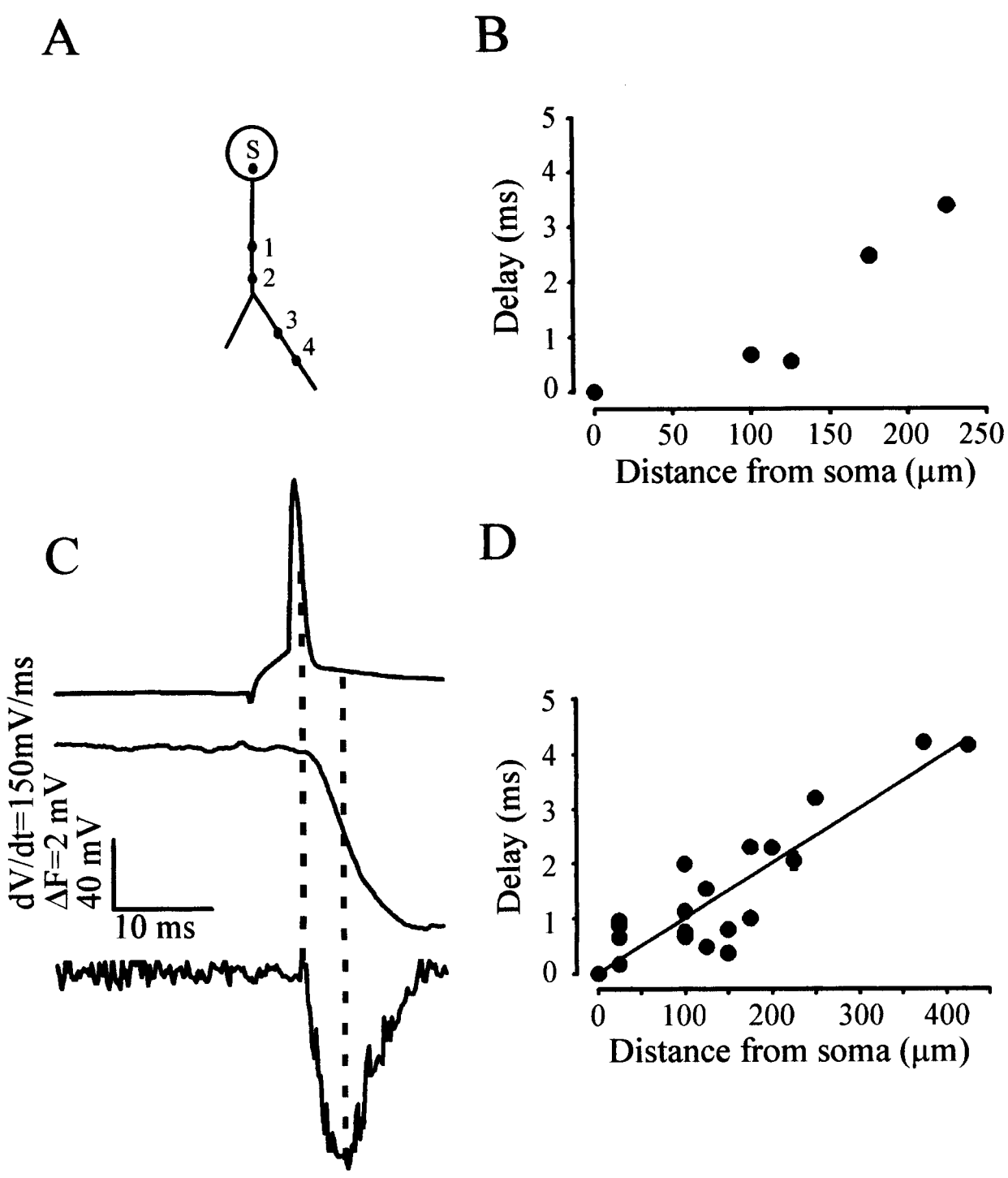
A
S
1
2
3
4
B
Delay (ms)
0
1
2
3
4
5
0
50
100
150
200
250
Distance from soma (μm)
C
dV/dt=150mV/ms
ΔF=2 mV
40 mV
10 ms
D
Delay (ms)
0
1
2
3
4
5
0
100
200
300
400
Distance from soma (μm)

Figure 8.

The time delay of action potential-evoked Ca^{2+} transient backpropagation into dendrites is proportional to the distance from the soma.

The delay between an action potential onset in the soma and its onset in the main shaft of apical dendrites is proportional to the distance between the two points. This conclusion was based on the data obtained in the experiments with dual whole-cell patch-clamp recordings in neocortical and CA1 pyramidal neurons (Stuart and Sakmann 1994; Spruston et al. 1995). If a backpropagating action potential causes changes in $[Ca^{2+}]_i$ by opening voltage-controlled Ca^{2+} channels, then the delay for such changes should also be proportional to the distance from the soma.

Figure 8 shows the results of a series of experiments where we used high speed optical recording of an action potential evoked Ca^{2+} transient from a single point in the dendritic tree (n=11). A delay between the peak of an action potential recorded in the soma of CA1 pyramidal neuron and a maximum of the first derivative of the calcium transient was proportional to the distance between soma and a position of the point of interest in the main shaft of the dendrite.

5-HT evokes hyperpolarization and increase of membrane conductance in dendrites

Bath application of 5-HT (10 μM) hyperpolarized the membrane by 8-10 mV (resting mebrane potential was -64±3.7 mV). The hyperpolarization was accompanied by an increase in conductance in both somatic recordings (35.7±5.3%; data not shown) and in dendritic recordings at the distance of 200-300 μm from the soma (n=7; Fig. 9A) If 5-HT remained in the bath for more than 5 min, the membrane potential relaxed to the original resting potential and sometimes depolarized the cell by 4-6 mV (n=3). If during

hyperpolarization depolarizing current was injected into the dendrites to restore the potential to the resting level, the conductance increase remained (Fig. 9B). This demonstrates that the conductance increase was not induced by the voltage-shift. Serotonin did reduce the sag in the voltage response (Fig. 9C). The hyperpolarization was prevented by spiperone (10 μM), a 5-HT_{1A} receptor antagonist, added to the bath >10 min before the addition of 5-HT (data not shown). These results from dendritic recordings are similar to those previously reported from somatic recordings (e.g. Andrade and Nicoll 1987; McCormick and Pape 1990), suggesting that 5-HT_{1A} receptors are the dominant mediator of this effect.

Figure 9 Serotonin hyperpolarized the dendrites of pyramidal neurons and increased the membrane conductance.

A. Constant current hyperpolarizing pulses (500 ms duration) were given every 30 s through the recording electrode as 10 μM 5-HT was washing into the bath. Each vertical line is a compressed version of the response. The length of each line represents the difference between the membrane potential before the current injection and the steady-state hyperpolarization before the end of the pulse. Individual responses are shown in C. At the recording site (215 μm from the soma) the cell hyperpolarized by 8 mV. The amplitude of the voltage responses diminished, indicating that the conductance increased. After returning to control solution, the membrane potential and conductance slowly recovered (n=7). **B.** A similar experiment except that at the peak of the response additional depolarizing current, in step increments, was injected through the recording electrode. The potential was restored to the resting level, but the conductance increase remained. **C.** Selected responses from this experiment on an expanded time scale.

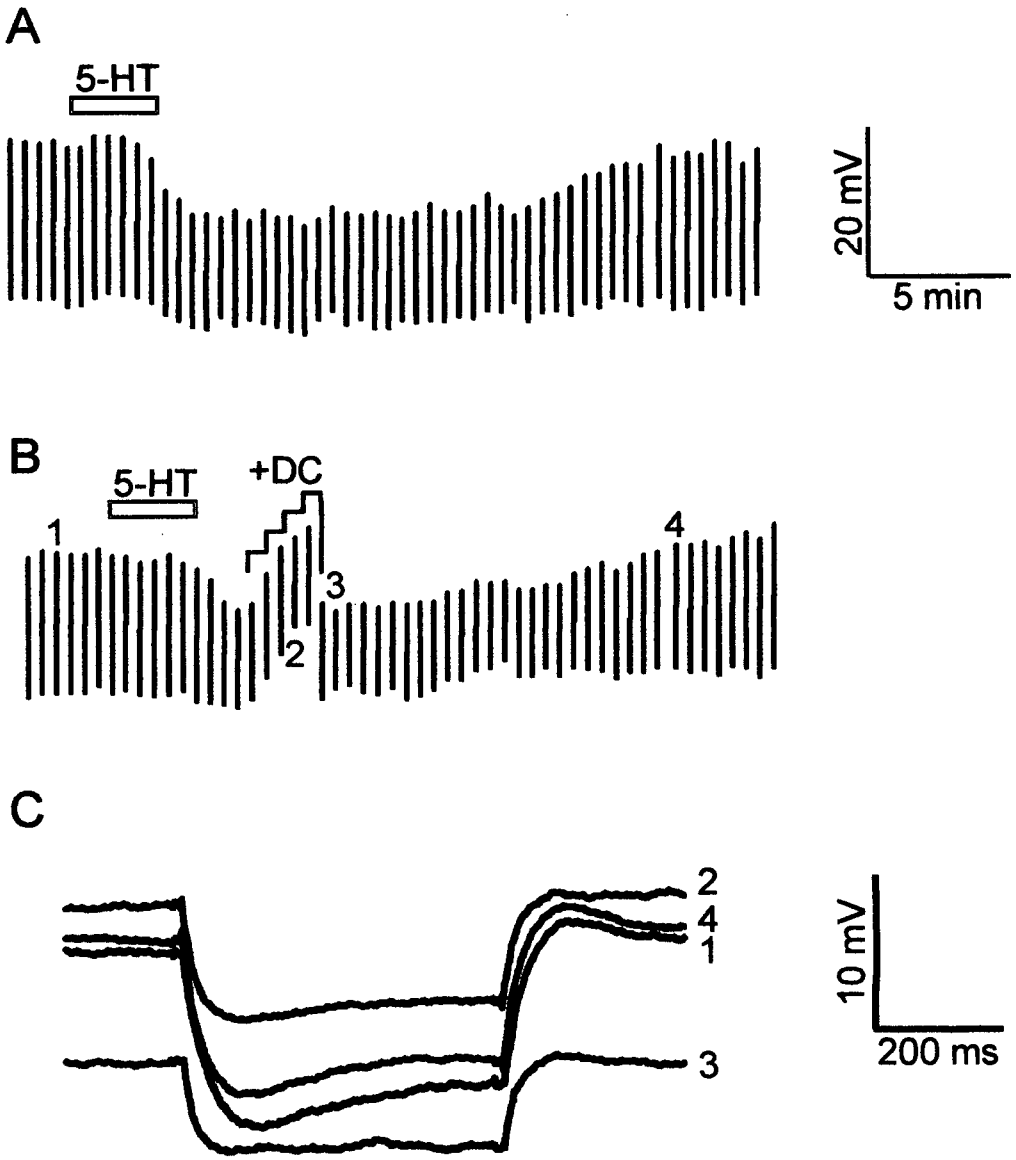

Figure 9.

Dendritic hyperpolarization was also observed in response to focal pressure-applied 5-HT on the distal apical dendrites (not shown), suggesting that 5-HT receptors and coupled K^+ channels are found in this region. This result is consistent with the immunocytochemical localization of 5-HT_{1A} receptors on hippocampal pyramidal cell dendrites (Kia et al. 1996).

Serotonin reduces the peak potential and the absolute amplitude of backpropagating action potentials recorded in the apical dendrites

To test the effects of 5-HT on spike amplitude we evoked action potentials antidromically with stimulating pulses in the alveus in the presence of CNQX (10 μM) and APV (50 μM) to block fast glutamatergic synaptic transmission. Under these conditions, single action potentials of almost constant amplitude were recorded with patch electrodes in the dendrites (200-300 μm from the soma). The amplitude of the first action potential in the dendrites was smaller than the 101±3.1-mV (n=17) amplitude usually recorded in the soma with patch electrodes, similar to the observations reported by Tsubokawa and Ross (1996). (Amplitude was measured as the difference between the peak potential and the potential just before evoking the spike). When spikes were evoked at 20 Hz, their amplitudes declined during the train (Fig. 10A, control) as previously reported (Fig. 6E; Callaway and Ross 1995; Spruston et al. 1995). 5-HT (10 μM) added to the bath hyperpolarized the cell and reversibly decreased the peak amplitude (absolute membrane potential) of all the spikes in the train (Fig. 10A). On average the peak potentials of the earlier spikes were reduced by 14 mV and of the later spikes by 10 mV (Fig. 10B). Since the membrane hyperpolarized only by about 8 mV, the absolute amplitude decreased

slightly (4-6 mV). Figure 10 C, D summarizes the effect of 5-HT on the peak potential and absolute amplitude of the action potentials in a train (n=9).

Figure 10 Serotonin reduces the peak potential and the absolute amplitude of backpropagating action potentials recorded in the apical dendrites.

A. Train of 10 spikes evoked at 50 ms intervals recorded 270 μm from the soma in normal ACSF. Spike amplitudes decrement in an activity dependent manner. 10 μM 5-HT hyperpolarized the cell and reduced the peak potential of the action potentials. Washing out the 5-HT almost restored the control recording. **B.** Summary of the effect of 5-HT on the changes in peak potential and absolute amplitude. Nine cells were analyzed; all were recorded 200-300 μm from the soma. The early spikes in the train were reduced by about 15 mV; later spikes were reduced by 8-10 mV. The absolute amplitude was reduced by a few mV or stayed the same for all spikes in the train. **C.** Summary of the peak potentials of the ten spikes in normal and 5-HT containing ACSF. **D.** Summary of the absolute amplitudes of the action potentials under the same conditions.

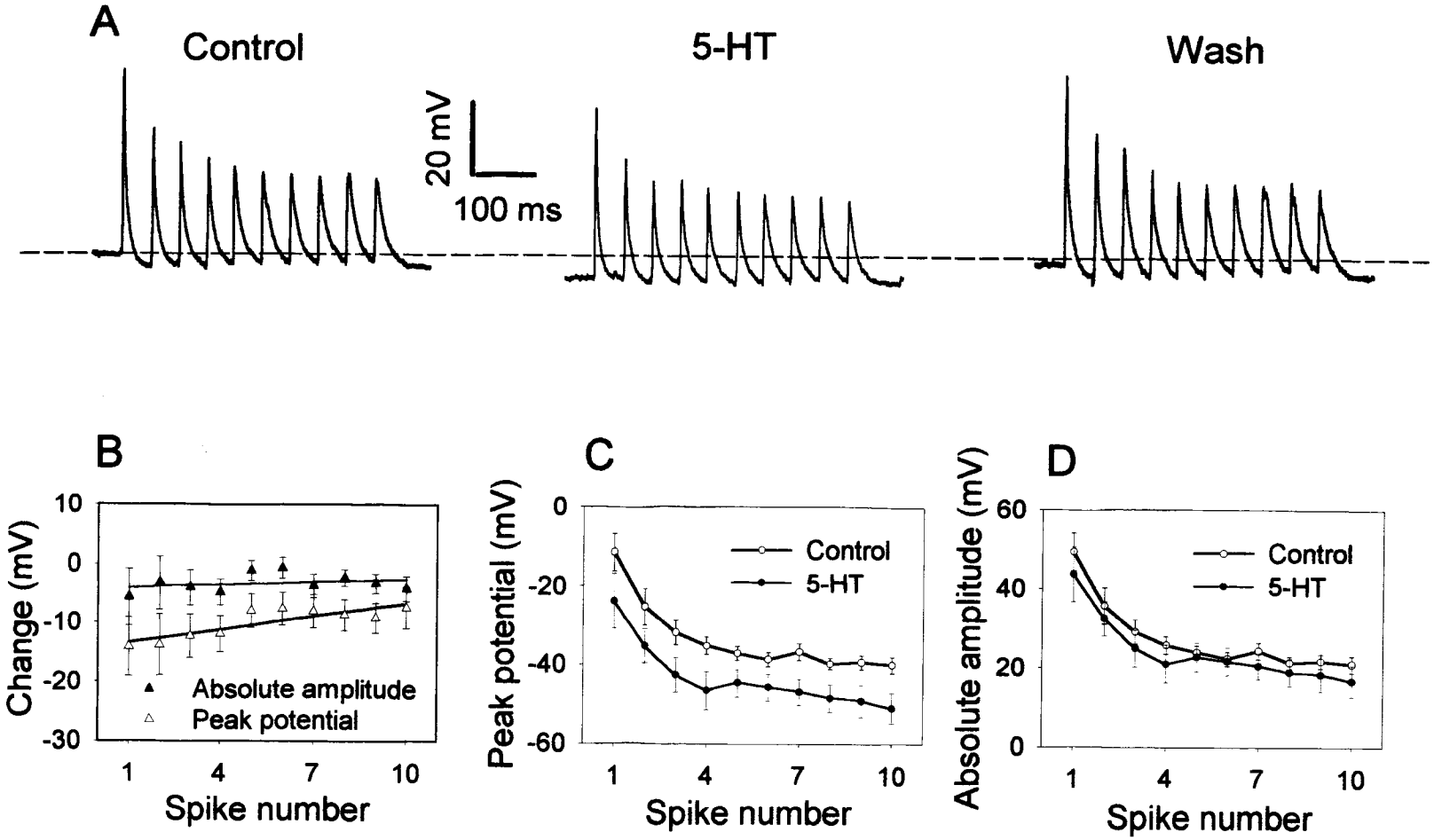
A
Control
5-HT
Wash
20 mV
100 ms
B
Change (mV)
10
0
-10
-20
-30
Absolute amplitude
Peak potential
1
4
7
10
Spike number
C
Peak potential (mV)
0
-20
-40
-60
Control
5-HT
1
4
7
10
Spike number
D
Absolute amplitude (mV)
60
40
20
0
Control
5-HT
1
4
7
10
Spike number

Figure 10.

The weak effect of 5-HT on action potentials recorded in dendrites resembled the effect of membrane hyperpolarization evoked by current injection into the dendrites (Tsubokawa and Ross 1996). To compare directly the two effects we combined the application of 5-HT and current injection in different combinations in the same cell. Fig. 11 (typical of experiments on 3 cells) shows that –0.08 nA mimicked the effect of 10 μM serotonin, and +0.08 nA in the presence of 5-HT restored the spike profile to the control response. This result differs from that observed with carbachol (Tsubokawa and Ross 1997) where current injection could not reproduce or reverse the carbachol response.

Figure 11 Current injection into the dendrites mimics the effect of 5-HT on dendritic action potentials.

Control recordings at 270 μm from the soma demonstrate the typical activity-dependent amplitude profile. Injection of –0.08 nA steady current lowers the resting potential and reduces the peak spike potential. The first, larger amplitude spike is more affected. Removal of the current and application of 10 μM 5-HT has a similar effect. Injection of +0.08 nA in the presence of 5-HT restores the spike profile to the control response. (One spike failed in this trial). Finally, removal of current and washout of 5-HT for 5 min partially restores the control response.

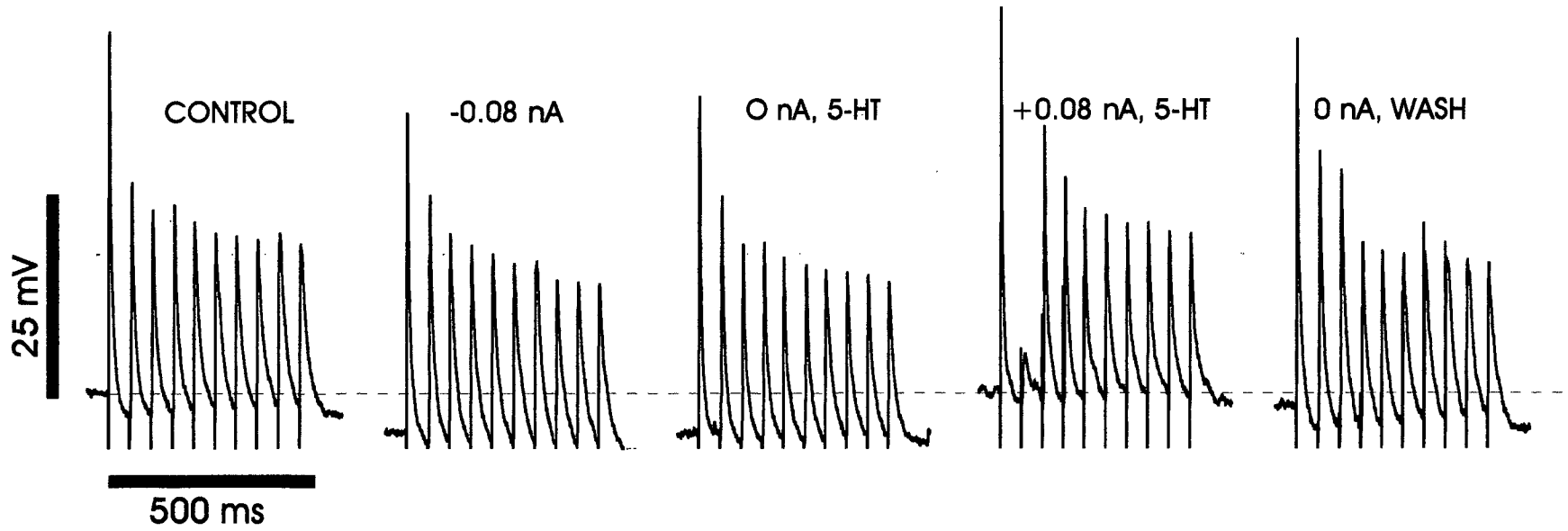

Figure 11.

Serotonin increases the absolute amplitude of action potentials in the soma with little effect on the peak potential

It has been previously shown (Tsubokawa and Ross 1996) that membrane hyperpolarization due to current injection had little effect on the peak amplitude of APs recorded at the soma. Therefore, we repeated the serotonin experiments with somatic recordings to test whether the 5-HT-induced hyperpolarization also affected the spikes in the two regions differently. Fig. 12A shows that antidromically-evoked action potentials increased in absolute amplitude by 8 mV whereas their peak potentials did not change when the soma was hyperpolarized by 8 mV. Note that in both normal conditions and in 5-HT all of the somatic spikes in the train have about the same amplitude (Callaway and Ross 1995; Spruston et al. 1995). Fig. 12C shows that on average, the peak potentials of all somatic spikes in the train decreased by about 3 mV and the absolute amplitude increased by about 4 mV. Fig. 12D, E summarize the effects on the peak potential and absolute amplitude in the soma (n=14).

Figure 12 Serotonin increases the absolute amplitude of action potentials in the soma with little affect on the peak potential.

A. Train of 10 antidromic spikes evoked at 50 ms intervals. All spikes have about the same amplitude. In 10 μM 5-HT the cell hyperpolarized but the peak potential was unchanged. **B.** Overlay of the first spikes in control and 5-HT containing ACSF. Only the amplitude was affected by 5-HT. **C.** Summary of the effect of 5-HT on the changes in peak potential and absolute amplitude in 14 recordings from the soma. The absolute amplitude of all spikes increased by about 4 mV. The peak potential was reduced by 2-3 mV. **D.** Summary of the peak potential in the soma of the ten spikes in normal and 5-HT containing ACSF (n=14). **E.** Summary of the absolute amplitudes of the spikes under the same conditions in the same cells (n=14). The larger error bars in D and E, compared with C, reflect cell to cell variation.

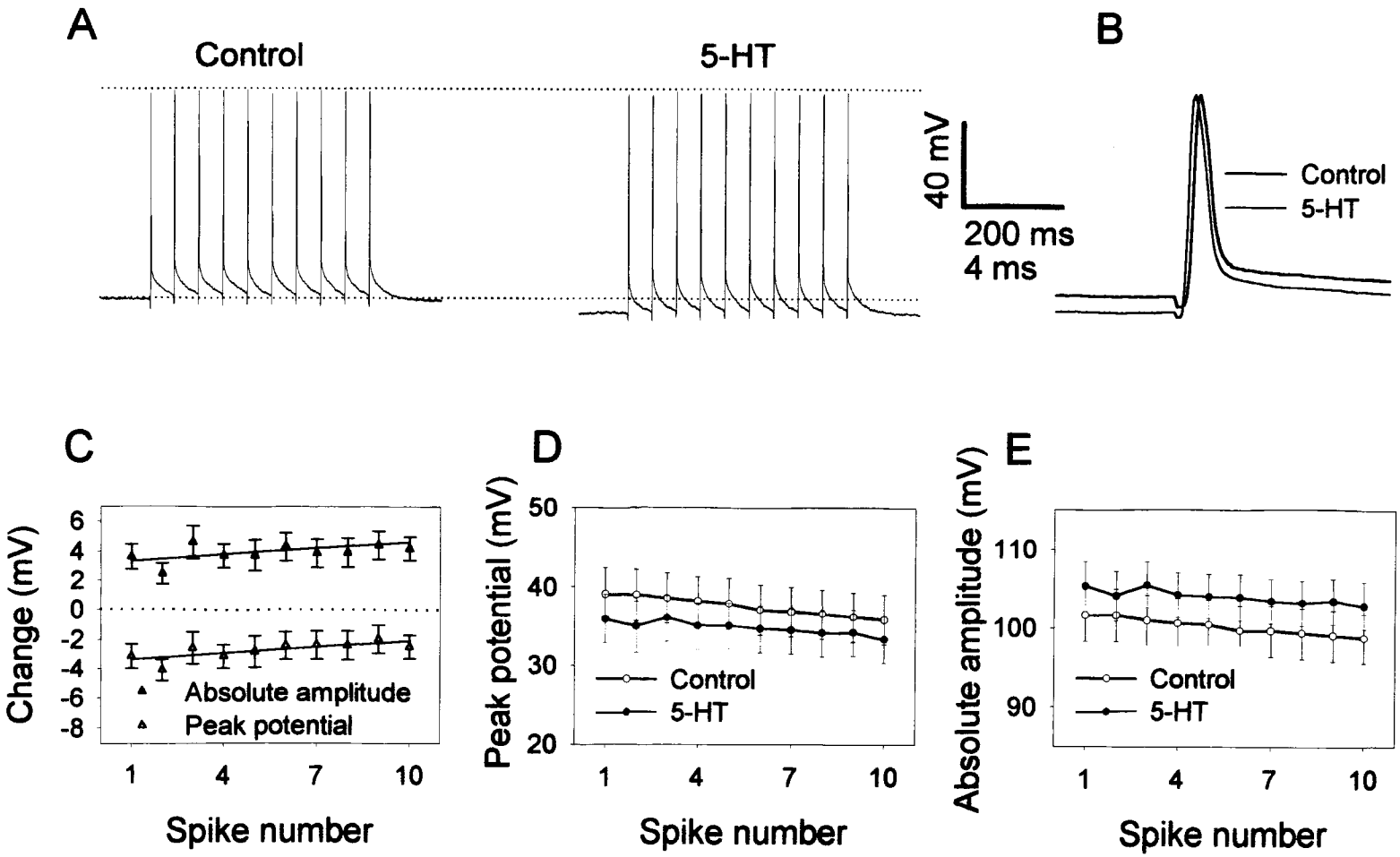
A
Control
5-HT
B
40 mV
200 ms
4 ms
Control
5-HT
C
Change (mV)
6
4
2
0
-2
-4
-6
-8
Absolute amplitude
Peak potential
1
4
7
10
Spike number
D
Peak potential (mV)
50
40
30
20
Control
5-HT
1
4
7
10
Spike number
E
Absolute amplitude (mV)
110
100
90
Control
5-HT
1
4
7
10
Spike number

58

Figure 12.

Serotonin reduces spike-evoked $[Ca^{2+}]_i$ changes in soma and dendrites of CA1 pyramidal neurons

One important consequence of spike backpropagation into the dendrites was that these action potentials caused large changes in $[Ca^{2+}]_i$ in this region (e.g. Jaffe et al. 1992). The mechanisms that alter backpropagation change the magnitude and spatial extent of these changes (Tsubokawa and Ross 1996; Tsubokawa and Ross 1997). Since 5-HT reduced spike amplitude in the dendrites, we reasoned that this reduction would also affect the associated $[Ca^{2+}]_i$ change. The experiments shown in Figure 13 confirmed this idea. In normal ACSF backpropagating action potentials caused $[Ca^{2+}]_i$ increases at all locations (cf. Jaffe et al. 1992; Regehr and Tank 1992; Callaway and Ross 1995). In 5-HT (10 μM) the $[Ca^{2+}]_i$ increase evoked by a train of 10 action potentials was reversibly reduced by about 20% in the dendrites (Fig. 13B). In addition, 5-HT reduced the somatic $\Delta F/F$ change by 30% although the peak potential was not significantly reduced in this region. The resting fluorescence level (F) did not change in 5-HT (not shown), suggesting that there was no change in resting $[Ca^{2+}]_i$. Figure 13C summarizes the results of 5 experiments. In all regions of the neuron, the reduction in $\Delta F/F$ was greater than 20%. The reductions were all statistically significant ($p<0.002$).

A difficulty in these experiments was that the concentration of bis-fura-2 in the dendrites rarely reached a stable value in less than 30 min. The indicator slowly diffused to these distal sites from the site of injection in the soma. As the indicator concentration increased, buffering of the $[Ca^{2+}]_i$ change increased, reducing $\Delta F/F$ for constant levels of Ca^{2+} entry (Helmchen et al. 1996). In addition, higher values of indicator fluorescence

altered the significance of background fluorescence. To minimize these effects, we waited as long as possible after breaking into the cell before making the measurements. We typically waited at least 15 min before making the first control measurement and 30 minutes before making the first measurement in ACSF containing 5-HT. We also bracketed all measurements with control observations after returning to normal ACSF.

Figure 13 Serotonin reduces spike-evoked $[Ca^{2+}]_i$ changes in all parts of patch-loaded pyramidal neurons.

A. Fluorescence image of bis-fura-2 loaded pyramidal neuron. Rectangles indicate regions from which time-dependent traces are taken. Scale 20 μm. **B.** Fluorescence changes in three regions in response to a train of 10 antidromic action potentials evoked at 50 ms intervals. Control recordings made just before changing to ACSF containing 10 μM 5-HT and 32 min after breaking into the cell. 5-HT recording: 4 min after changing the solution. Wash recording: 9 min after returning to normal ACSF. Serotonin was in the bath for 3 min. Three trials were averaged for each condition. Voltage traces show the first of the three responses. Spike amplitudes did not completely return to control values, but the fluorescence change recovered. **C.** Summary of changes in three regions for five cells. Control values were normalized to 100%. The middle (M) and distal (D) boxes were typically 100 and 200 μm from the soma (S).

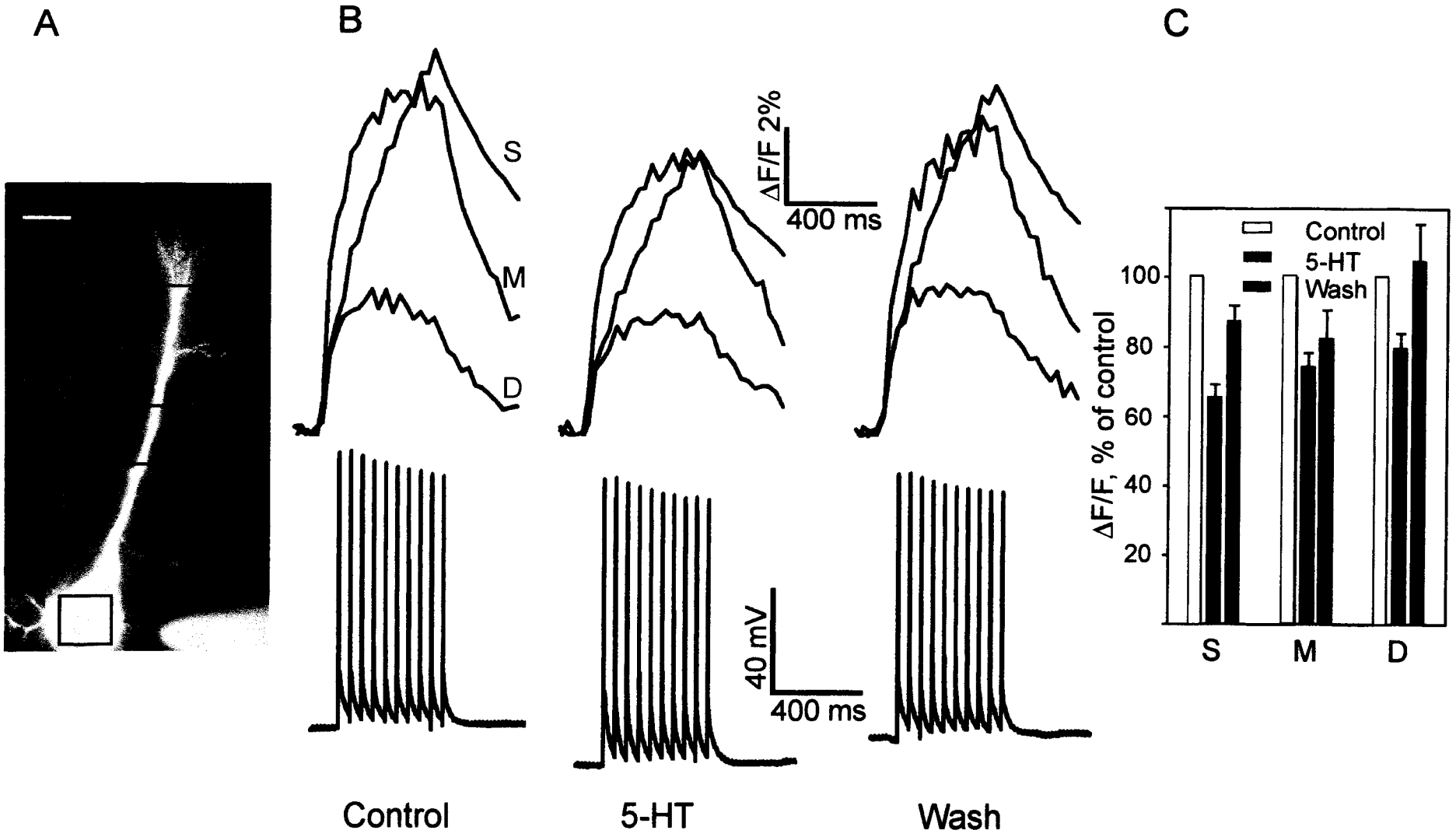
A
B
C
S
M
D
ΔF/F 2%
400 ms
40 mV
400 ms
Control
5-HT
Wash
ΔF/F, % of control
100
80
60
40
20
Control
5-HT
Wash
S
M
D

Figure 13.

Serotonin reduces action potential-evoked $[Ca^{2+}]_i$ changes in the soma of fura-2-AM loaded CA1 pyramidal neurons

In another series of experiments, we tried to avoid the problem of uneven and slow dye diffusion by loading pyramidal neurons in the slice with the acetoxymethylester form of fura-2 (Grynkiewicz et al. 1985). Using this procedure, all parts of the neuron were loaded simultaneously and diffusion was not a problem. The final concentration of fura-2 in the cells was unknown. However, the half recovery time for single spike-evoked fluorescence transients typically was less than 200 ms in the soma and less than 150 ms in the dendrites (Fig. 14A). If the indicator in these experiments responded similarly to indicator loaded from patch pipettes then these fast recovery times would indicate that the final concentration was less than 100 μM (Helmchen et al. 1996). The protocol for these experiments was similar to the whole-cell experiments except that there was no electrode in the cell. While this procedure was not able to directly monitor the potentials in the neurons, it had the advantage of avoiding washout of important intracellular constituents. We confirmed that the pyramidal cells fired antidromic action potentials by observing the all-or-none fluorescence response as the stimulus intensity in the alveus was increased. Subthreshold synaptic stimulation evoked small Ca^{2+} transients, probably due to Ca^{2+} influx through low-threshold Ca^{2+} channels (not shown). These fluorescence changes were blocked by adding TTX (1 μM) to the bath, implying that they depended on Na^+ spikes (n=3; not shown). Figure 14B shows results from a typical experiment. Fluorescence transients were evoked with a train of 10 antidromic action potentials. Serotonin (10 μM) caused a reversible reduction of about 35% in spike-evoked $\Delta F/F$ in

the soma. Transients recorded in the dendrites, 200 μm from the soma, had a low signal-to noise ratio. Hence, it was impossible to measure them accurately with this technique. Analysis of 19 cells (Fig. 14C) shows that 10 μM 5-HT reduced the $[Ca^{2+}]_i$ changes in the soma on average by 27% ($p<0.0005$), similar to the level observed in whole-cell experiments (Fig. 13C).

Figure 14 Serotonin reduces spike-evoked $[Ca^{2+}]_i$ changes in the cell bodies of fura-2-AM-loaded pyramidal neurons.

A. Fluorescence image of a hippocampal slice loaded with fura-2-AM. The cell body and proximal dendritic region of one neuron are indicated. Scale 50 μm. The traces below the image show the fluorescence change in the two regions in response to a single stimulus to the alveus. No averaging was required. Note the fast recovery times of the transients. **B.** Effect of 5-HT on the amplitude of the action potential-evoked fluorescence changes. Each point represents the average of 5 trials of 10 antidromically-activated action potentials. The line is arbitrary smooth curve fit to the points. Selected traces are shown below the time points. **C.** Summary of results from 19 cells in 4 slices.

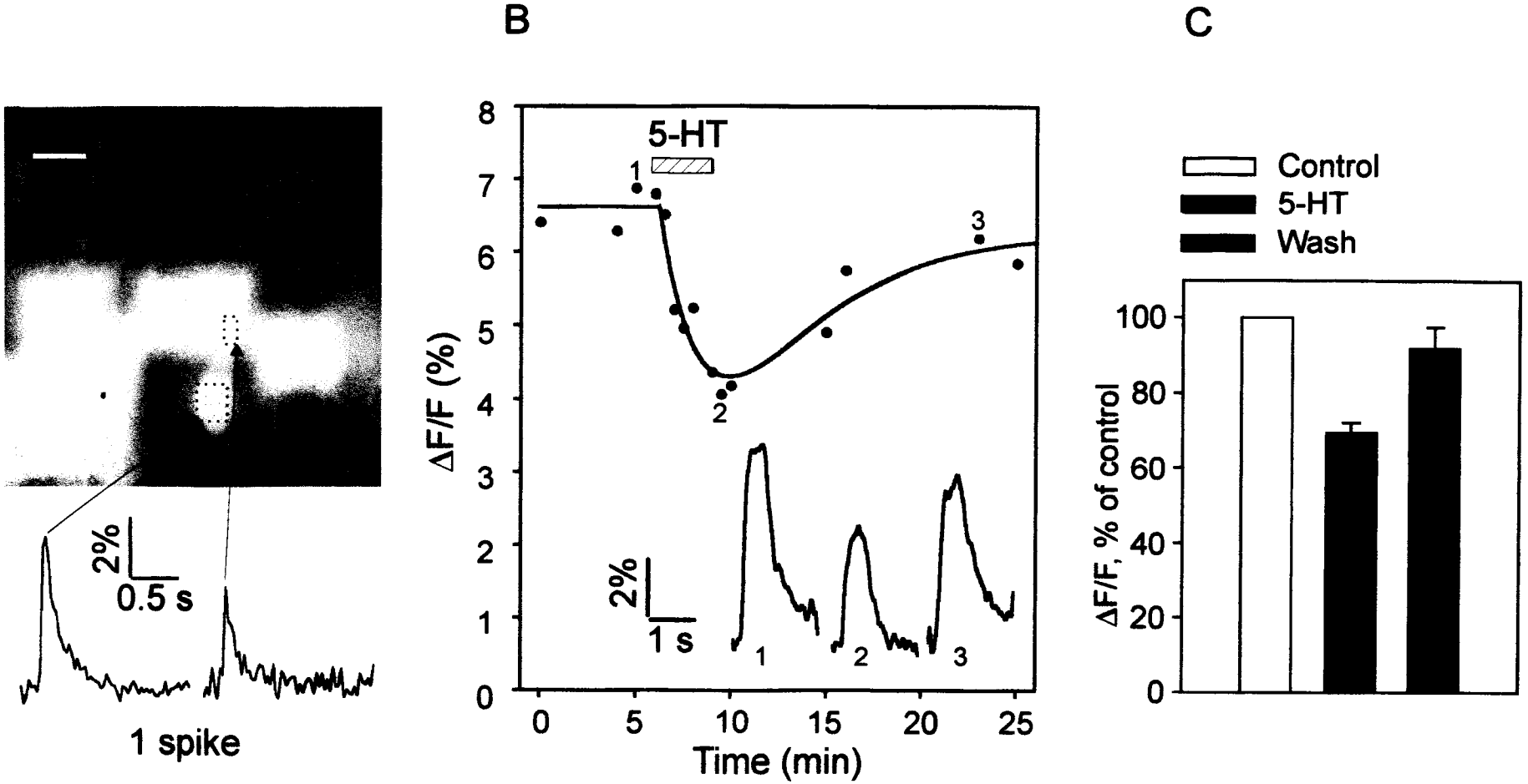
A
B
C
2%
0.5 s
1 spike
5-HT
1
2
3
ΔF/F (%)
2%
1 s
Time (min)
Control
5-HT
Wash
ΔF/F, % of control

Figure 14.

Effects of membrane hyperpolarization on the action potential evoked $[Ca^{2+}]_i$ changes in the soma and dendrites of CA1 pyramidal neurons recorded in the whole-cell mode.

Since 5-HT hyperpolarized the resting potential, it is possible that this hyperpolarization was responsible for the reduced $[Ca^{2+}]_i$ change, even though the peak spike potential was unchanged. To test this possibility, we hyperpolarized the soma with current and compared the $[Ca^{2+}]_i$ increase to that recorded without injected current. Figure 15 shows that the $[Ca^{2+}]_i$ increase was unchanged when the soma was hyperpolarized by 10 mV. In four measurements from the soma of this neuron the ratio of $\Delta F/F$ in hyperpolarized and normal conditions was 0.98 ± 0.06. Similar results were found in five other neurons (0.97 ± 0.2). In all experiments the difference between amplitude of Ca^{2+} transients measured in control and during hyperpolarization was not signifficant (ANOVA, $p>0.2$).

Figure 15 Membrane hyperpolarization, by itself, does not reduce spike evoked $[Ca^{2+}]_i$ increases.

A. Fluorescence increases in the soma and proximal dendrites evoked by 10 antidromic action potentials. The image shows the two selected regions and the recording electrode in the soma. Scale 50 μm. **B.** Fluorescence increases from the same regions when the soma was hyperpolarized by 10 mV with current through the recording electrode. The fluorescence changes are about the same as in A ($0.97\pm0.2\%$).

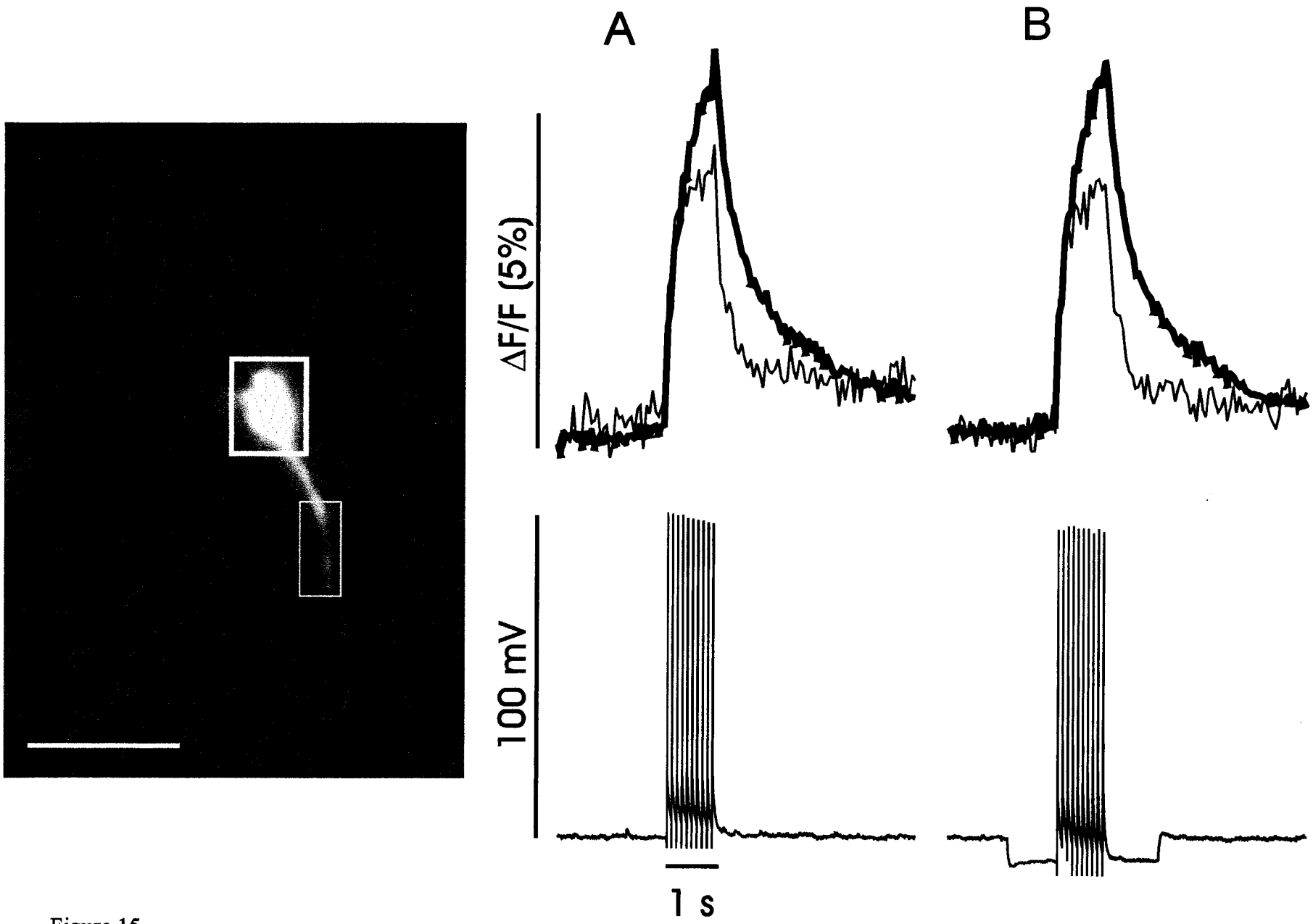

Figure 15.

Serotonin reduces synaptically activated backpropagating action potentials recorded in the apical dendrites of CA1 pyramidal neurons

In the experiments presented so far, the action potentials were evoked by intrasomatic depolarization or antidromic stimulation. To test whether 5-HT could affect dendritic spike amplitudes under more physiological protocols we synaptically stimulated the pyramidal cells while recording in the dendrites. For these experiments, APV and CNQX were not included in the bathing solution. When the stimulating electrode was in the stratum radiatum (SR) the peak spike potentials were not significantly reduced in 5-HT (data not shown). These unchanged spike amplitudes, even when the neuron was hyperpolarized, probably were due to the large EPSP producing the action potential at the recording site, counteracting the hyperpolarization caused by 5-HT. To avoid this problem we placed the stimulating electrode in the stratum oriens (SO), evoking EPSPs in the basal dendrites. EPSPs that were at threshold in the somatic region were electrotonically reduced to lower amplitudes at the recording site in the apical dendrites. Under these conditions, 5-HT (10 μM) reversibly reduced the peak potential of the dendritically recorded action potentials (Fig. 16, top). This reduction was greater for earlier spikes than for later ones in the train. This differential effect on earlier spikes is similar to the effect of direct hyperpolarization on distal dendrites (Fig. 12; see also Tsubokawa and Ross 1996). Thus, in some protocols 5-HT modulates synaptically activated backpropagating action potentials.

Figure 16 Serotonin reduces synaptically activated action potentials in the dendrites when stimulated in the stratum oriens.

Left. Response to 10 stimuli in the SO at 50 ms intervals in normal ACSF. Recording was performed at the distance of 250 μm from the soma. The first response was below threshold. Later responses facilitated and evoked spikes. The first two responses (time window indicated by solid line) are shown in the expanded trace below. ***Center***. Responses in 10 μM 5-HT. The membrane hyperpolarized and spike potentials were reduced. The expanded traces below (time window indicated by dotted line) show that the amplitudes measured from threshold (arrows) also were reduced. ***Right.*** Return to normal ACSF restored the control responses.

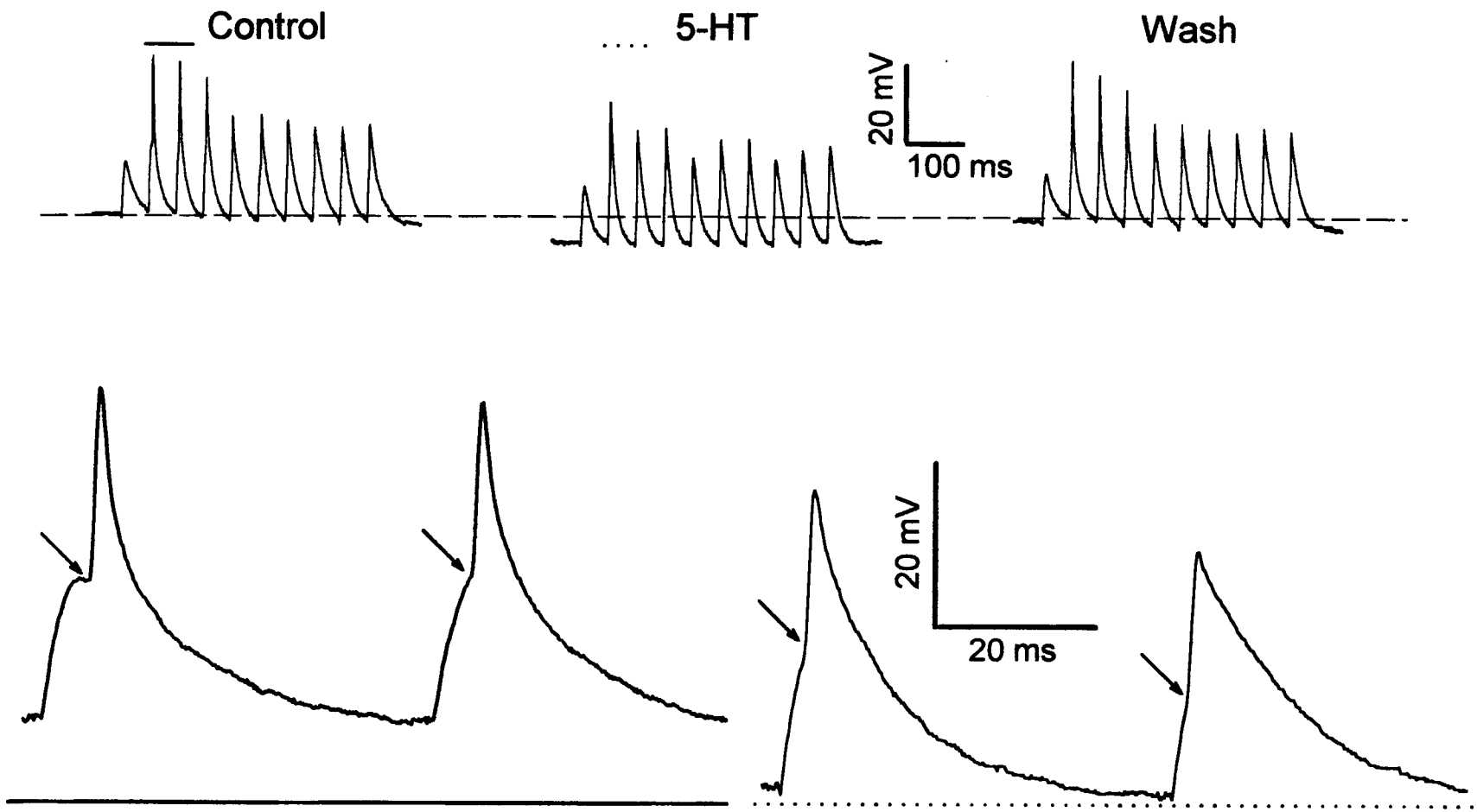

Figure 16.

Serotonin and action potentials synergistically release calcium from internal stores in dendrites of CA1 hippocampal pyramidal cells

Serotonin (10 μM), by itself, usually caused little change in resting $[Ca^{2+}]_i$. When a train of 10 antidromic action potentials was evoked, 5-HT produced two effects on the $[Ca^{2+}]_i$ changes. First, as described above, the Ca^{2+} transients were reduced at all locations. The other effect was a generation of a localized calcium wave in the proximal or middle dendrites which was not accompanied by a change in membrane potential and often lasted much longer than the train of action potentials. This effect was considered to be caused by release of Ca^{2+} from internal stores. It was not observable in all cells, but has been registered in 13 experiments (Fig. 17).

Figure 17 A train of action potentials and 5-HT synergistically release calcium from internal stores.

A. Fluorescent image of a neuron filled with *bis*-fura-2. **B.** A train of action potentials causes elevation of $[Ca^{2+}]_i$ in both soma and dendrites of the neuron. **C.** When 5-HT (10μM) is applied, a train of action potentials evokes a calcium wave in the dendrites which is not reflected in the electrical recordings made in the soma. Colors of the optical traces in B and C correspond to the colors of rectangles in A.

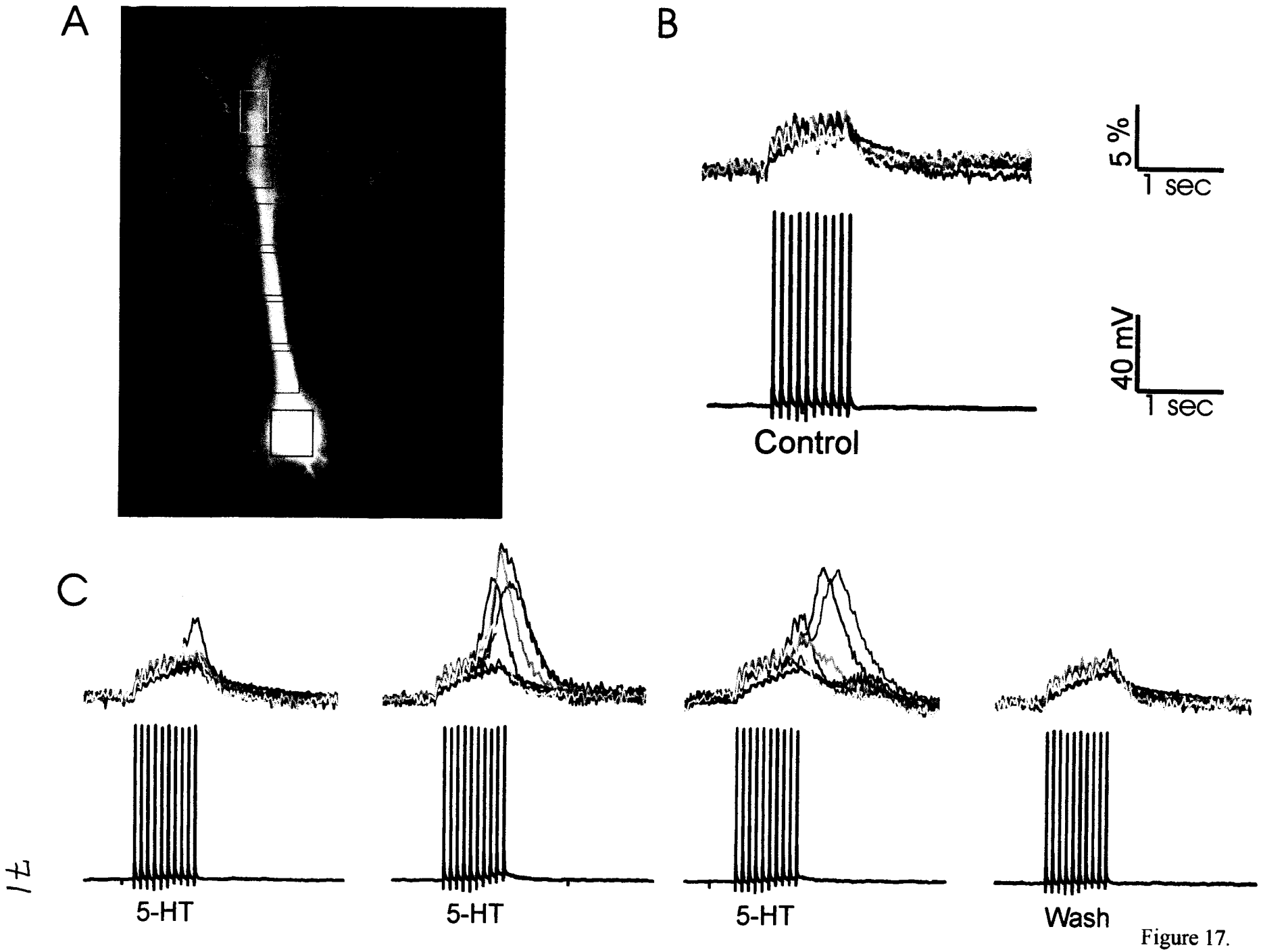

Figure 17.

The Ca^{2+} wave, assumed to represent release of Ca^{2+} from internal stores, was not directly linked to, but required the action potentials. No other electrical correlate of the release was noticed. The onset of release was rapid, usually before the end of the train. Its magnitude was much larger than the spike-evoked $[Ca^{2+}]_i$ increase in the absence of 5-HT (Fig. 18C). Most commonly, it was localized to the proximal and middle region of the apical dendrites. However, both dendritic and somatic release was recorded in one experiment. When evoked, the release was evident as a slow wave, propagating over a limited part of the apical arbor towards soma (Fig. 18). In the soma and distal dendrites the $[Ca^{2+}]_i$ increase retained the temporal profile of spike-evoked Ca^{2+} entry. Although the release signal was large and had some characteristics of a wave, the half recovery time of the event was rapid, usually similar to the duration of spike-evoked transients.

Figure 18 Propagation of a Ca^{2+} wave evoked by APs in the presence of 5-HT.

A. A series of "pseudocolor" images showing a distribution of $[Ca^{2+}]_i$ at selected periods of time. The time is shown underneath each image. Green and red numbers correspond to the time of the first and the last spike in the train of action potentials. **B.** Electrical recording form the soma and optical recordings from the selected regions along the dendritic tree of the neuron used in the experiment represented in A. Colors of the Ca^{2+} signals in B correspond to the colors of the rectangles in C. **C.** A fluorescent image of the cell filled with *bis*-fura-2 through a patch pipette.

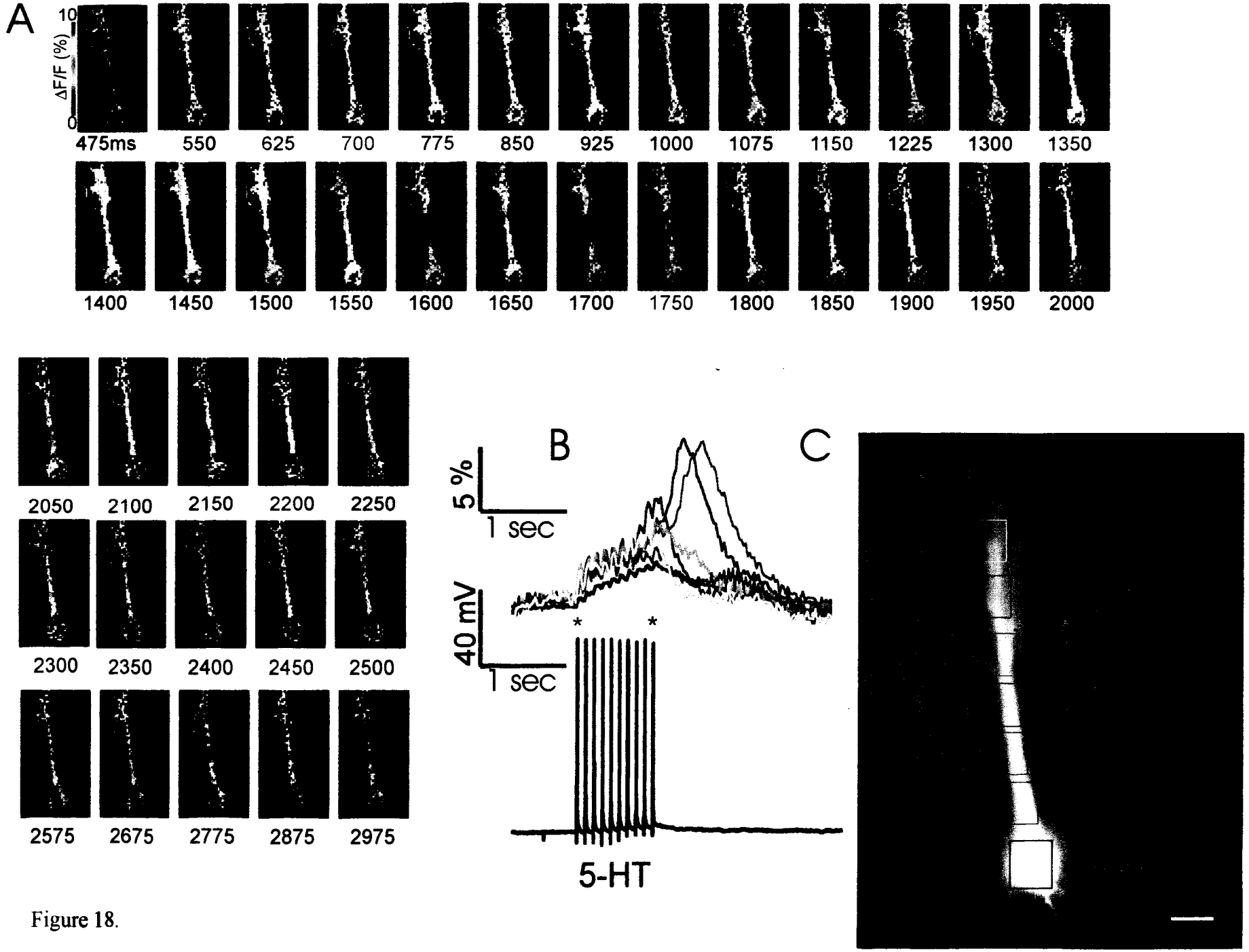
A
10
ΔF/F (%)
0
475ms
550
625
700
775
850
925
1000
1075
1150
1225
1300
1350
1400
1450
1500
1550
1600
1650
1700
1750
1800
1850
1900
1950
2000
2050
2100
2150
2200
2250
2300
2350
2400
2450
2500
2575
2675
2775
2875
2975
B
5 %
1 sec
40 mV
1 sec
5-HT
C

Figure 18.

A minimal number of action potentials is required for the Ca^{2+} release in the presence of 5-HT

When serotonin (10 μM) was applied, trains containing random numbers of antidromic action potentials were presented in a random order. The results of the experiment are shown in the Figure 17. A calcium wave, attributable to calcium release, was observed only when we evoked 5 or more action potentials (at 50 ms intervals). Progressively larger number of evoked action potentials induced progressively larger amplitudes of the calcium release wave. The greatest release signal was observed for 10 antidromic action potentials (Fig. 19). This implied that a minimal Ca^{2+} influx evoked by APs is necessary to trigger the described effect.

Figure 19 A minimal number of action potentials in a train is required to evoke calcium release in the presence of 5-HT.

A. A fluorescent image of the cell filled with *bis*-fura-2. **B.** Electrical recording from the soma and optical recordings from the selected regions along the dendritic tree of the neuron before 5-HT application. **C.** 5 or more spikes in a train of action potentials were required to trigger calcium release when 5-HT was bath applied. Colors of optical traces correspond to the colors of the rectangles in A.

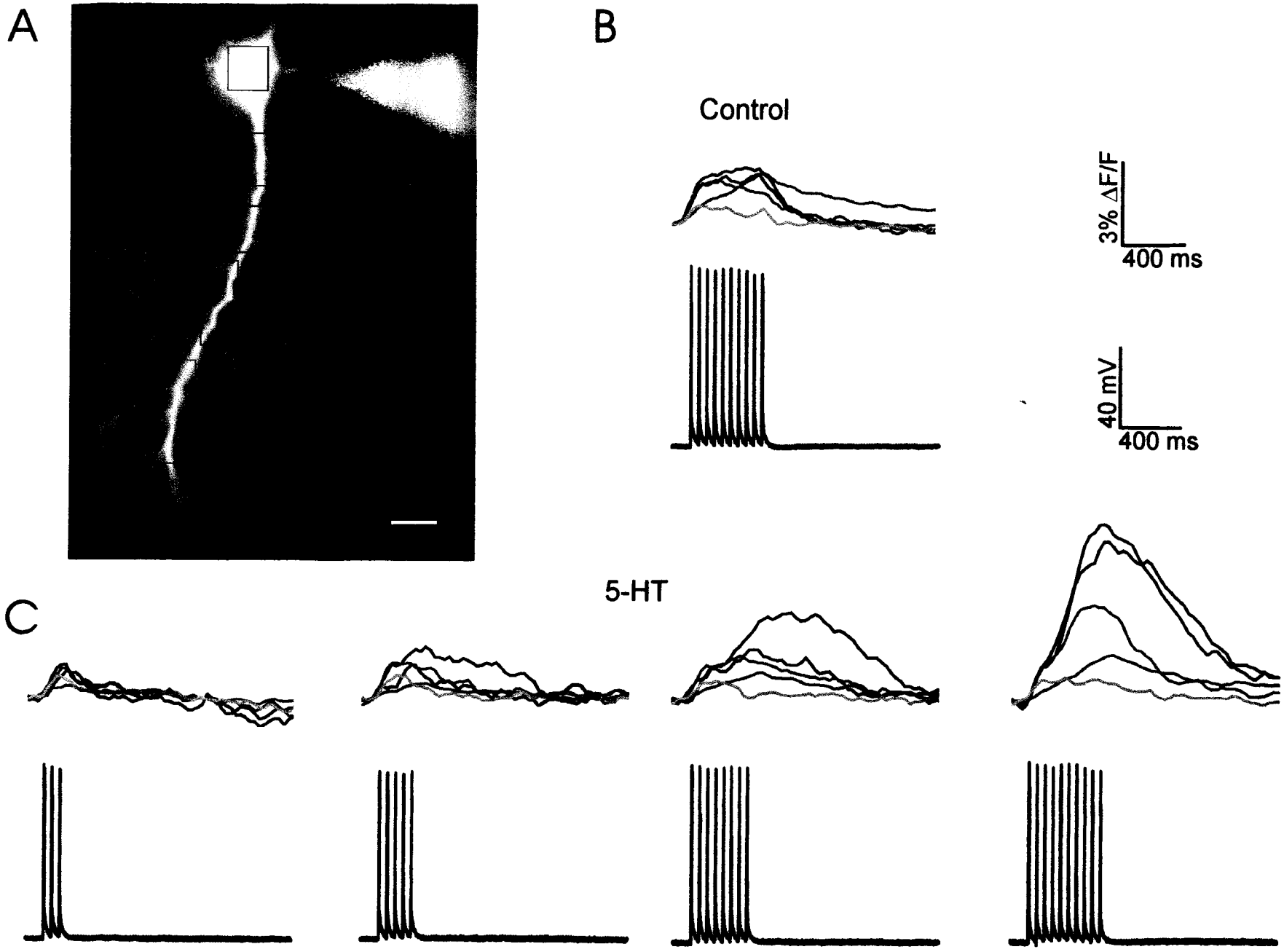

Figure 19.

Properties of Ca^{2+} transients induced by antidromic stimulation in fura-2-AM loaded hippocampal CA1 pyramidal neurons

Changes of intracellular Ca^{2+} concentration were recorded in CA1 pyramidal neurons from hippocampal slices following antidromic stimulation in the alveus. When the stimulus intensity was increased, Ca^{2+} transients occurred in an all-or-none fashion in individual somas (Fig. 20 and 21) and were entirely blocked by TTX (1 μM; Fig. 21D). On a single stimulus (1 pulse, 100-500 μA, 200 μs), the occurrence of a Ca^{2+} signal was correlated to the generation of action potentials in a neuron recorded in the whole-cell configuration (Fig. 25).

Figure 20 Recording of all-or-none Ca^{2+} transients in CA1 neurons triggered by a single antidromic pulse.

A. Changes of $[Ca^{2+}]_i$ during a single pulse of increasing intensity. Upper panels: ΔF/F pseudocolor images calculated for the moment of stimulation showing a clear spot of high ΔF/F corresponding to a single CA1 neuron. Lower traces: each trace corresponds to the spatial average of ΔF/F over a 5x5 pixels area positioned over the stimulated neuron. **B.** Plot of maximal spatial averages of ΔF/F against the stimulus intensity. **C.** Bright field DIC image of the stimulated neuron. **D.** Fluorescence image of the same neuron excited at 380 nm. Scale bar is 20 μm in C and D.

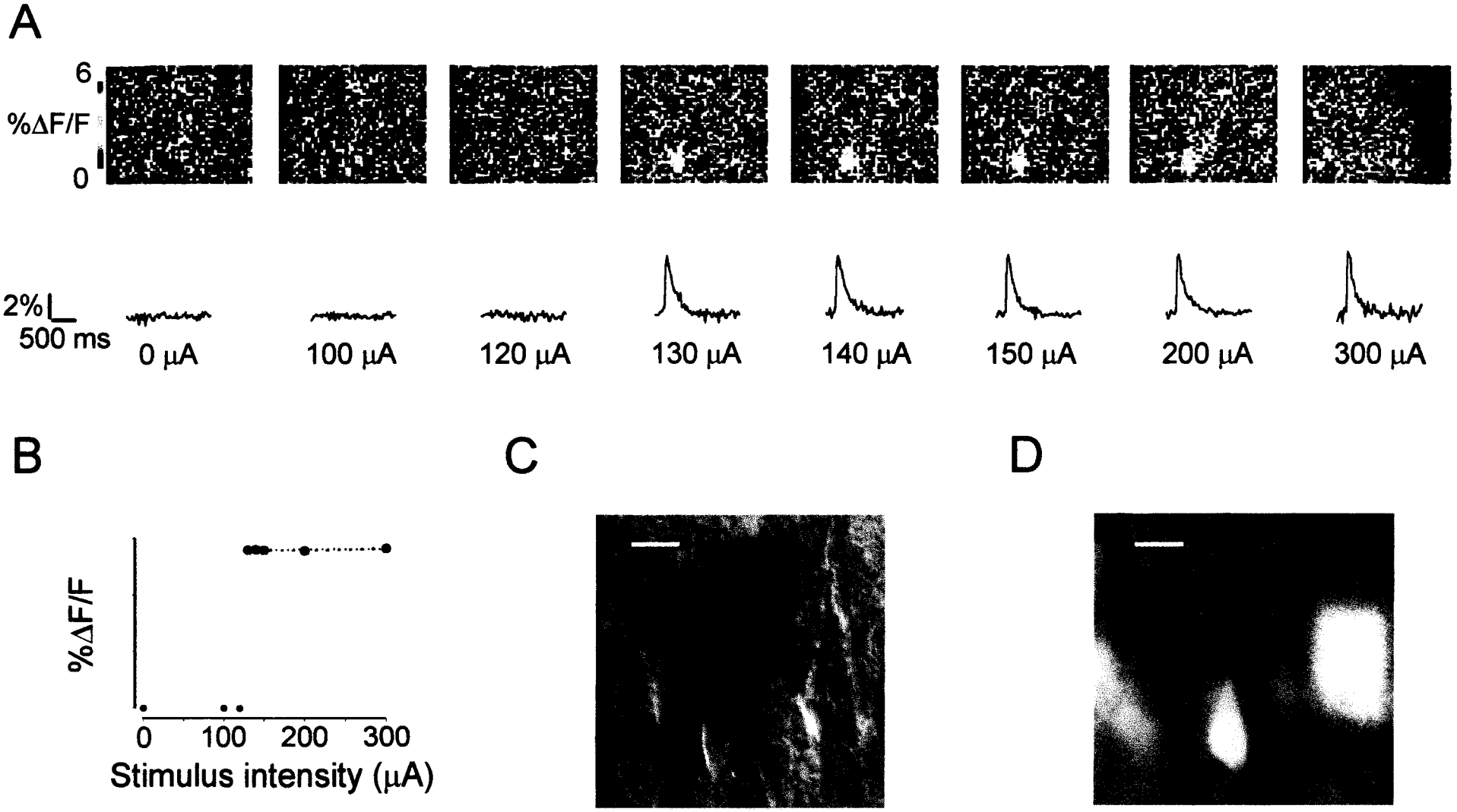
A
6
%ΔF/F
0
2%
500 ms
0 μA
100 μA
120 μA
130 μA
140 μA
150 μA
200 μA
300 μA
B
%ΔF/F
0
100
200
300
Stimulus intensity (μA)
C
D

Figure 20.

This indicates that Ca^{2+} transients were triggered by antidromically evoked action potentials. Ca^{2+} transient amplitudes, given in $\Delta F/F$ with no background correction, were on an average of 1.85 ± 0.14% (n=29 cells) for a single spike, with decay time constants of 273.2 ± 32.1 ms (n=17 cells). These fast kinetics suggests that the fura-2 concentration inside neurons was below 50 μM according to calculations of Helmchen et al. (1996). Thus, dye-buffering probably was low in our Ca^{2+} recordings.

It has been suggested previously that ryanodine-insensitive internal Ca^{2+} stores may amplify by >30 fold, Ca^{2+} transients evoked by field stimulation in cultured hippocampal neurons (Jacobs and Meyer 1997). This finding relied on the lack of a dependence of the Ca^{2+} transient amplitude on external Ca^{2+} concentration ($[Ca^{2+}]_o$) between 0.05 and 2 mM, as well as on the slow rise-time (10-15 ms) of Ca^{2+} transients. By using the low-affinity indicator furaptra, however, Ross et al. (1998) have shown that Ca^{2+} transients can rise in ≈ 1 ms when evoked by a single action potential in CA1 neurons. Furthermore, we now show that Ca^{2+} transient amplitude depended on extracellular $[Ca^{2+}]_o$ within the same $[Ca^{2+}]_o$ range.

When $[Ca^{2+}]_o$ was reduced from 2 mM to 1 mM and 100 μM, amplitudes of Ca^{2+} transients were 88.2±2.5 % (n=9 cells) and 36.3±3.0 % of control signals respectively (n=14 cells, Fig 21. *E,F*). Although different from previously published data in hippocampal cultured neurons (Jacobs and Meyer 1997), these results do not eliminate the possibility of CICR contribution to the $[Ca^{2+}]_i$ change evoked by an action potential. Therefore, we further examined the participation of Ca^{2+} stores in action potential-evoked Ca^{2+} signals in CA1 neurons from hippocampal slices.

Figure 21 Properties of Ca^{2+} transients simultaneously recorded in several CA1 pyramidal neurons.

A. ΔF/F pseudocolour image of maximal response to 5 antidromic stimulating pulses. Note that at least 6 neurons are stimulated. **B.** Corresponding fluorescence image (380 nm) showing that high ΔF/F regions correspond to the fura-2_AM loaded neurons in the CA1 pyramidal cell layer. The alveus is upward in the micrograph. **C.** Ca^{2+} transients corresponding to the neurons numbered in B are shown. The light blue trace was sampled from region 5 to illustrate a background signal; there was no visibly loaded neuron in the region. Inset: example of a Ca^{2+} transient abolished by TTX application (1 μM). **D.** Dependence of Ca^{2+} transients evoked by 5 action potentials on external $[Ca^{2+}]$ (5-20 cells for each concentration). Inset: Log plot of the same data. $[Ca^{2+}]_o$ was changed randomly from the normal ($[Ca^{2+}]_o$=2 mM) to the lowered values and then back to the normal one. **E.** Ca^{2+} transients in response to 5 antidromic action potentials in the control ACSF and ACSF with $[Ca^{2+}]_o$= 0.1 mM. Taller red trace is control, taller blue trace is return to normal ACSF. Two smaller traces are repeats at $[Ca^{2+}]_o$= 0.1 mM. Traces correspond to the points in the graph shown in F. **F.** Dependence of Ca^{2+} transients evoked by 5 action potentials on external $[Ca^{2+}]_o$ in a representative experiment. In contrast to the data shown in D, $[Ca^{2+}]_o$ was changed sequentially from normal to low (red) and from low to normal (blue). Arrows show the direction of $[Ca^{2+}]_o$ change. In all experiments samples were taken ≥5 min. after the change of solutions.

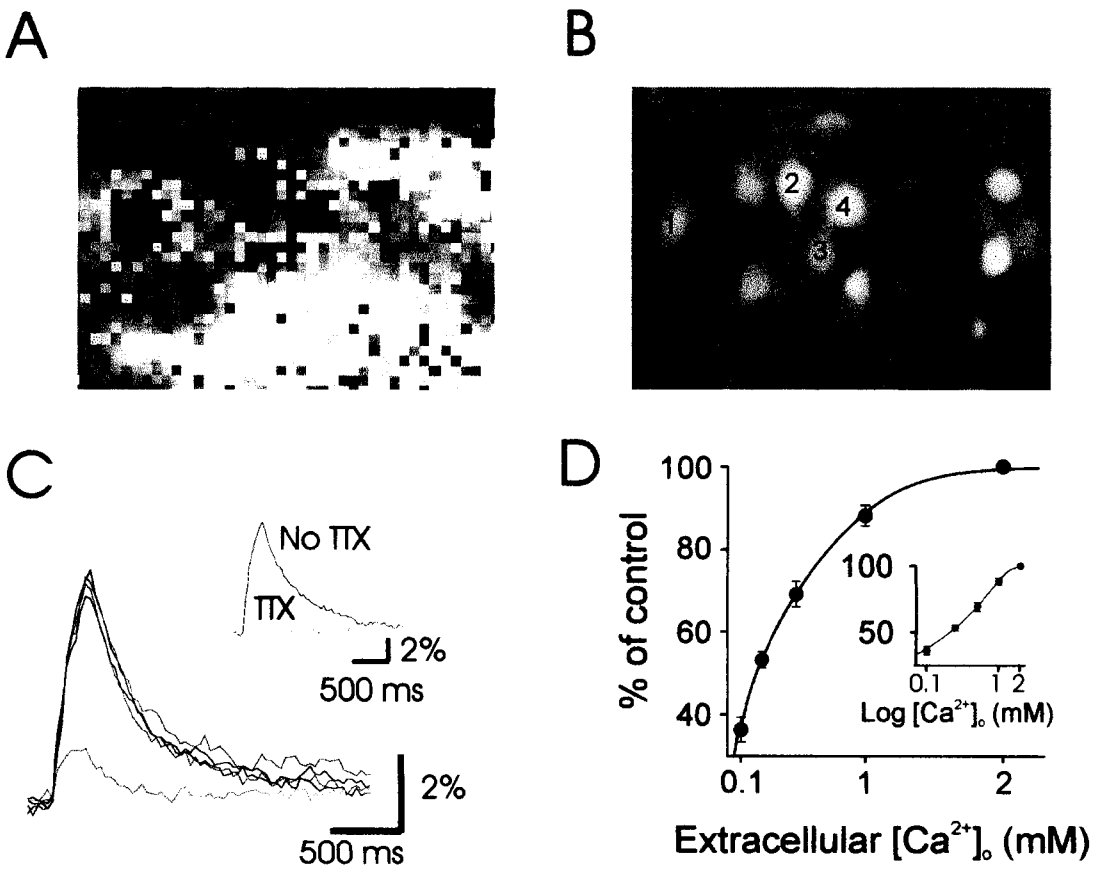
A
B
2
4
3
C
No TTX
TTX
2%
500 ms
2%
500 ms
D
100
80
60
40
% of control
100
50
0.1
1 2
Log [Ca2+]o (mM)
0.1
1
2
Extracellular [Ca2+]o (mM)
E
1 %
500 ms
F
3
2
1
ΔF/F (%)
0.1
0.25
0.5
1
2
Extracellular [Ca2+]o (mM)

Figure 21.

Pressure-applied caffeine induces increase in $[Ca^{2+}]_i$ in soma and dendrites of CA1 pyramidal neurons

The experiments were conducted in hippocampal slices with CA1 pyramidal neurons loaded with fura-2-AM. Pressure-applied caffeine (200-1000 ms pulse of 10 mM caffeine dissolved in ACSF) evoked a transient increase of $[Ca^{2+}]_i$ in the region of the neuron immediately adjacent to the application pipette, as well as in some cells positioned in close vicinity of the pipette (n=9; Fig. 22). Calcium transients were observed in both soma (Fig. 22B) and dendrites (wherever dendrites were available for observations; n=4). TTX (1 μM) was bath applied in order to exclude action potential generation. The origin of these transients was studied by Garaschuk et al. (1997).

Figure 22 Pressure-applied caffeine induces a transient increase in $[Ca^{2+}]_i$ in hippocampal CA1 pyramidal neurons.

A. Fluorescent image of a part of a hippocampal slice with fura-2-AM loaded neurons. The experimental arrangement is shown on the right. An application pipette, containing 10mM caffeine dissolved in ACSF, was brought into close proximity of the loaded neuron. It was directed either to the soma or to the dendrite of the cell. In addition to the standard cocktail of neurotransmission blockers described in methods, TTX (1μM) was bath applied. **B.** A 1-second application of caffeine evoked a $[Ca^{2+}]_i$ increase in the soma. The colors of selected optical traces, shown in the center, correspond to the colors of rectangles in the fluorescent image on the left. A pseudo-color image shows maxima of $[Ca^{2+}]_i$ (ΔF/F %) change in response to caffeine application.

C. Same as in B but for the dendritic caffeine application.

Figure 22.

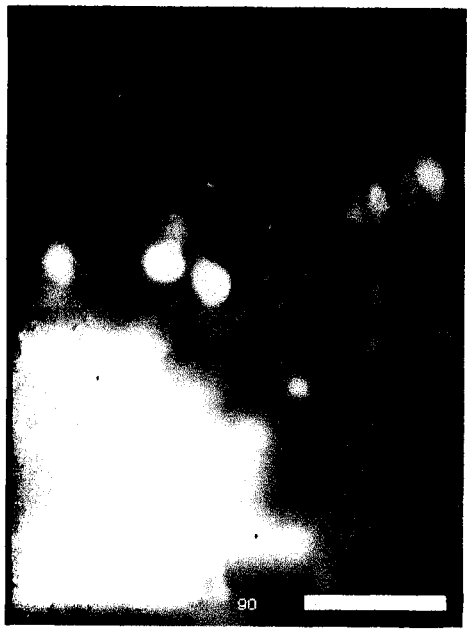

A

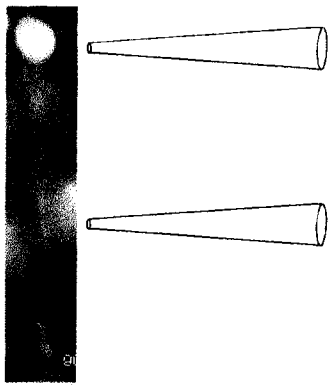

Caffeine 10 mM puff
TTX 1 μM

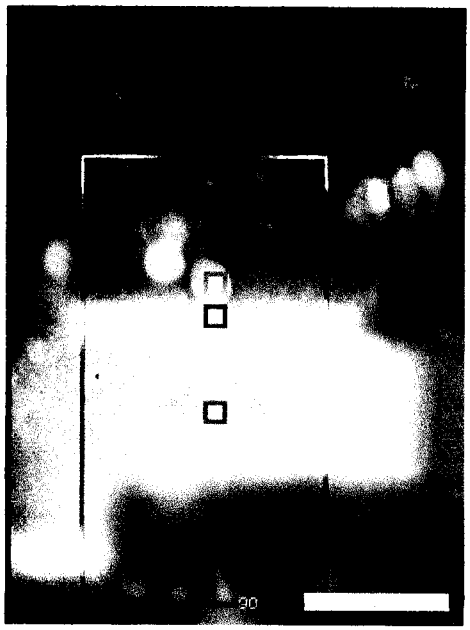

B

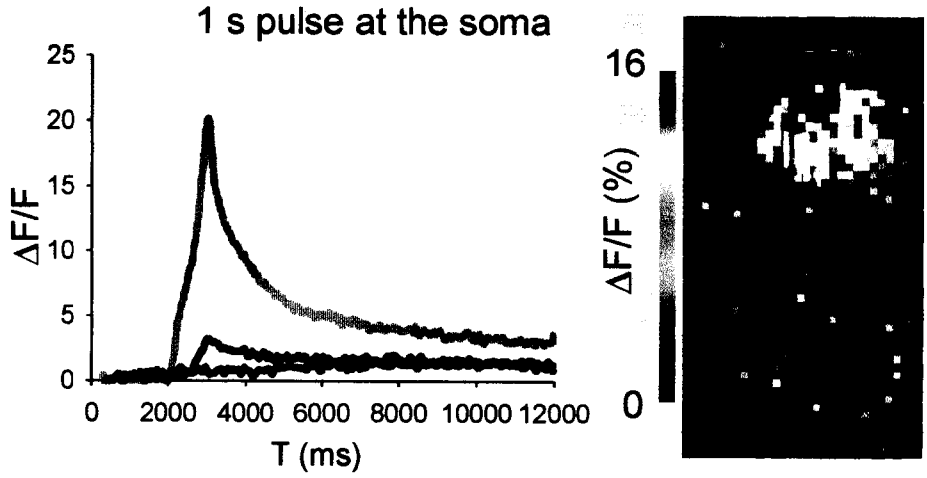

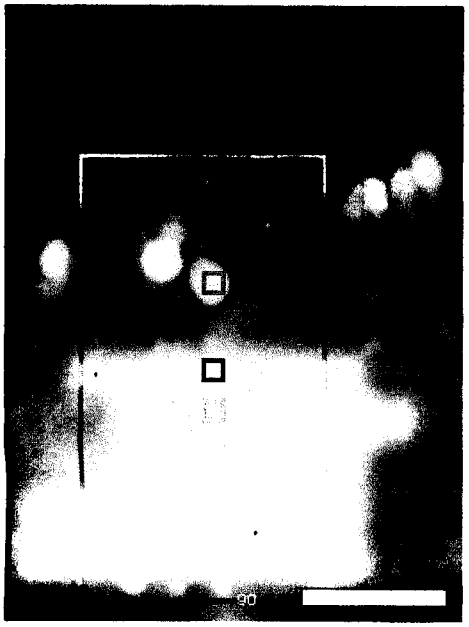

C

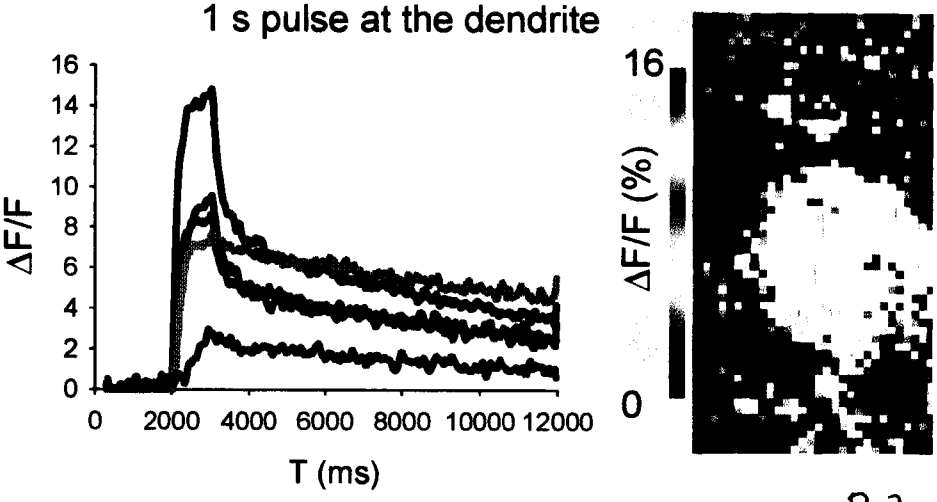

These authors suggested that they are calcium release from endoplasmic reticulum through RyR channels. These experiments suggest that, indeed, calcium stores in CA1 pyramidal neurons are loaded with calcium at rest.

Caffeine induces either a transient increase or decrease of action potential-evoked Ca^{2+} signals

To examine whether Ca^{2+}-induced Ca^{2+}-release (CICR) contributed to Ca^{2+} signals evoked by action potentials, the xanthine derivative caffeine was used. Caffeine readily crosses plasma membranes and accumulates inside cells (Toescu et al. 1992) where it binds to RyRs. If CICR occurs when a neuron generates an action potential, caffeine can either increase a Ca^{2+} transient by sensitizing RyR channels (Sitsapesan and Williams 1990) or decrease it by partial depletion of internal Ca^{2+} stores (Usachev et al. 1993; Shmigol et al. 1996).

In a first series of experiments, caffeine (5 mM) induced a small and reversible potentiation of Ca^{2+} signals evoked by action potentials (Fig. 23). When caffeine was bath applied for 5 min, a potentiation to 115.4±4.9%, 122.5±4.8% and 116.2±4.9% was observed within 1-3 minutes for 1, 5 and 10 spikes respectively (Fig 23). Neurons which did not show the potentiation with caffeine were included in the statistics. The potentiation reached up to 178 % and was observed in 90% of neurons (see histogram, Fig. 23E, n=103 cells, $p<0.001$). Ca^{2+} transients returned to control values after 10 min of wash. The effect of caffeine was associated with neither a change in basal F recorded in the soma nor a change in background fluorescence (Fig. 23D).

Figure 23 Caffeine increases Ca^{2+} transient amplitude evoked by 1-10 antidromic stimulations. Experiments are conducted in Fura-AM loaded slices.

A. Ca^{2+} transients evoked by a single action potential were potentiated by application of caffeine (5 mM) for 5 min (left traces). Averages are illustrated in the right panel. **B.** Same as in A, except that 5 action potentials were evoked. **C.** Same as in A, except that 10 action potentials were evoked. Averages shown in A, B, and C are from (10-16 cells and at least three different slices). **D.** Time course of caffeine action is shown. Traces were recorded at 5 min intervals. Basal F values with no stimulation are plotted bellow each trace. Basal F at the location of the cell (○) and background F (❑, see Methods) are plotted with their difference (●) to indicate background fluorescence contribution. **E.** Histogram of the changes of Ca^{2+} transient amplitudes caused by caffeine application is shown. Inset: control histogram of the changes between two consecutive control Ca^{2+} transients recorded at a 5min interval. The bold-curve in the histogram of caffeine action represents a gaussian fit of the control histogram. Experiments were conducted in fura-2-AM loaded slices.

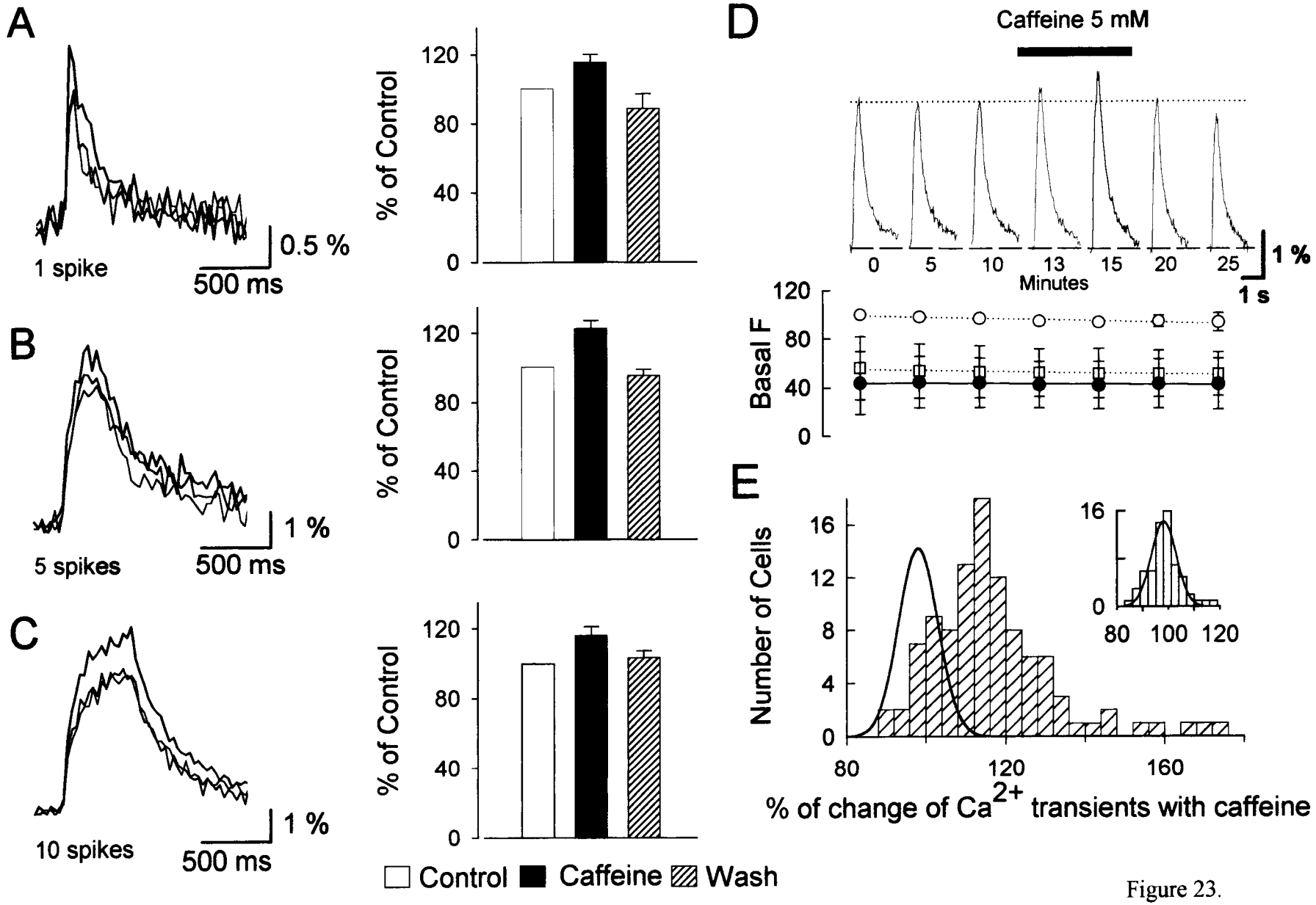
A
1 spike
0.5 %
500 ms
B
5 spikes
1 %
500 ms
C
10 spikes
1 %
500 ms
% of Control
120
80
40
0
Control
Caffeine
Wash
D
Caffeine 5 mM
0
5
10
13
15
20
25
Minutes
1 %
1 s
Basal F
E
Number of Cells
16
12
8
4
0
80
120
160
% of change of Ca2+ transients with caffeine

Figure 23.

The results of previous experiments implied that a low concentration of caffeine would facilitate CICR in pyramidal cells. A higher concentration of caffeine should lead to a reduction of the amplitudes of the Ca^{2+} signals since the degree of caffeine-induced store depletion is dependent on caffeine concentration (Usachev et al. 1993). To check this, 20 mM of caffeine was applied. Control Ca^{2+} signals were recorded in ACSF containing 20 mM of sucrose to mimic the change in osmolarity when 20 mM of caffeine was added to the test solution. Application of caffeine (20 mM) for 5 min caused a reduction of the amplitudes of the Ca^{2+} signal to 91.1±6.1% (n=21 cells, $p<0.005$, not shown). We observed a partial recovery. This result is consistent with an expected reduction of Ca^{2+} signals by caffeine depleting Ry-sensitive internal Ca^{2+} stores; it indicates a contribution of CICR to spike-evoked Ca^{2+} transients in CA1 neurons.

Caffeine-induced potentiation of action potential evoked calcium transients is independent of action potential properties

Simultaneous whole-cell recordings and Ca^{2+} imaging were performed to determine whether caffeine changed the action potential properties in pyramidal neurons. CA1 pyramidal neurons were filled with *bis*-fura-2 (200 μM) through a patch-pipette. A single antidromic pulse (200 μs, < 500 μA) evoked an action potential and associated Ca^{2+} transients of 2.0±0.3% (ΔF) in the soma and 3.5±0.7% (ΔF) in the dendrites (n=5 neurons). Caffeine application lead to a potentiation of these Ca^{2+} signals, with no significant change in action potential amplitude (non-significant difference, p=0.79, n=5 neurons) or width (non-significant difference, p=0.39, n=5 cells; Fig. 24). Action potential

amplitudes were 101.5±6.4 mV and 99.1±6.3 mV before and during caffeine application respectively (n=5 neurons). The effect of caffeine (increase of Ca^{2+} transient amplitude) was 116.4±5.7% (n=5 cells) in the soma and 113.8±1.6% (n=5 cells) in the dendrites. The caffeine effect was not associated with a change in basal F in these experiments. We conclude that caffeine potentiates Ca^{2+} transients without modification of the amplitude or shape of the action potential.

Figure 24 Caffeine-induced increase of Ca^{2+} transients did not depend on a change of action potential properties of a neuron recorded with whole-cell patch-clamp.

A. Caffeine (5 mM) applied for 3 min potentiated Ca^{2+} transients both in the soma and in the proximal dendrite of a CA1 neuron recorded in current clamp mode. **B.** Action potentials before, during, and after caffeine application are superimposed and at two different time resolutions. No significant change of action potential waveform was observed during the caffeine application.

Figure 25 The time course of the caffeine effect in a neuron recorded in the whole-cell configuration.

A. Three controls are shown, separated by 5 min intervals. Fourth traces were recorded at ~3 min of caffeine application. Basal F values with no stimulation are plotted correspondingly to each trace. Basal F values in the soma (●) and dendrites (○) are shown in the third panel from the top. Action potential amplitude (mV) (●) and width (ms; ○) are shown in the bottom panel. **B.** Averaged data from 5 neurons recorded in whole-cell mode. Max ΔF/F of Ca^{2+} transients is increased in the presence of caffeine (red; upper panel). Basal fluorescence excited at 380 nm (F) slightly increases in the soma (left group of bars) and dendrites (right group of bars) but does not decrease after caffeine removal (middle panel). Spike amplitude and spike width were unaffected by application of caffeine (lower panel).

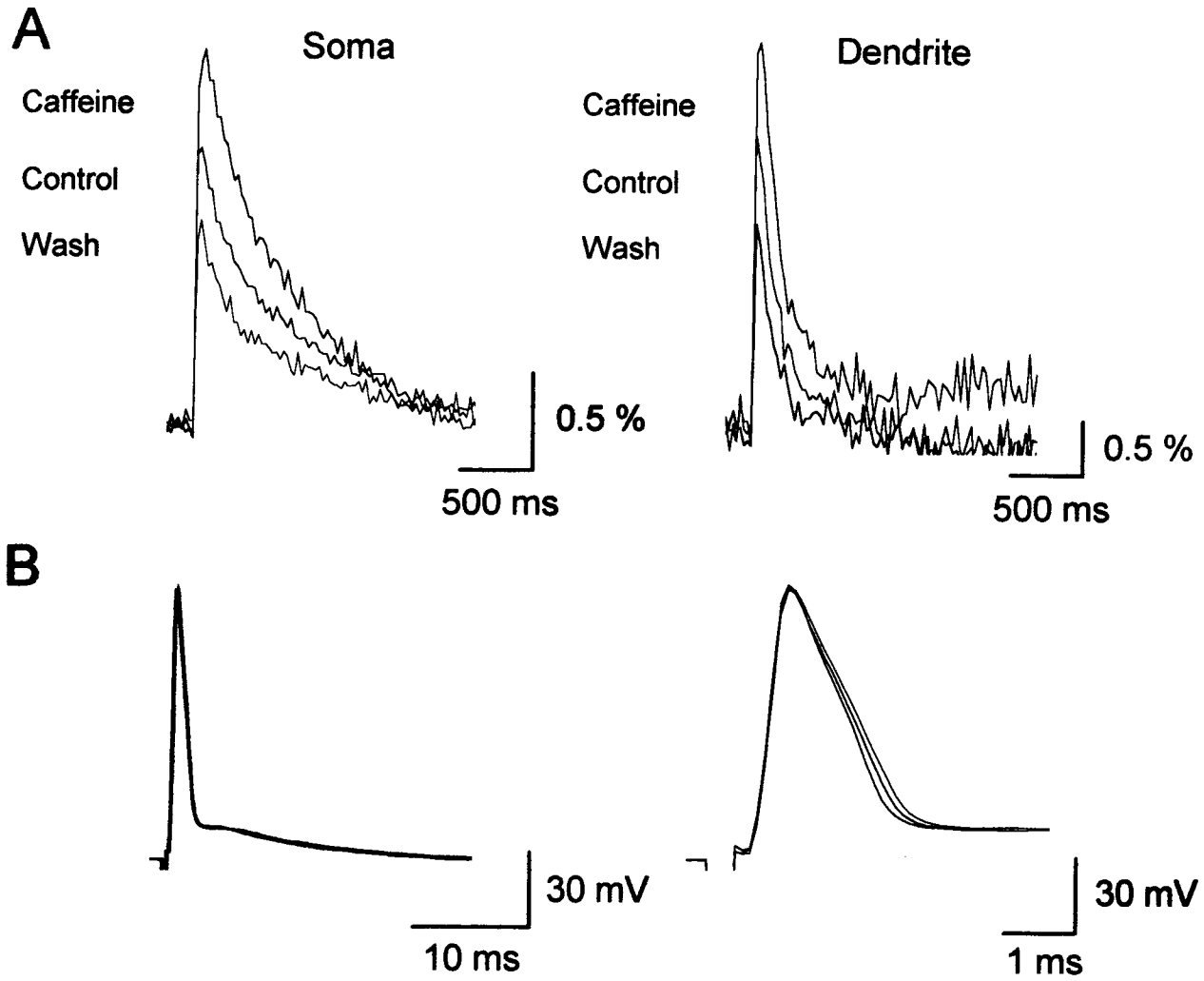
A
Soma
Caffeine
Control
Wash
0.5 %
500 ms
Dendrite
Caffeine
Control
Wash
0.5 %
500 ms
B
30 mV
10 ms
30 mV
1 ms

Figure 24

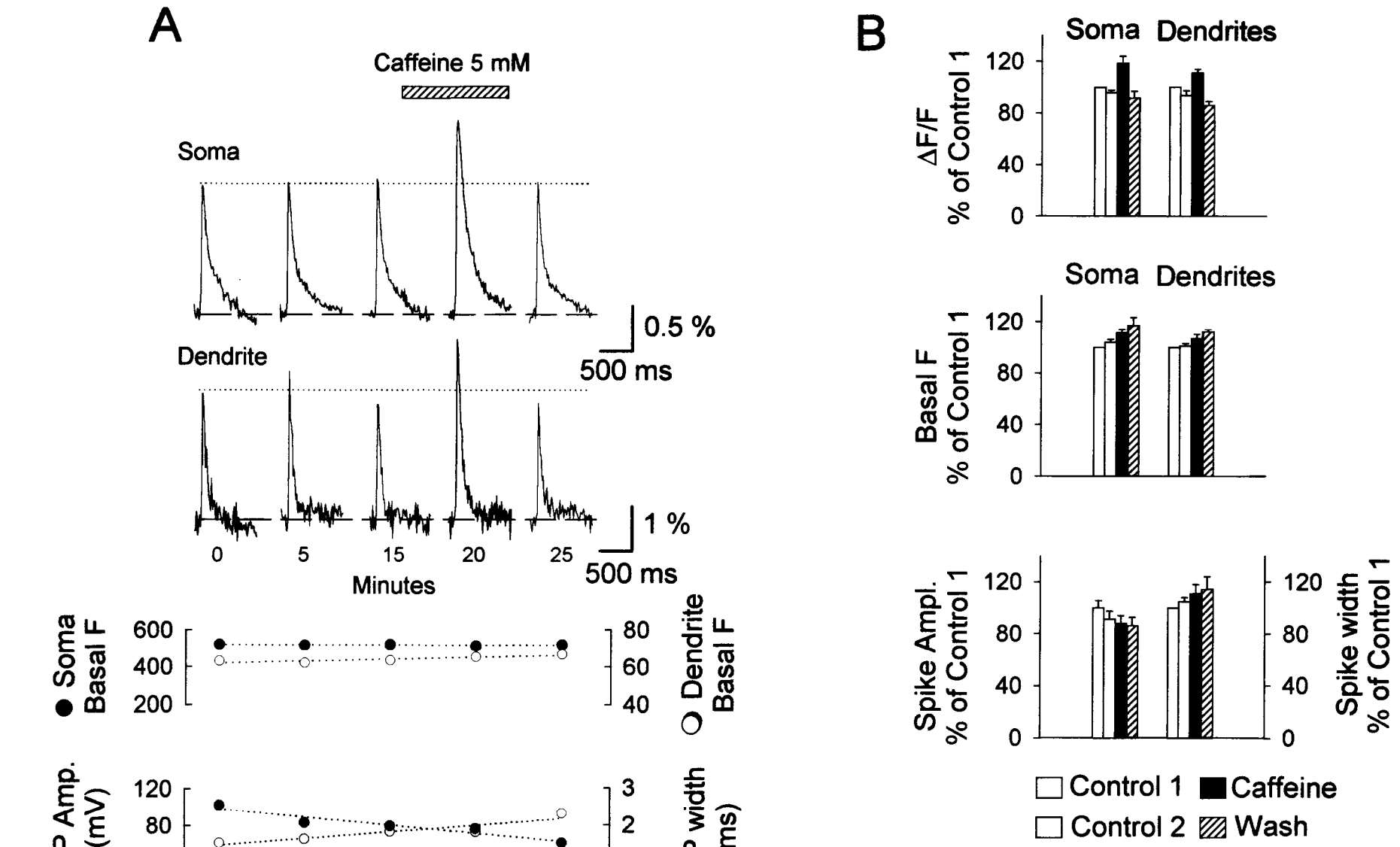
A
Caffeine 5 mM
Soma
0.5 %
500 ms
Dendrite
1 %
500 ms
0
5
15
20
25
Minutes
● Soma Basal F
600
400
200
○ Dendrite Basal F
80
60
40
● AP Amp. (mV)
120
80
40
○ AP width (ms)
3
2
1
B
Soma Dendrites
ΔF/F % of Control 1
120
80
40
0
Soma Dendrites
Basal F % of Control 1
120
80
40
0
Spike Ampl. % of Control 1
120
80
40
0
Spike width % of Control 1
120
80
40
0
Control 1
Caffeine
Control 2
Wash

Figure 25.

The caffeine effect is not mediated by protein phosphorylation

Caffeine is a known antagonist of phosphodiesterases (PDEs, Butcher, 1962) and can trigger protein phosphorylation by increasing cAMP and/or cGMP levels (Beavo and Reifsnyder 1990). Thus, a caffeine-induced potentiation of Ca^{2+} signals could be due to an increased Ca^{2+} influx mediated by a phosphorylation of Ca^{2+} voltage-dependent channels as recently reported for CA1 neurons (Kavalali et al. 1997) (Fig. 26A).

To exclude this possibility we used 1-methyl-3-isobutylxanthine (IBMX), a non-specific PDEs inhibitor related to, but ≈100 times more potent than caffeine (Wells et al. 1975; Fig 27A). When IBMX (100 μM) was bath applied for 5 min, a transient potentiation of Ca^{2+} signals was observed (Fig. 27A, 112.2±5.6%, n=19 neurons; p=0.01). In the presence of IBMX, Ca^{2+} signals returned below control values within 15 min (Fig. 27A, 86.7±4.6%, n=19 cells). After at least 10 min of IBMX bath application, caffeine then was co-applied.

Figure 26 Schematic representation of several possible pathways that can lead to phosphorylation of voltage-dependent calcium channels and experimental strategies used to rule out their contribution.

A. Caffeine blocks phosphodiesterases (PDEs, red arrows) which ultimately leads to enhanced phosphorylation of voltage-dependent calcium channels (VCC) (green arrow). Protein kinases A and G (PKA, PKG) can be implicated in phosphorylation of VCCs (green arrows). **B.** Forskolin activates adenylyl cyclase (green arrow) leading to an increase of cAMP and PKA production. H-89 blocks both PKA and PKG. IBMX blocks PDEs. This prevents cAMP, cGMP degradation and ultimately leads to increase of PKA and PKG concentrations.

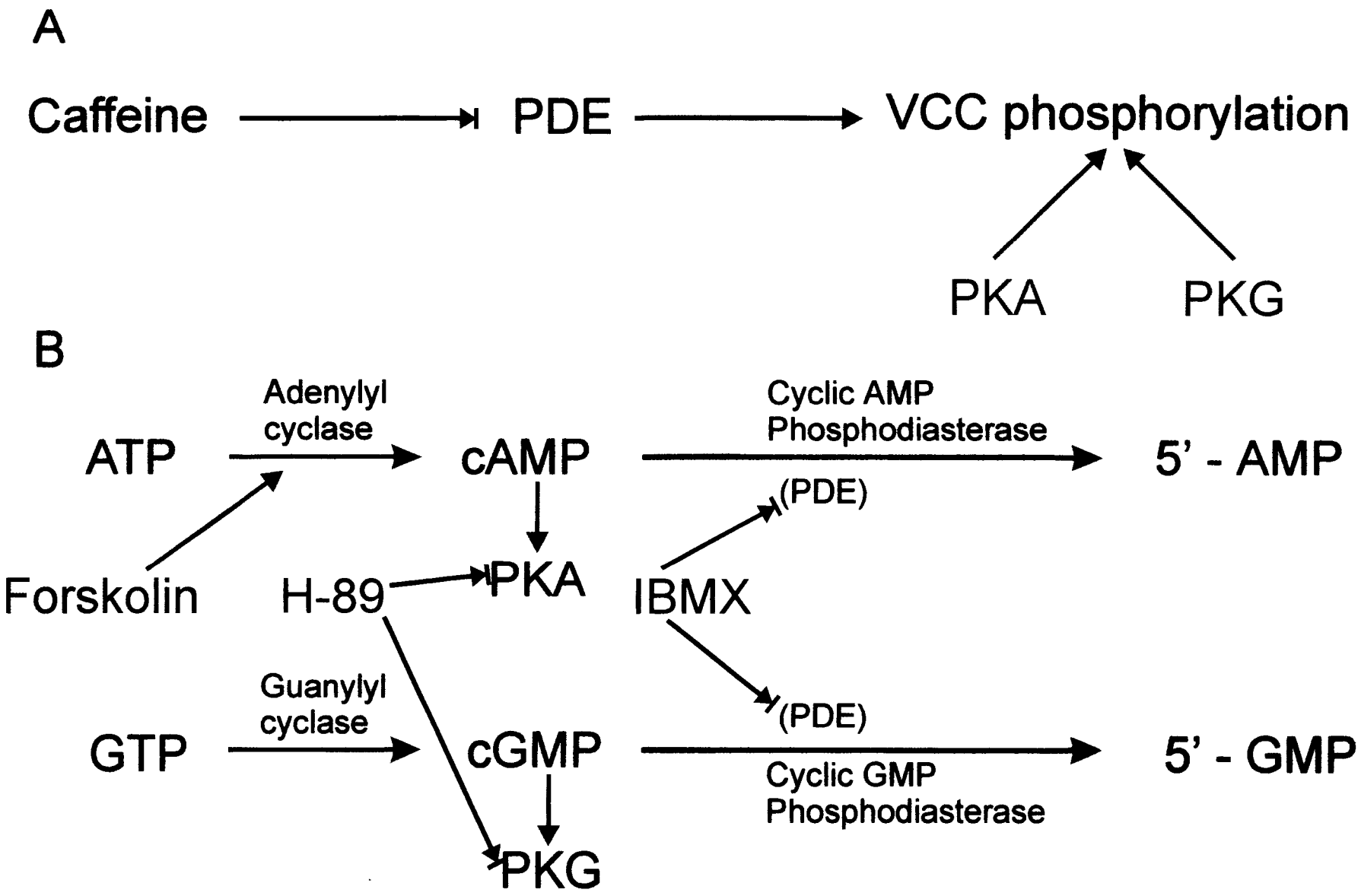
A
Caffeine
PDE
VCC phosphorylation
PKA
PKG
B
ATP
Adenylyl cyclase
cAMP
Cyclic AMP Phosphodiasterase
5' - AMP
(PDE)
Forskolin
H-89
PKA
IBMX
Guanylyl cyclase
GTP
cGMP
(PDE)
5' - GMP
Cyclic GMP Phosphodiasterase
PKG

Figure 26.

This protocol did not prevent the potentiation of Ca^{2+} signals by caffeine which was 110.5±2.5% for 5 action potentials (Fig. 27A and D, $p<0.001$, n=19 cells).

This result suggests that caffeine action is not mediated by an increase in cyclic nucleotides.

Caffeine-induced increase of Ca^{2+} transients is not mediated by a rise in cyclic nucleotides.

Using forskolin, an activator of adenylyl cyclase in the brain (Seamon, Vaillancourt et al. 1985), we examined the contribution of cAMP to the potentiation of Ca^{2+} signals. When a saturating dose of forskolin (5 μM) was bath applied for 10 min, no increase of Ca^{2+} signals was detected after either 5 or 10 min of incubation (100.7±3.1%, n=16 cells). This finding strongly supports that an increase of cAMP cannot account for a potentiation of action potential evoked Ca^{2+} signals recorded in our conditions.

Figure 27 Caffeine increase of Ca^{2+} transients is not mediated by a rise in cyclic nucleotides.

A. IBMX (100 μM) has little effect on Ca^{2+} transients (traces 2 and 3) and does not occlude caffeine action (traces 4 and 5). Traces are separated by 5 min unless otherwise indicated. Traces 4 and 5 were recorded after 1 and 3 min of caffeine application respectively for A, B and C. Trace 3 has been recorded after 20 min in IBMX. **B.** Same as in *A* except Forskolin (5 μM) was applied. **C.** Same as in *A* except H-89 was used. Two controls are shown separated by 5 min in A, B and C. Dashed blue bars indicate the time of application of IBMX, forskolin or H-89. Red bars indicate the 5 min caffeine application. **D.** Average data of caffeine action in the presence of Forskolin, IBMX or H-89 are shown. Data for every drug were obtained from 14-19 cells and at least three different slices. Application of Forskolin, IBMX or H-89 did not cause change of basal fluorescence (F). Experiments were conducted in fura-2-AM loaded slices.

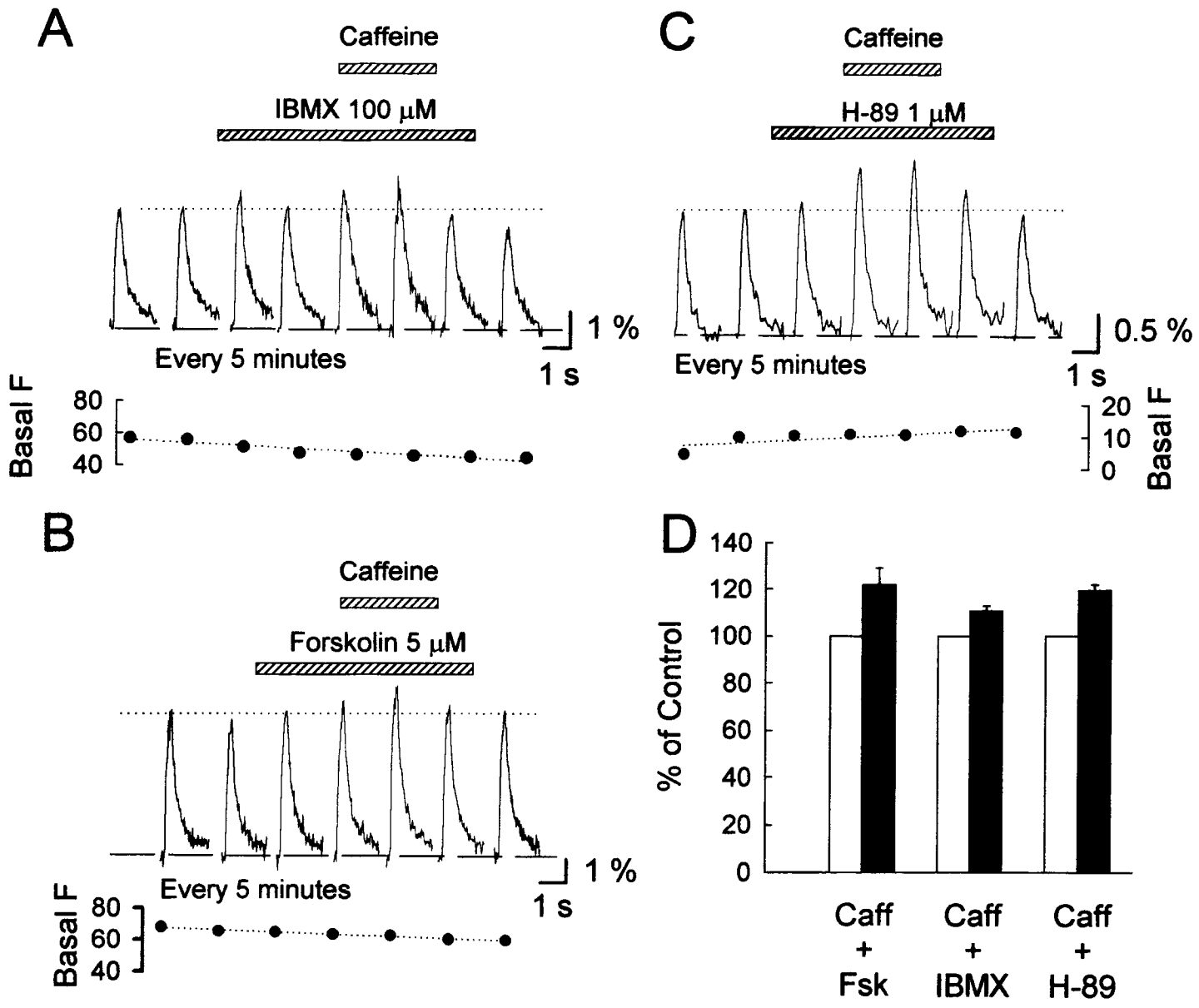
A
Caffeine
IBMX 100 μM
1 %
1 s
Every 5 minutes
Basal F
80
60
40
C
Caffeine
H-89 1 μM
0.5 %
1 s
Every 5 minutes
20
10
0
Basal F
B
Caffeine
Forskolin 5 μM
1 %
1 s
Every 5 minutes
Basal F
80
60
40
D
% of Control
140
120
100
80
60
40
20
0
Caff + Fsk
Caff + IBMX
Caff + H-89

Figure 27.

Furthermore, following a 10 min application of forskolin (5 μM), caffeine applied in the presence of forskolin caused a potentiation to 121.8±7.1% (n=16 cells, $p<0.001$; Fig. 27). This result demonstrates that caffeine can potentiate Ca^{2+} signals independently of cAMP production.

In order to reinforce these findings and to extend them to the cGMP-PKG pathway, H-89, an antagonist of both protein kinases at a concentration of 1 μM, was used (Chijiwa et al. 1990). H-89 alone had no effect on Ca^{2+} signals during a 10 min incubation (98.9±1.8%, n=14 cells). However, caffeine applied in the presence of H-89 caused a potentiation of Ca^{2+} signals to 119.5±2.4% (n=14 cells, Fig 27 C, D). We suggest that caffeine potentiates action potential-evoked Ca^{2+} signals independently of protein phosphorylation mediated by either cAMP or cGMP.

L-type channels are not required for caffeine-induced potentiation of Ca^{2+} signals

The previous experiments demonstrated that a cAMP-dependent phosphorylation of Ca^{2+} channels could not account for the potentiation of spike-evoked Ca^{2+} signals by caffeine. However, another pathway independent of kinases and involving L-type channels could be implicated. It has recently been proposed that caffeine modifies a direct interaction between RyRs and L-type channels, leading to an increase of RyRs' open probability (Chavis et al. 1996). We investigated this possibility in an experiment where we applied caffeine while blocking L-type channels by nifedipine (Tombaugh and Somjen 1997).

20 μM of nifedipine partially inhibited action potential-evoked Ca^{2+} signals by 18.8±0.1% (n=5cells, Fig. 28B). A 10 min preincubation with nifedipine (20 μM) did not,

however, prevent the caffeine-induced potentiation of the action potential-induced Ca^{2+} transients which remained at 114.0±2.3% (n=16 cells, $p<0.001$, Fig. 28A, C). This demonstrates that caffeine-induced enhancement of action potential-evoked Ca^{2+} signals does not require L-type Ca^{2+} channels. Thus an interaction between the RyRs and L-type channels is probably not responsible for this effect in CA1 neurons.

Ryanodine decreases action potential-evoked Ca^{2+} transients and occludes caffeine effects in CA1 pyramidal neurons

The findings presented thus far suggest that caffeine potentiated action potential-evoked Ca^{2+} transients independently of a modulation of Ca^{2+} influx. A possible explanation of the action of caffeine is that caffeine favors CICR by interacting with the RyR channels, thereby enhancing their open probability (Rousseau and Meissner 1989; Sitsapesan and Williams 1990). Ryanodine binds to the RyRs, irreversibly locks them in a low conductance open state (Coronado et al. 1994), and prevents caffeine action on the RyR channels (Sitsapesan and Williams 1990).

Figure 28 L-type Ca^{2+} channels are not required for caffeine potentiation of Ca^{2+} transients.

A. Nifedipine (20 μM) reduces Ca^{2+} transient amplitudes (traces 4 and 5) but does not occlude the caffeine action (traces 6 and 7). Three controls shown were separated by 5 min. intervals. Traces 6 and 7 were recorded after 1 and 3 min of caffeine application respectively. No change of basal fluorescence (F) was observed when the drugs were applied. **B.** dose-response curve of nifedipine for the reduction of Ca^{2+} transient amplitude. Each point is from 5-6 cells. **C.** Average data for caffeine (Caff) effect in the presence of nifedipine (Nif, 20 μM). Percentage of Control for nifedipine (Nif) and

nifedipine + caffeine (Nif + Caff) are given compared to the value of the last control. Experiments were conducted in fura-2-AM loaded slices.

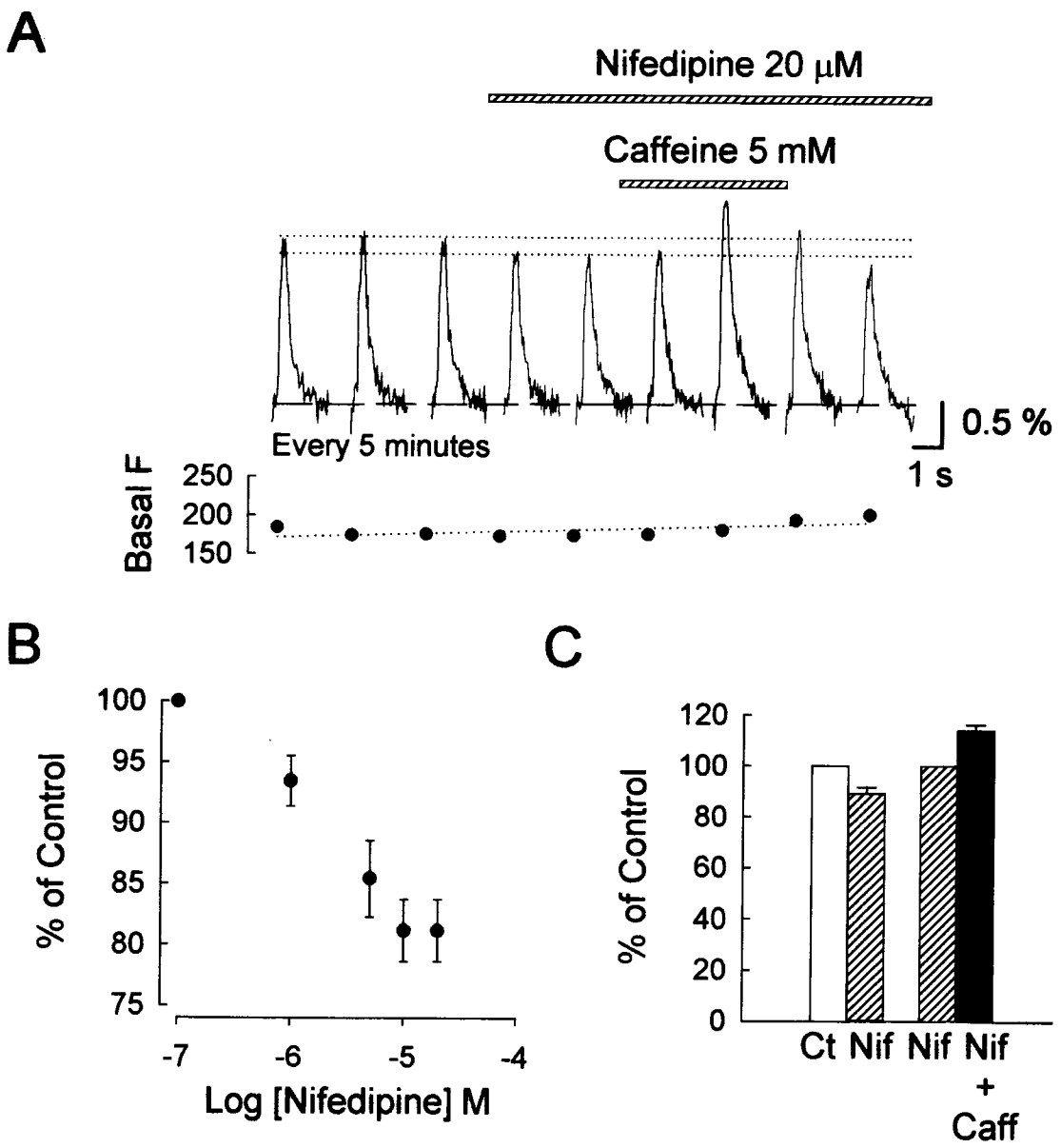
A
Nifedipine 20 μM
Caffeine 5 mM
0.5 %
1 s
Every 5 minutes
Basal F
250
200
150
B
100
95
90
85
80
75
% of Control
-7
-6
-5
-4
Log [Nifedipine] M
C
120
100
80
60
40
20
0
% of Control
Ct
Nif
Nif
Nif + Caff

Figure 28.

In addition, ryanodine has been shown to have no effect on voltage-gated Ca^{2+} currents and the resting potential in CA1 pyramidal neurons (Sitsapesan and Williams 1990; Belousov et al. 1995). Thus, ryanodine allowed us to further investigate the origin of the effect of caffeine on RyR channels. Ryanodine (20 μM; Belousov et al. 1995) irreversibly reduced Ca^{2+} transients to 77.8±4.0 % (n=24 cells) and to 72.9±2.9% (n=24 cells), when evoked by 1 and 5 action potentials respectively (Fig. 29A, B and C), without a change in baseline fluorescence. This effect was observed within 10-15 min of incubation. After the reduction had occurred, action potential-evoked Ca^{2+} signals remained stable (Fig. 29A). The percentage of reduction was greater when cells were stimulated by 5 action potentials every 20 sec (Fig. 29D and E). Such stimulation did not interfere with the stability of control Ca^{2+} transients; their amplitudes ($\Delta F/F$ values) were stable for more than 20 min under these conditions (Fig. 29D). When ryanodine was applied to stimulated neurons, Ca^{2+} transient amplitudes were reduced to 54.0±1.5 % of controls (n=30 cells, Fig. 29D, E). This larger reduction of Ca^{2+} transients in stimulated neurons is consistent with the known use-dependent block by ryanodine of caffeine-evoked Ca^{2+} transients observed in CA1 neurons (Garaschuk et al. 1997) and the Ca^{2+} dependence of ryanodine binding to RyRs (Coronado et al. 1994). The reduction of Ca^{2+} transients by ryanodine is unlikely to be attributable to Ca^{2+}-dependent inactivation of Ca^{2+} influx (Kramer et al. 1991), since no change of basal fluorescence was associated with ryanodine application (Fig. 29A and B). This indicates that the slow application of the drug (see Methods) did not trigger a change in basal $[Ca^{2+}]_i$ required to significantly modulate voltage-gated Ca^{2+} channels (Kramer et

al. 1991). The effects of ryanodine observed here are in agreement with a contribution of CICR to action potential-evoked Ca^{2+} transients.

If 20 μM ryanodine is able to prevent CICR triggered by action potentials in CA1 neurons, it should also be able to prevent the facilitation of CICR induced by caffeine application (5 mM). By applying caffeine in the presence of ryanodine (20 μM) we tested this assumption. When cells were stimulated with 5 action potentials at 20 Hz every 20 seconds in the presence of ryanodine, caffeine failed to induce a potentiation of Ca^{2+} signals (94.6±3.3%, n=30 cells, p=0.054, Fig. 29). These experiments show that ryanodine can occlude the action of caffeine. We therefore concluded that caffeine probably favored a CICR by interacting with the RyR channels, while ryanodine suppressed a CICR induced by action potentials.

Figure 29 Ryanodine reduces action potential-evoked Ca^{2+} transient amplitude and precludes caffeine action.

A, Ryanodine (20 μM) reduced the Ca^{2+} transient amplitude to a stable level both for 5 (left panels) and single spikes (right panels). Traces were recorded every 5 min. No change of basal fluorescence (F) is associated with the application of ryanodine. **B**, Average data of ryanodine (20 μM) action are shown. Data are from 26 cells. **C**, Ryanodine (20 μM) precludes caffeine action on Ca^{2+} transients evoked with 5 action potentials. Inset scale, 3% and 500 ms. **D**, Average data of the effects of ryanodine alone (Ry) and Ryanodine and caffeine (Ry + Caff) are given as percentage of control. **E**, Histogram of the effect of caffeine alone (red bars) and in the presence of ryanodine (blue bars) on Ca^{2+} transient amplitudes. Note that on average Ryanodine precludes caffeine potentiation of Ca^{2+} transients. Experiments were conducted in fura-2-AM loaded slices.

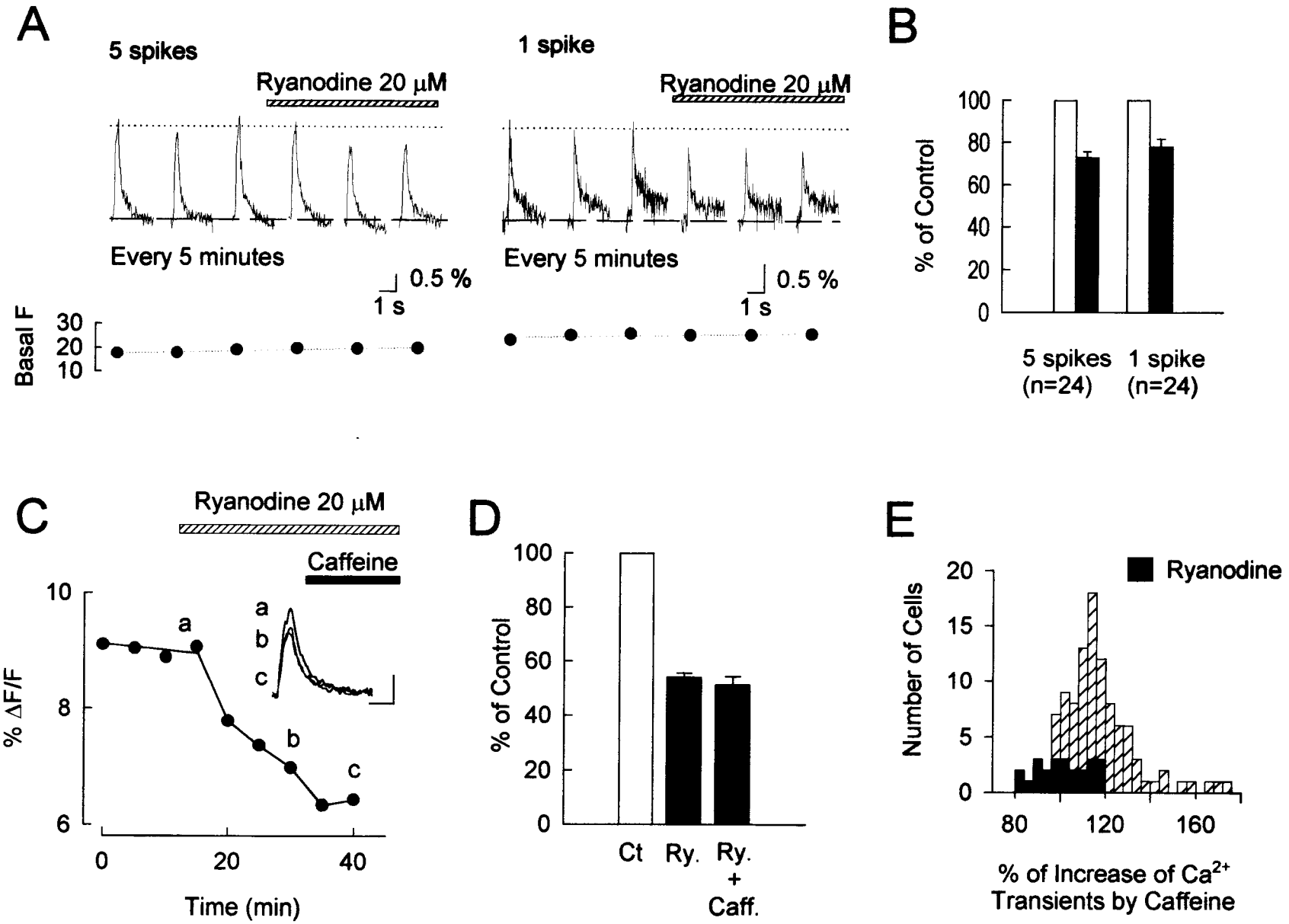
A
5 spikes
Ryanodine 20 μM
Every 5 minutes
0.5 %
1 s
Basal F
30
20
10
1 spike
Ryanodine 20 μM
Every 5 minutes
0.5 %
1 s
B
% of Control
100
80
60
40
20
0
5 spikes (n=24)
1 spike (n=24)
C
Ryanodine 20 μM
Caffeine
% ΔF/F
10
8
6
a
b
c
0
20
40
Time (min)
D
% of Control
100
80
60
40
20
0
Ct
Ry.
Ry. + Caff.
E
Ryanodine
Number of Cells
20
15
10
5
0
80
120
160
% of Increase of Ca2+ Transients by Caffeine

Figure 29.

Thapsigargin application decreases action potential-evoked Ca^{2+} transients and prevents caffeine effects in CA1 pyramidal neurons.

The involvement of internal Ca^{2+} stores in the spike-evoked Ca^{2+} transients was further examined by blocking endoplasmic Ca^{2+}-ATPases. Thapsigargin, a naturally occurring tumor-promoting sesquiterpene lactone, is an effective and irreversible inhibitor of endoplasmic ATPases (Thastrup et al. 1990; Thastrup 1990) without a known influence on plasma membrane ATPases (Lytton 1991). Due to a continuous Ca^{2+} release through RyR channels, thapsigargin (3 μM) appears to cause a gradual depletion of caffeine-sensitive internal Ca^{2+} stores in CA1 pyramidal neurons (Garaschuk et al. 1997). It does not affect either resting potential or action potential amplitude in neurons (Belousov et al. 1995).

Bath application of thapsigargin (500 nM and 3000 nM; Garaschuk et al. 1997) irreversibly reduced Ca^{2+} signals evoked by 1 or 5 action potentials to 82.9±3.4 % (n=16 cells) and 79.8±3.0 % (n=32 cells; Fig 30) respectively, in neurons loaded with fura-2-AM. The decrease of signal amplitude typically started after 15 min of thapsigargin application and reached a steady-state level of reduction in 30 min. Furthermore, thapsigargin caused a large change of Ca^{2+} signal kinetics with decays of the Ca^{2+} signal being much slower in the presence of thapsigargin (Fig. 30B, inset). No change of basal fluorescence was observed during thapsigargin application, consistent with the reported lack of thapsigargin effects on resting $[Ca^{2+}]_i$ in neurons (Shmigol et al. 1995). A similar effect of thapsigargin (3 μM) was obtained in neurons loaded with bis-fura-2 (60-100 μM) and recorded using whole-cell patch clamp mode, both in the soma and proximal

dendrites. In these experiments, resting potential and action potential amplitudes were unaffected by the drug (n=5 cells). Taken together, these results suggest that thapsigargin prevents CICR by depleting Ca^{2+} stores.

If thapsigargin depletes internal Ca^{2+} stores, caffeine applied in the presence of thapsigargin should not increase action potential-evoked Ca^{2+} signals. Caffeine (5 mM), applied after 30 min of thapsigargin incubation, failed to induce a potentiation of Ca^{2+} signals (Fig. 30). On the contrary, caffeine further reduced Ca^{2+} signals to 63.4±5.8 % (n=5 cells) and 69.1±3.0 % (n=32 cells, Fig. 30) for 1 and 5 action potentials respectively. This is consistent with an assumption that caffeine further depleted the internal Ca^{2+} stores in the presence of thapsigargin. No potentiation by caffeine was observed in these experiments. These results further imply that the caffeine action required replenished internal Ca^{2+} stores.

Figure 30 Thapsigargin reduced Ca^{2+} transient amplitude and occluded the caffeine effect.

A. Thapsigargin (3 μM) reduces the spike-evoked Ca^{2+} transient amplitude to a stable level and occludes caffeine action on Ca^{2+} transients. **B.** Selected traces (a,b and c) corresponding to the points labeled a,b and c in the plot are shown. Inset: trace b has been scaled to the amplitude of trace a to visualize the change of kinetics induced by thaspigargin. Scale: 500 ms and 1%. **C.** Average data for the effects of thapsigargin (Thap) and caffeine in the presence of thapsigargin (Thap + Caff). Data are from 16 cells. **D.** Histogram of the effect of caffeine alone (open bars) and the effect of caffeine in the presence of thapsigargin (closed bars) on Ca^{2+} transient amplitudes. Note that on average thapsigargin occludes caffeine potentiation of Ca^{2+} transients. Ca^{2+} transients were evoked with 5 action potentials for A-D. Experiments were conducted in fura-2-AM loaded slices.

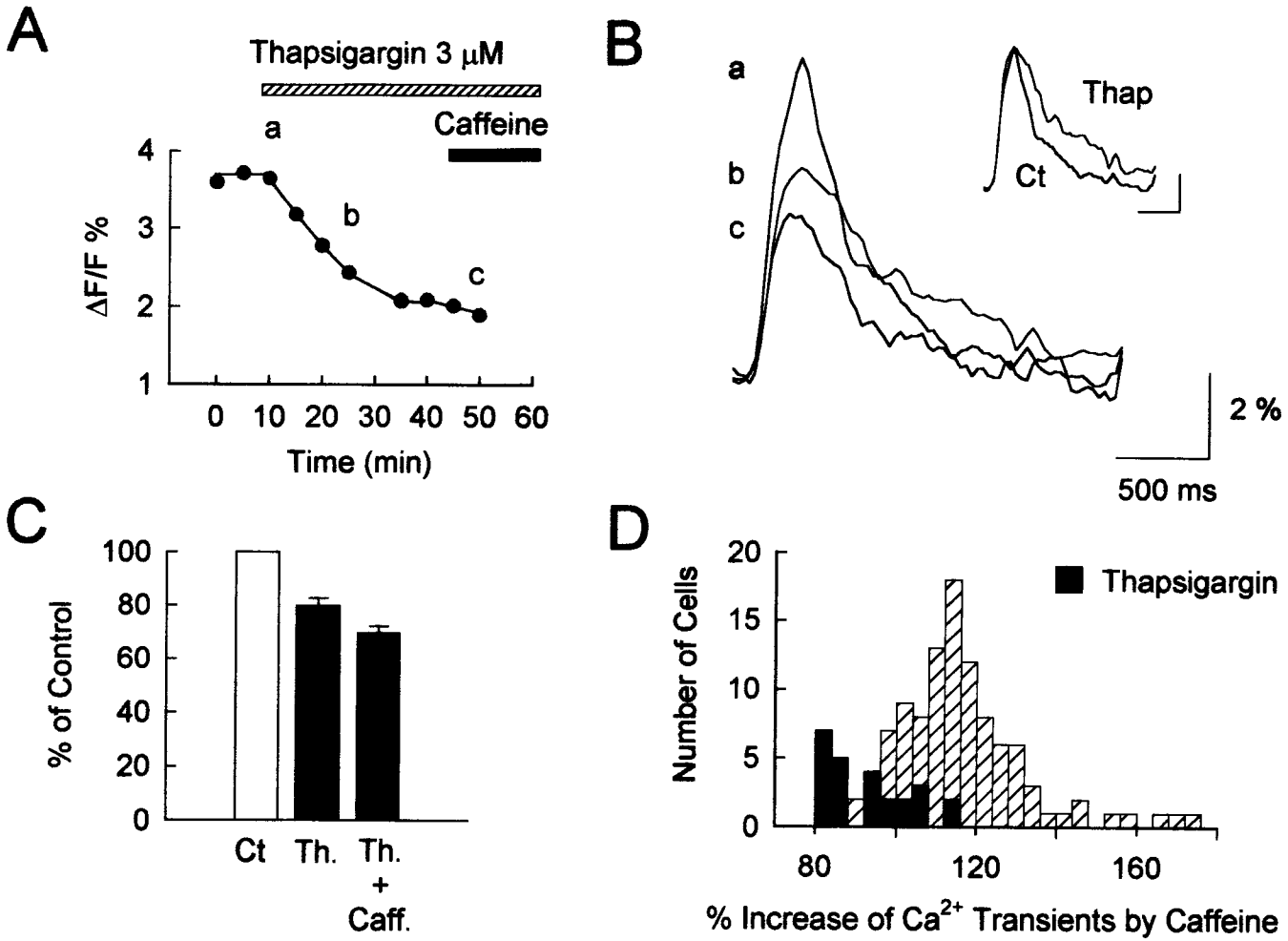
A
Thapsigargin 3 μM
Caffeine
a
b
c
ΔF/F %
4
3
2
1
0 10 20 30 40 50 60
Time (min)
B
a
b
c
Thap
Ct
2 %
500 ms
C
% of Control
100
80
60
40
20
0
Ct
Th.
Th. + Caff.
D
Number of Cells
20
15
10
5
0
Thapsigargin
80
120
160
% Increase of Ca2+ Transients by Caffeine

Figure 30.

Cyclopiazonic acid decreases action potential-evoked Ca^{2+} transients in CA1 pyramidal neurons

Because thapsigargin is an irreversible antagonist (Thastrup et al. 1990) and because it may partially inhibit Ca^{2+} influx in some cells (Rossier et al. 1993; Nelson et al. 1994; Shmigol et al. 1995), we used cyclopiazonic acid (CPA), a reversible and more specific blocker of SERCAs. CPA (in the μM range) has been shown to have no effects on Ca^{2+} channels, resting potential, and action potential amplitude in neurons (Ishii et al. 1992; Nelson et al. 1994). These properties enabled us to study the effect of a reversible Ca^{2+} store depletion on the action potential-evoked Ca^{2+} signals.

A 10 min application of CPA (30 nM) reduced Ca^{2+} transients to 80.4±2.6 % (n=20 cells). Recovery by > 96% of control signals occurred in about 75% of cells upon wash out of CPA (n=20 cells, Fig. 31). No change in basal fluorescence was detected when CPA was applied (Fig. 31A). This result indicates that Ca^{2+} transient amplitude can be reduced when internal Ca^{2+} stores are emptied in a reversible manner. However, at such low concentration, the effect of CPA was probably partial since the reduction of Ca^{2+} transient amplitude and the effect on Ca^{2+} signal kinetics were smaller than those observed with thapsigargin. For this reason, CPA was used at higher concentrations between 1 and 20 μM. CPA (>1 μM) had a similar effect on Ca^{2+} signal kinetics as the one observed with thapsigargin. Furthermore, a reversible reduction of Ca^{2+} signals to 67.0±5.2 % was observed in 4 out of 10 cells (Fig. 31) with Ca^{2+} signal amplitude recovering to more than 95 % of control signals upon wash out of the drug. This result shows that the reversible effect of CPA is dose-dependent (Fig. 31B). In the remaining cells, the reduction of Ca^{2+}

signal amplitude failed to recover, even after up to 1h of wash (n=32 cells, not shown) and a marked decrease of basal F was observed (by 27.6±7.3 %, n=27 cells). This is in agreement with previous reports showing that CPA can increase resting $[Ca^{2+}]_i$ in some cells (Carmignoto et al. 1998), thereby masking a recovery upon washout of CPA. Such decrease of basal F was never observed in cells, which recovered from CPA, and in cells treated with thapsigargin (0.5-3 μM) or ryanodine (20 μM). We conclude that the amplitude of action potential-evoked Ca^{2+} transient is reduced in a reversible manner, when internal Ca^{2+} stores are slowly emptied with no change in basal $[Ca^{2+}]_i$. These results further establish a role for CICR in setting the amplitude of action potential-evoked Ca^{2+} signals in CA1 neurons.

Figure 31 Cyclopiazonic acid reversibly reduces action potential-evoked Ca^{2+} transient amplitude.

A. CPA (30 nM), applied for 10 min, reduced Ca^{2+} transient amplitudes (traces 4 and 5). The reduction continues after a partial wash of CPA (trace 6). Full wash of CPA led to complete recovery of Ca^{2+} transients (trace 8). Traces were recorded every 5min. No detectable change of basal fluorescence (F) is associated with the application of CPA. **B.** Average results for the effect of CPA (300nM; left group of bars) and CPA (30 nM; right group of bars). **C.** Same as in A. CPA concentration is 20 μM. **D.** Effect of CPA (20 μM) on the decay of Ca^{2+} transients. Recording traces have been scaled for comparison of their decay kinetics. Experiments were conducted in fura-2-AM loaded slices.

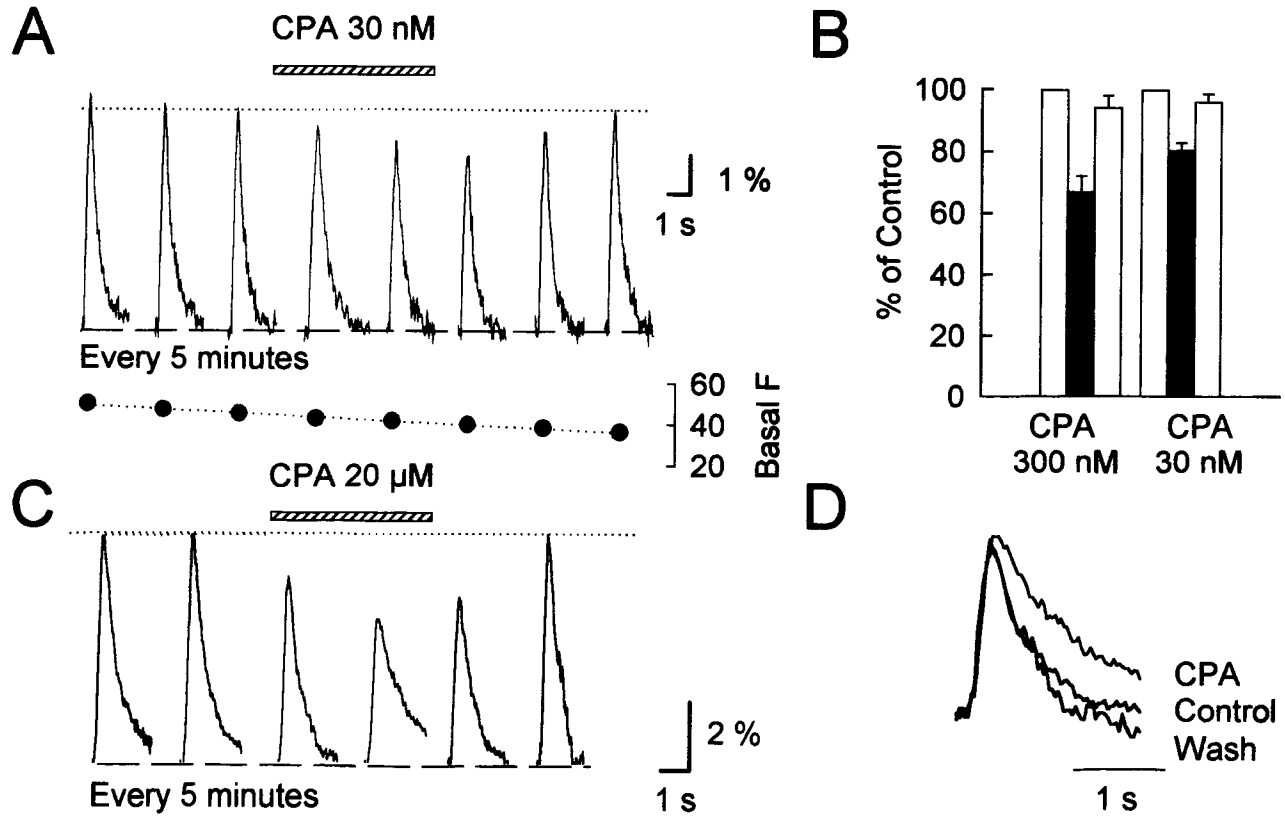
A
CPA 30 nM
1 %
1 s
Every 5 minutes
60
40
20
Basal F
B
100
80
60
40
20
0
% of Control
CPA
300 nM
CPA
30 nM
C
CPA 20 µM
2 %
1 s
Every 5 minutes
D
CPA
Control
Wash
1 s

Figure 31.

DISCUSSION

Modulation of action potential backpropagation and associated calcium signals by 5-HT

The experiments described above show that serotonin has at least two effects on dendritic properties and action potential induced $[Ca^{2+}]_i$ changes in CA1 pyramidal neurons. First, it hyperpolarized the membrane potential recorded in dendrites and increased the membrane conductance. This hyperpolarization matched the change measured in the soma and probably reflects the same 5-HT_{1A} receptor-mediated increase in K^+ conductance determined previously (Andrade and Nicoll 1987; Colino and Halliwell 1987). The hyperpolarization may also reflect the accelerated onset and voltage-shift of activation of I_h in 5-HT, as described by McCormick and Pape (1990).We do not know the spatial distribution of the conductance increase in these cells, but the high density of 5-HT_{1A} receptors on the dendrites (Kia et al. 1996) implies that some of the increase occurs in this part of the cell.

Dendritic recordings also revealed a reduction in the peak potential of backpropagating action potentials. The 5-HT induced reduction in AP amplitude usually was greater than the reduction of the resting potential, decreasing slightly the amplitude of the earlier spikes in the train. In contrast, 5-HT lowered the resting potential in the soma without affecting the peak potential. Consequently, the action potential amplitude increased at that location. These effects are similar to the effects of injected hyperpolarizing current (Tsubokawa and Ross 1996).

The study of carbachol (CCh; cholinergic agonist) effects on action potential backpropagation is the only known study that directly addresses the question as to how a neurotransmitter can modulate action potential backpropagation in CA1 pyramidal neurons

(Tsubokawa and Ross 1997). Hence, it is interesting to compare effects of 5-HT and CCh application on action potential backpropagation and associated $[Ca^{2+}]_i$.

The almost equal reduction in peak dendritic spike potential for all action potentials in the train, without a significant change in amplitude, differs from the effects of carbachol on backpropagating spikes (Tsubokawa and Ross 1997). In those experiments, CCh reversed the activity-dependent amplitude reduction in a train, resulting in spikes that have almost equal amplitude when recorded in the dendrites. Both the peak potential and amplitude of later spikes were enhanced by CCh. There was little effect on the first spike in the train. In the hippocampus 5-HT affects almost all spikes equally, whether they are isolated or occur in bursts. In contrast, cholinergic modulation appears to have more dramatic effects on closely spaced action potentials than on isolated spikes.

This conclusion may not apply to the most distal dendrites (more than 300 μm from the soma). At this distance, CCh was ineffective in reversing the activity-dependent reduction in spike amplitude (Tsubokawa and Ross 1997). In addition, hyperpolarization of the distal dendrites by current injection was particularly effective in reducing the amplitude of the first (and sometimes second) back-propagating action potential. Spikes later in the train were not reduced because they had already failed at a more proximal location. Peak potentials of all spikes were lowered (Tsubokawa and Ross 1996). Serotonin acts similarly to a maintained hyperpolarization at this location.

Since the peak spike potential is largely due to the balance of conductances at that time, the different effects in the soma and dendrites are probably a result of a different proportion of Na^+ and K^+ conductances in these two regions. If the balance in the soma is dominated by the Na^+ conductance, then a small increase in K^+ conductance and

hyperpolarization mediated by 5-HT would not lower the peak potential significantly. However, if the balance in the dendrites is more equal, then an increase in K^+ conductance and hyperpolarization would lower the peak potential in that region. One possibility is that there is a high density of Na^+ channels near the soma – perhaps in the axon hillock as traditionally assumed. However, Colbert and Johnston (1996) found that the density of Na^+ channels was not significantly different in the axon hillock than in other regions of hippocampal pyramidal neurons. A second possibility is that the density of K^+ channels is higher in the dendrites. Recently, (Hoffman et al. 1997) it has been found that the conductance underlying the A-current increased with distance away from the soma in pyramidal neurons. Since the A-current activates rapidly during the upstroke of the action potential, the higher conductance in the dendrites could be responsible for the lower spike amplitude in this region. Other K^+ conductances, including those active at the resting potential, also could contribute to the balance of currents in the dendrites.

The second effect of 5-HT was the reduction in the spike-mediated $[Ca^{2+}]_i$ increase in both the soma and dendrites. Some of this reduction probably was due to the reduction in peak spike potential in the dendrites. The lower potential would open fewer Ca^{2+} channels causing less Ca^{2+} entry. A similar reduction in spike-evoked $[Ca^{2+}]_i$ increase by 5-HT was recently observed (Chen and Lambert 1997) in hippocampal neurons loaded with fura-2-AM. The authors used dendritic field potential recordings to support the idea that spike peak reduction is responsible for the reduction in the $[Ca^{2+}]_i$ change. One important difference between their experiments and ours is that we observed a consistent 5-HT-mediated reduction in the spike-evoked $[Ca^{2+}]_i$ change in the soma. They observed a much smaller effect of 5-HT in this region. A possible explanation for the difference is that they used adenosine as an agonist in most of

their experiments. Although adenosine and 5-HT are thought to act through similar pathways (Hille 1994), it is possible that the distribution of receptors on pyramidal neurons is different. A second possible explanation of the difference in observations is that they detected the $[Ca^{2+}]_i$ changes from all alveus-stimulated neurons in a field of view. These may have included some interneurons. In contrast, in both our experiments with whole-cell-loaded and fura-2-AM-loaded cells we recorded from single identified pyramidal neurons.

The reduction of the spike-evoked $[Ca^{2+}]_i$ change in the soma, where the action potential peak potential was not reduced and the amplitude increased, implies that 5-HT also affects Ca^{2+} channels directly. This conclusion is consistent with the fact that the action potential shape was not altered by 5-HT (Fig. 14B) and by the observation that membrane hyperpolarization by itself did not affect the $[Ca^{2+}]_i$ change (Fig. 16). Previous work suggests that 5-HT modulates several different kinds of Ca^{2+} channels in CNS neurons, although not to the same extent (Anwyl 1991; Hille 1994). In particular, N- and P-channels appear to be more susceptible than L- or T-channels (Bayliss, et al. 1995; Foehring 1996). These modulations generally occur through membrane-delimited G-protein mechanisms. Imaging (Christie et al. 1995), electrophysiological (Magee and Johnston 1995), and immunocytochemical (Westenbroek et al. 1990) studies indicate that several Ca^{2+} channels types are expressed in pyramidal cells. All channel types are found in all regions of the cell. However, L-type channels appear to be more concentrated near the soma and T-type channels more concentrated in the dendrites. The distribution of other high-threshold channels, including N-type, is more uniform (Magee and Johnston 1995). Our experiments made no attempt to distinguish which channel type was affected by serotonin. Assuming that some Ca^{2+} channels were affected in all regions of the cell, our results suggest that in the dendrites the reduction in the $[Ca^{2+}]_i$ change was

caused by both a reduction in peak spike amplitude and direct modulation of Ca^{2+} channels. However, the relative contribution of each effect was not determined in these experiments. Modulation of dendritic Ca^{2+} channels is consistent with the demonstration of G-protein mediated inhibition of voltage-gated Ca^{2+} currents in isolated dendritic segments (Kavalali et al. 1997).

Previously, it was demonstrated that spike propagation and dendritic $[Ca^{2+}]_i$ changes could be affected by synaptic inhibition and muscarinic modulation. The dramatic reduction in spike-evoked $[Ca^{2+}]_i$ in the distal dendrites caused by synaptic inhibition (Tsubokawa and Ross 1996) clearly was due to a reduction in spike amplitude. No change in Ca^{2+} channel properties would be expected from $GABA_A$-mediated inhibition. $GABA_B$-mediated changes in channel properties are possible (Anwyl 1991), but are inconsistent with the narrow time window for the inhibitory effect in those experiments. The carbachol-mediated increase in $[Ca^{2+}]_i$ change in the dendrites resulting from a train of action potentials (Tsubokawa and Ross 1997) was predominantly due to the enhanced backpropagation of spikes later in the train. Modulation of Ca^{2+} channel properties was not a major contributor to this effect. One piece of evidence for this conclusion is that neither the amplitude of the first spike nor the $[Ca^{2+}]_i$ increase evoked by this spike were significantly altered by carbachol. However, details of the effect of carbachol on dendritic Ca^{2+} channels were not examined.

Since inhibition and cholinergic modulation affected $[Ca^{2+}]_i$ changes via changes in spike amplitude, the changes in $[Ca^{2+}]_i$ were restricted to the dendrites where the amplitude change was greatest. The largest changes were in the distal processes. Spike amplitudes and associated $[Ca^{2+}]_i$ changes in the soma were unaffected. Serotonin, in contrast, affected

spike-evoked $[Ca^{2+}]_i$ changes in all parts of the cell even though spike potentials in the soma were not significantly reduced.

The functional consequences of the reduction in action potential amplitude in the dendrites and the associated $[Ca^{2+}]_i$ change are unknown. A role for backpropagating action potentials in synaptic plasticity has been demonstrated (Magee and Johnston 1997; Markram, Lubke et al. 1997). Either the action potentials themselves or the spike-evoked $[Ca^{2+}]_i$ changes contribute to this effect. Serotonin has been shown to inhibit the induction of LTP in the hippocampus in some experiments (Corradetti et al. 1992; Sakai and Tanaka 1993; Villani and Johnston 1993). However, it is not known if the effects on spike backpropagation described here would contribute to this inhibition. The magnitude of the changes we observed was not large. Therefore, it is possible that the effects of 5-HT on dendrites are not relevant to changes in synaptic plasticity.

A second possible role for backpropagating spikes is the variations in control of membrane conductances in different parts of the cell, possibly by activating Ca^{2+}-sensitive K^+ conductances (Storm 1993). These conductances could shape dendritic EPSPs and IPSPs, influencing synaptic integration and spike accommodation. Related to this possibility, Torres et al. (1996) recently have shown that 5-HT reduced the fast Ca^{2+}-dependent afterhyperpolarization in CA1 pyramidal neurons.

Calcium induced calcium release through IP_3 sensitive channels.

Application of 5-HT combined with a train of action potential evoked a large calcium wave in the proximal and middle dendrites. A train of action potentials probably evoked this

wave by triggering calcium induced calcium release through IP_3 sensitive channels. Several arguments favor this supposition.

First, the lack of electrical correlate of the described effect measured in soma argues against a possibility of a dendritic calcium spike. CA1 pyramidal neurons are electrotonically compact; a change of membrane potential by 1.2 mV at a distance of more than 500 μm from soma causes a change of membrane potential of about 1 mV in the soma (Stuart and Spruston 1998). Thus calcium spike evoked in the proximal or middle dendrites (50-200 μm from the soma) should have been recorded in the soma with a patch pipette.

Second, 5-HT_2 type receptors are coupled through the phosphoinositol second messenger cascade to phospholipase C (PLC) and eventually to IP_3 production. IP_3 binds to the IP_3 sensitive channels in the ER and increases their sensitivity to cytoplasmic [Ca^{2+}] (Finch et al. 1991). The sensitivity of IP_3 sensitive channels to the cytoplasmic [Ca^{2+}] in the presence of IP_3 has a strong non-linear character (Bezprozvanny et al. 1991). Its concentration dependence described by a bell-shaped curve with a maximum probability of IP_3 sensitive channels opening at 0.2 μM of free Ca^{2+} (Bezprozvanny et al. 1991). A similarly shaped curve describing Ca^{2+} dependence of IP_3 sensitive channels in the nuclear membrane has been described by Stehno-Bittel et al. (1995). These authors have shown that the maximal activation of the channels by Ca^{2+} is achieved at [Ca^{2+}] around 1 μM. Unfortunately, it is impossible to compare directly the results described above because the experiments were conducted at different holding membrane potentials, 0 mM and +30 mV respectively (Bezprozvanny et al. 1991; Stehno-Bittel et al. 1995). IP_3 dependent channels have been shown to be sensitive to the changes in membrane potential (Stehno-Bittel et al. 1995).

Taking this information into account we decided to estimate the $[Ca^{2+}]_i$ in the described experiments. In order to calculate $[Ca^{2+}]_i$ we used the following formula:

$$[Ca^{2+}]_i = \frac{[Ca^{2+}]_{rest} + K_d\left(\frac{\frac{\Delta F}{F}}{\left(\frac{\Delta F}{F}\right)_{max}}\right)}{\left(1-\left(\frac{\frac{\Delta F}{F}}{\left(\frac{\Delta F}{F}\right)_{max}}\right)\right)},$$

where bis-fura-2 K_d=525 nM, $(DF/F)_{max}$=80% and $[Ca^{2+}]_{rest}$=60 nM (Jaffe et al. 1992). The time course of a calculated $[Ca^{2+}]_i$ for one experiment is shown in the Figure 32. One can see that the initial point of the $[Ca^{2+}]_i$ wave lies at the level of about 200 nM, which is the exact concentration where IP_3 sensitive channels are the most sensitive to the $[Ca^{2+}]_i$ in the presence of IP_3, according to the data of Bezprozvanny et al. (1991). At rest, the level of IP_3 in the cytoplasm is probably low and that is why action potential evoked changes of $[Ca^{2+}]_i$ are not sufficient to induce significant shift of IP_3 sensitive channels open probability. This explains why this effect was not observed in control conditions. When serotonin was applied, the activation of 5-HT_2 type receptors led to an increase of IP_3 production and an increase of its background concentration. This created conditions when an elevation of $[Ca^{2+}]_i$ caused by action potentials was sufficient to trigger a positive feedback type process of calcium induced calcium release from endoplasmic reticulum through IP_3 sensitive channels (Bezprozvanny et al. 1991). Such a positive feedback mechanism might exist when the $[Ca^{2+}]_i$ is below the sensitivity peak of IP_3

sensitive chanels. When [Ca^{2+}] reached hundreds of nanomolar, the open probability of IP_3 sensitive channels decreased, leading to the observed decay of the calcium wave (Fig. 32). This effect fits the hypothetical negative feedback mechanism proposed by Bezprozvanny et al. (1991). The negative feedback mechanism is assumed to become dominant when $[Ca^{2+}]_i$ grows to values above 200 nM. Such high $[Ca^{2+}]_i$ values inhibit IP_3 sensitive channels.

Figure 32 Calcium release starts at the $[Ca^{2+}]_i$ level of maximal IP_3 channel sensitivity. **A.** Formula used for calculation of free $[Ca^{2+}]_i$ in the cytoplasm and parameters used for the calculation. **B.** Fluorescent image of the CA1 pyramidal neuron filled with *bis*-fura-2. **C.** A figure from (Bezprozvanny et al. 1991) showing bell-shaped curve of IP_3 sensitive channel activation in dependence of $[Ca^{2+}]_i$. Maximal open probability of these channels is reached at 0.2 mM of $[Ca^{2+}]_{free}$. **D.** Calculated change of $[Ca^{2+}]_i$ evoked by a train of action potentials in the presence of 5-HT. Colors of the traces correspond to the colors of rectangles in B.

A

K_d = 525 nM

$(\Delta F/F)_{max}$ = 80%

$[Ca^{2+}]_{rest}$ = 60 nM

$$[Ca^{2+}] = \frac{[Ca^{2+}]_{rest} + K_d \dfrac{\frac{\Delta F}{F}}{\left(\frac{\Delta F}{F}\right)_{max}}}{1 - \left(\dfrac{\frac{\Delta F}{F}}{\left(\frac{\Delta F}{F}\right)_{max}}\right)}$$

B

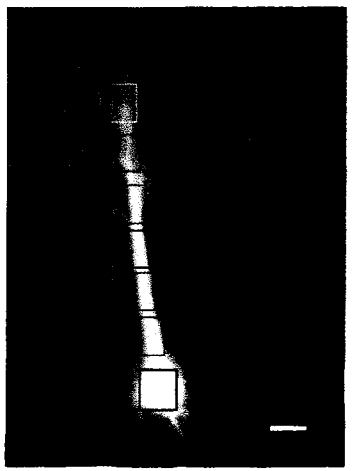

C

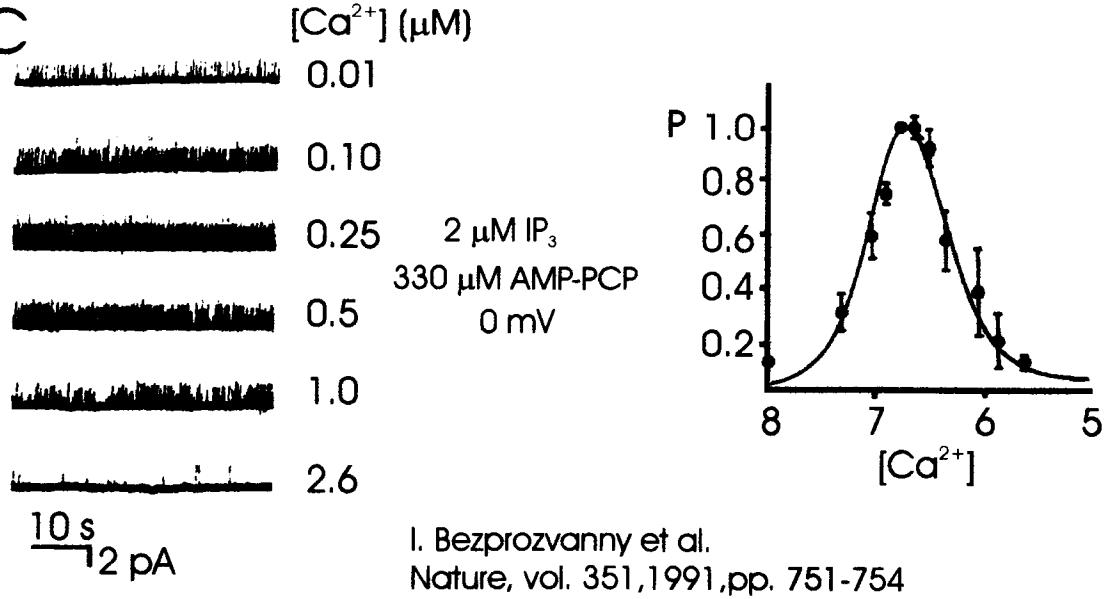

I. Bezprozvanny et al.
Nature, vol. 351,1991,pp. 751-754

D

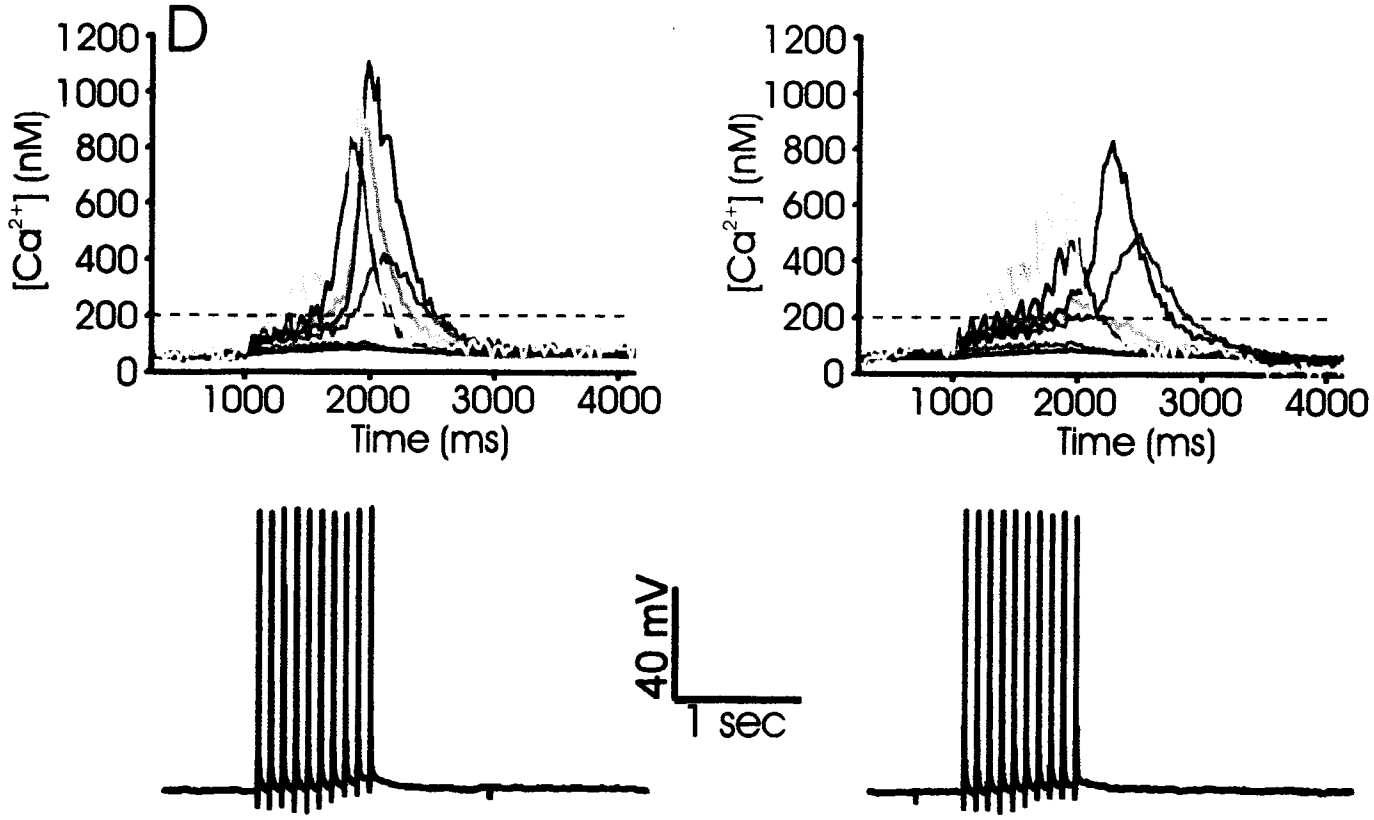

Figure 32.

Calcium induced calcium release through RyR channels

Our results provide new evidence for a contribution of internal Ca^{2+} stores to the action potential-induced elevations of $[Ca^{2+}]_i$ in CA1 hippocampal pyramidal neurons. This conclusion is based on pharmacological manipulations of CICR, which can either increase or decrease action potentials-evoked Ca^{2+} transients in these cells. While this contribution does not seem predominant in magnitude, the contribution of internal Ca^{2+} stores to action potential-evoked Ca^{2+} transients may profoundly influence the sub-cellular patterns of $[Ca^{2+}]_i$ increases. In addition, the CICR may present new targets for neuromodulators controlling the amplitude of Ca^{2+} transients in the soma and dendrites of neurons.

A main argument in favor of a contribution of CICR to action potential-evoked change of $[Ca]_i$ was the caffeine sensitivity of Ca^{2+} transients. They were enhanced by a low concentration (5 mM) and reduced by a higher concentration (20 mM) of caffeine. Such caffeine sensitivity of Ca^{2+} transients has been reported in various neuronal cell types (Friel and Tsien 1992; Usachev et al. 1993; Verkhratsky and Shmigol 1996) and is usually attributed to the known sensitivity of isolated RyRs to caffeine (Sitsapesan and Williams 1990). Low concentrations of caffeine increase the open probability of the RyR channels only in the presence of Ca^{2+}, thus favoring CICR once a suprathreshold $[Ca^{2+}]_i$ is reached. Higher caffeine concentrations increase the sensitivity of RyRs to Ca^{2+}, causing depletion of calcium stores at resting $[Ca]_i$. Our experiments support these views because low concentration (5 mM) of caffeine had no measurable effect on resting $[Ca^{2+}]_i$, but enhanced Ca^{2+} transients evoked by action potentials in a ryanodine-sensitive manner. Finally, several controls ruled out non-specific effects of caffeine. This strengthened our

conclusion that caffeine could be used to reveal CICR as previously reported for other types of neurons (Kano, et al. 1995; Usachev and Thayer 1997).

Caffeine has been used in CA1 neurons to show that ryanodine-sensitive Ca^{2+} stores contain releasable Ca^{2+} at rest (Garaschuk et al. 1997). Our results are in agreement with this finding since caffeine-induced potentiation required filled Ca^{2+} stores and was occluded by depletion of these Ca^{2+} stores. However, because caffeine was slowly bath applied in our study, it did not induce a detectable rise in resting $[Ca^{2+}]_i$. A possible slow Ca^{2+} release due to caffeine application may have been counteracted by both extrusion and uptake mechanisms. To observe caffeine evoked calcium release, a fast change of RyRs sensitivity to Ca^{2+} is required. Under these conditions Ca^{2+}-dependent inactivation of the RyRs has no time to occur (Hernandez-Cruz et al. 1997). A rapid picospritzer-applied bolus of caffeine can, in fact, release large amounts of Ca^{2+} (Hernandez-Cruz et al. 1997; Garaschuk et al. 1997), while slow caffeine applications are ineffective. Other Ca^{2+} releasing agents such as ryanodine, thapsigargin or CPA did not affect resting $[Ca^{2+}]_i$ either, which can be explained similarly.

Experiments with caffeine did not provide direct evidence that CICR could be triggered by action potentials. Our data obtained with ryanodine, thapsigargin and CPA further suggested that internal Ca^{2+} stores not only participate in the clearance of Ca^{2+} from the cytoplasm as shown before (Markram et al. 1995; Fierro et al. 1998), but also contributing to the amplitude of action potential-evoked Ca^{2+} transients. Ryanodine has been shown to reduce action potential-evoked Ca^{2+} transients in several peripheral neurons (Cohen et al. 1997; Usachev and Thayer 1997; Moore et al. 1998), in agreement with an underlying CICR. Our results show that ryanodine application reduces Ca^{2+} transients

during a single action potential in CA1 neurons. Furthermore, the use-dependent block of Ca^{2+} signals by ryanodine, observed in the present study, agrees with the reported action of ryanodine on RyRs in other central neurons (Kano, et al. 1995; Garaschuk et al. 1997). The block of SERCAs by thapsigargin or CPA also reduced Ca^{2+} transients and affected their time course. Although thapsigargin was shown to block voltage-dependent Ca^{2+} channels in some cells (Rossier et al. 1993; Nelson et al. 1994; Shmigol et al. 1995), a low concentration reduced depolarization-induced Ca^{2+} transients in DRG neurons with no effect on calcium influx (Shmigol et al. 1995). In agreement, we observed that the effect of thapsigargin on decay and amplitude of Ca^{2+} transients developed almost synchronously, suggesting that the reduction in Ca^{2+} transient amplitude was related to the depletion of Ca^{2+} stores. Furthermore, the dose-dependent and reversible inhibition observed with CPA, which was shown to block caffeine-induced release in CA1 neurons (Garaschuk et al., 1997), supports our conclusions that store depletion affects action potential-evoked Ca^{2+} transients. Finally, the effects of ryanodine, thapsigargin and CPA cannot be explained by a Ca^{2+}-dependent modulation of voltage-dependent Ca^{2+} currents since resting $[Ca^{2+}]_i$ appeared unchanged in our experimental conditions. Such modulation was reported when resting $[Ca^{2+}]_i$ rose above 100 nM as a result of rapid picospritzer - application of Ca^{2+}-releasing agents (Kramer et al. 1991). We therefore conclude that a CICR component underlies action-potential Ca^{2+} transients and involves RyRs. A participation of other stores such as IP_3-sensitive Ca^{2+} stores or a novel type of Ca^{2+} store (Jacobs and Meyer 1997) is nevertheless not excluded.

The small contribution of CICR to the action potential-evoked Ca^{2+} transients described here raises the question of its role. Properties of RyRs, morphological evidence

and theoretical calculations suggest that CICR would be most effective when calcium influx creates localized Ca^{2+} microdomains of a few tens of μM, reaching ≈100 μM within 1 μs with RyRs positioned in the close apposition to the plasma membrane (Bezprozvanny et al. 1991; Berridge 1998; Neher 1998). Within this narrow time and space range, CICR would be favored by the ineffectiveness of both Ca^{2+} buffering (Neher 1998) and Ca^{2+}-dependent inactivation of RyRs (Hernandez-Cruz et al.1997). Berridge (1998) recently revised morphological data concerning the subplasmalemmal localization of RyRs in neurons and emphasized that ER can be at a distance of 20-80 nm from the plasma membrane similar to cardiac muscle. Measurements of Ca^{2+} signals which rise in ≤1 ms also favor the idea that CICR might be locally important (Ross et al., 1998). Although some studies using confocal microscopy have suggested that CICR may occur in close vicinity to the plasma membrane, allowing Ca^{2+} diffusion to the nucleus (Usachev and Thayer 1997; Jacobs and Meyer 1997), more detailed studies of local $[Ca^{2+}]_i$ increase at the plasmalemmal level are needed to prove localized CICR. Such CICR has been suggested to control neuronal excitability by producing slow after-hyperpolarizations of peripheral and central neurons (for review, Berridge 1998), including hippocampal CA1 neurons (Torres et al. 1996). In addition, CICR could occur more widely within the cytoplasm and dendrites under conditions where second messengers such as cADPribose or IP_3 might be produced. In such a scenario, the role of CICR might be relevant to synaptic plasticity and coupling of synaptic inputs to gene transcription in the nucleus.

POSSIBLE FUNCTIONAL SIGNIFICANCE

Almost fifty years ago, in 1949, D. O. Hebb had proposed a hypothesis of associative learning in the central nervous system. Later, this hypothesis became known as a set of Hebb's rules of synaptic modification. These rules read:

1. Synaptic connections between synchronously active neurons are reinforced.
2. Synaptic connections between asynchronously active neurons are suppressed.

Long term synaptic modification (potentiation/depression) in hippocampus is one of the most striking examples for these rules in the brain. Simultaneous activation of both presynaptic and postsynaptic sites that is accompanied by an increase of $[Ca^{2+}]_i$ is required for its induction (Bliss and Collingridge 1993; Malinow 1991).

Until recently, the main paradigm of cellular neurobiology stated that an action potential is evoked as a result of summation of synaptic inputs impinging onto the dendrites and that it is generated in the initial segments of an axon. When generated, an action potential recruits soma and propagates down the axon.

A discovery of existence of Na^+, Ca^{2+} and K^+ conductances in dendrites, and active backpropagation of action potentials into the dendrites, required reexamination of the dogma (Fig. 1). It also offered a possible explanation of an old paradox of Hebb's rules (Magee and Johnston 1997): How does a postsynaptic site "know" that the neuron generated an action potential?

A long distance between the place of action potential generation and a site of synaptic transmission requires a fast feedback mechanism that would be capable of forming an association between an action potential, as an ultimate expression of neuronal

activity, and synaptic transmission. Such feedback could be provided by a backpropagating action potential that causes elevation of $[Ca^{2+}]_i$ in the postsynaptic site (Svoboda et al. 1996; Svoboda et al. 1997) which is known to be a minimal requirement for synaptic modification (Magee and Johnston 1997; Fig 1). Thus an understanding of the nature and the origin of action potential evoked calcium changes is of fundamental interest.

Figure 33 The main paradigm of cellular neurobiology has changed.

A. A schematic representation of the modified paradigm that includes an active action potential backpropagation into dendrites (yellow dots). **B.** Schematic representation of the Hebb's rules. On the left, three neurons are monosynaptically connected. The top and middle neurons fire action potentials synchronously. The bottom neuron is asynchronous to the middle one. On the right, the blown out sites of the synaptic transmission with a hypothetical mechanism of a change of synaptic efficacy are shown schematically. An arrow from the left to the right shows the direction of synaptic transmission. The arrows from the right to the left with a question mark show a suggested involvement of a retrograde messenger (e.g. Bolshakov and Siegelbaum 1995). **C.** Dendritic action potentials are required for the induction of synaptic plasticity in CA1 pyramidal neurons. Panel E shows normalized EPSP amplitudes in response to paired stimulation with and without backpropagating action potential blockade by TTX (J.C. Magee and D. Johnston, Science 1997; 275, 209-213).

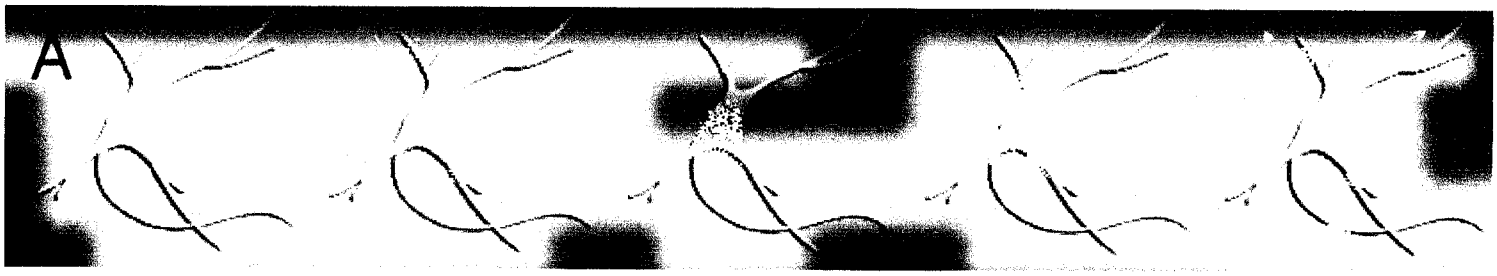

www.cajal.com

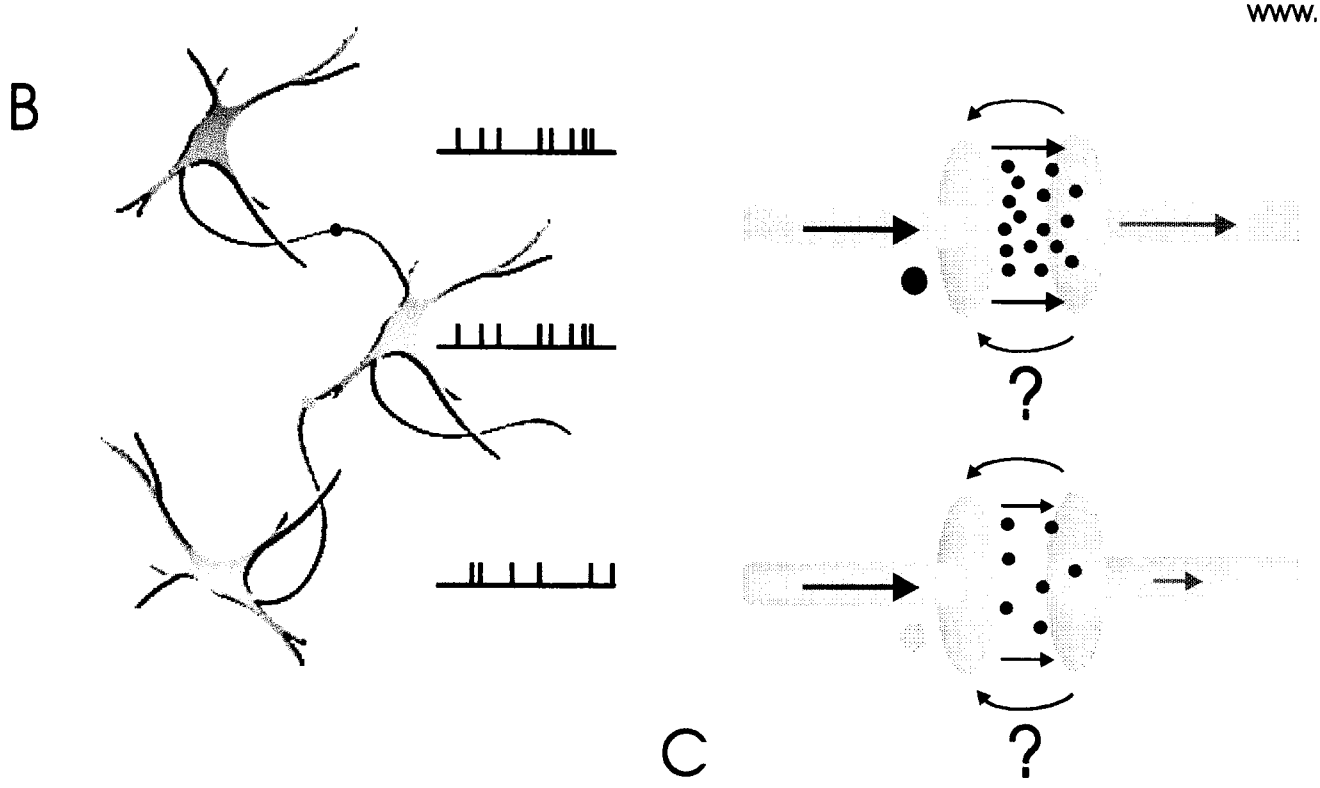

C

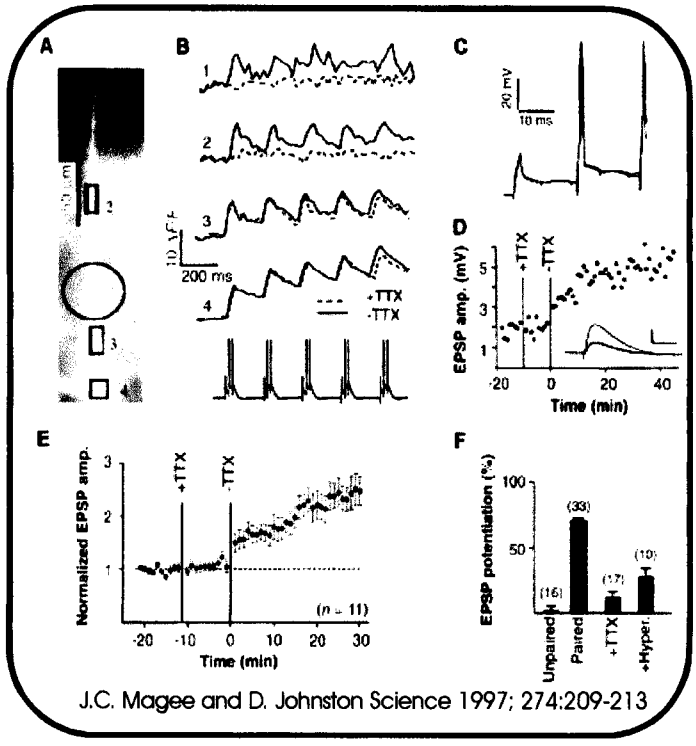

Hebb's rules

1. Synaptic contacts between synchronously active neurons are reinforced.

2. Synaptic contacts between asynchronously active neurons are depressed.

Figure 33.

This study examined the modulation of spike backpropagation and associated changes of calcium concentration in hippocampal CA1 pyramidal neurons. It also approached the question of the origin of $[Ca^{2+}]_i$ changes induced by action potentials and argued in favor of a contribution of calcium induced calcium release through ryanodine sensitive channels. Finally it demonstrated, for the first time, evidence that action potentials and the neurotransmitter serotonin can cause a synergistic calcium induced calcium release through IP_3 sensitive channels located in the endoplasmic reticulum.

REFERENCES

Andrade, R. and R. A. Nicoll (1987). "Pharmacologically distinct actions of serotonin on single pyramidal neurones of the rat hippocampus recorded in vitro." J Physiol (Lond) 394: 99-124.

Andrade, R. and R. A. Nicoll (1987). "Pharmacologically distinct actions of serotonin on single pyramidal neurones of the rat hippocampus recorded in vitro." J Physiol (Lond) 394: 99-124.

Andreasen, M. and J. D. Lambert (1995). "Regenerative properties of pyramidal cell dendrites in area CA1 of the rat hippocampus." J Physiol (Lond) 483(Pt 2): 421-41.

Anwyl, R. (1991). "Modulation of vertebrate neuronal calcium channels by transmitters." Brain Res Brain Res Rev 16(3): 265-81.

Ashley, R. H. and A. J. Williams (1990). "Divalent cation activation and inhibition of single calcium release channels from sheep cardiac sarcoplasmic reticulum." J Gen Physiol 95(5): 981-1005.

Baba-Aissa, F., Raeymaekers L., Wuytack, F.,Callewaert, G., Dode, L. Missiaen, L. Casteels, R. (1996). "Purkinje neurons express the SERCA3 isoform of the organellar type Ca(2+)-transport ATPase." Brain Res Mol Brain Res 41: 169-74.

Barbara, J.-G., Sandler, V.M., and W.N. Ross (1998) "A possible involvement of calcium stores in action-potential evoked calcium transients in CA1 hippocampal pyramidal neurons." Society for Neuroscience 28th Annual Meeting, Los Angeles, CA, 1998.

Bayliss, D. A., Umemiya M., Berger, A. J. (1995). "Inhibition of N- and P-type calcium currents and the after- hyperpolarization in rat motoneurones by serotonin." J Physiol (Lond) 485(Pt 3): 635-47.

Baimbridge, K. G., Celio, M. R. and J. H. Rogers (1992). "Calcium-binding proteins in the nervous system." Trends Neurosci 15(8): 303-308.

Bear, M. F. and R. C. Malenka (1994). "Synaptic plasticity: LTP and LTD." Curr Opin Neurobiol 4(3): 389-99.

Beavo, J. A. and D. H. Reifsnyder (1990). "Primary sequence of cyclic nucleotide phosphodiesterase isozymes and the design of selective inhibitors." Trends Pharmacol Sci 11(4): 150-5.

Beech, D. J., Bernheim, L., Mathie, A., Hille, B. (1991). "Intracellular Ca2+ buffers

disrupt muscarinic suppression of Ca2+ current and M current in rat sympathetic neurons." Proc Natl Acad Sci U S A 88(2): 652-6.

Belousov, A. B., Godfraind, J. M., Krnjevic, K. (1995). "Internal Ca2+ stores involved in anoxic responses of rat hippocampal neurons." J Physiol (Lond) 486(Pt 3): 547-56.

Berridge, M. J. (1997). "The 1996 Massry Prize. Inositol trisphosphate and calcium: two interacting second messengers." Am J Nephrol 17(1): 1-11.

Berridge, M. J. (1998). "Neuronal calcium signaling [In Process Citation]." Neuron 21(1): 13-26.

Berridge, M. J. and R. F. Irvine (1984). "Inositol trisphosphate, a novel second messenger in cellular signal transduction." Nature 312: 315-21.

Bezprozvanny, I. and B. E. Ehrlich (1993). "ATP modulates the function of inositol 1,4,5-trisphosphate-gated channels at two sites." Neuron 10: 1175-84.

Bezprozvanny, I. and B. E. Ehrlich (1994). "Inositol (1,4,5)-trisphosphate (InsP3)-gated Ca channels from cerebellum: conduction properties for divalent cations and regulation by intraluminal calcium." J Gen Physiol 104: 821-56.

Bezprozvanny, Watras, I., J., Ehrlich, B. E. (1991). "Bell-shaped calcium-response curves of Ins(1,4,5)P3- and calcium-gated channels from endoplasmic reticulum of cerebellum." Nature 351: 751-4.

Blanton, M. G., Lo Turco, J. J., Kriegstein, A. R. (1989). "Whole cell recording from neurons in slices of reptilian and mammalian cerebral cortex." J Neurosci Methods 30(3): 203-10.

Bliss, T. V. and G. L. Collingridge (1993). "A synaptic model of memory: long-term potentiation in the hippocampus." Nature 361(6407): 31-9.

Bolshakov, V. Y. and S. A. Siegelbaum (1995). "Hippocampal long-term depression: arachidonic acid as a potential retrograde messenger." Neuropharmacology 34(11): 1581-7.

Borst, J. G. and B. Sakmann (1996). "Calcium influx and transmitter release in a fast CNS synapse [see comments]." Nature 383(6599): 431-4.

Brandl, C. J., deLeon, S., Martin, D. R., MacLennan, D. H. (1987). "Adult forms of the Ca2+ATPase of sarcoplasmic reticulum. Expression in developing skeletal muscle." J Biol Chem 262(8): 3768-74.

Brandl, C. J., Green, N. M., Korczak, B., MacLennan, D. H. (1986). "Two Ca2+ ATPase

genes: homologies and mechanistic implications of deduced amino acid sequences." Cell 44: 597-607.

Buzsaki, G., Penttonen, M., Nadasdy, Z., Bragin, A. (1996). "Pattern and inhibition-dependent invasion of pyramidal cell dendrites by fast spikes in the hippocampus in vivo." Proc Natl Acad Sci U S A 93(18): 9921-5.

Callaway, J. C. and W. N. Ross (1995). "Frequency-dependent propagation of sodium action potentials in dendrites of hippocampal CA1 pyramidal neurons." J Neurophysiol 74(4): 1395-403.

Callaway, J. C. and W. N. Ross (1995). "Frequency-dependent propagation of sodium action potentials in dendrites of hippocampal CA1 pyramidal neurons." J Neurophysiol 74(4): 1395-403.

Cannell, M. B., Cheng, H., Lederer, W. J. (1995). "The control of calcium release in heart muscle." Science 268: 1045-9.

Cannell, M. B. and C. Soeller (1997). "Numerical analysis of ryanodine receptor activation by L-type channel activity in the cardiac muscle diad." Biophys J 73: 112-22.

Carmignoto, G., Pasti, L., Pozzan, T. (1998). "On the role of voltage-dependent calcium channels in calcium signaling of astrocytes in situ." J Neurosci 18(12): 4637-45.

Chavis, P., Fagni, L., Lansman, J. B., Bockaert, J. (1996). "Functional coupling between ryanodine receptors and L-type calcium channels in neurons." Nature 382(6593): 719-22.

Chen, H. and N. A. Lambert (1997). "Inhibition of dendritic calcium influx by activation of G-protein- coupled receptors in the hippocampus." J Neurophysiol 78(6): 3484-8.

Chijiwa, T., Mishima, A., Hagiwara, M., Sano, M., Hayashi, K., Inoue, T., Naito, K., Toshioka, T., Hidaka, H. (1990). "Inhibition of forskolin-induced neurite outgrowth and protein phosphorylation by a newly synthesized selective inhibitor of cyclic AMP-dependent protein kinase, N-[2-(p-bromocinnamylamino)ethyl]-5-isoquinolinesulfonamide (H-89), of PC12D pheochromocytoma cells." J Biol Chem 265(9): 5267-72.

Chow, R. H., Klingauf, J., Neher, E. (1994). "Time course of Ca2+ concentration triggering exocytosis in neuroendocrine cells." Proc Natl Acad Sci U S A 91(26): 12765-9.

Christie, B. R., Eliot, L. S., Ito, K., Miyakawa, H., Johnston, D. (1995). "Different Ca2+ channels in soma and dendrites of hippocampal pyramidal neurons mediate spike-induced Ca2+ influx." J Neurophysiol 73(6): 2553-7.

Cohen, A. S., Moore, K. A., Bangalore, R., Jafri, M. S., Weinreich, D., Kao, J. P. (1997). "Ca(2+)-induced Ca2+ release mediates Ca2+ transients evoked by single action potentials in rabbit vagal afferent neurones." J Physiol (Lond) 499(Pt 2): 315-28.

Colbert, C. M. and D. Johnston (1996). "Axonal action-potential initiation and Na+ channel densities in the soma and axon initial segment of subicular pyramidal neurons." J Neurosci 16(21): 6676-86.

Colino, A. and J. V. Halliwell (1987). "Differential modulation of three separate K-conductances in hippocampal CA1 neurons by serotonin." Nature 328(6125): 73-7.

Cook, E. P. and D. Johnston (1997). "Active dendrites reduce location-dependent variability of synaptic input trains." J Neurophysiol 78(4): 2116-28.

Coronado, R., Morrissette, J., Sukhareva, M., Vaughan, D. M. (1994). "Structure and function of ryanodine receptors." Am J Physiol 266: C1485-504.

Corradetti, R., Ballerini, L., Pugliese, A. M., Pepeu, G. (1992). "Serotonin blocks the long-term potentiation induced by primed burst stimulation in the CA1 region of rat hippocampal slices." Neuroscience 46(3): 511-8.

Denk, W., Strickler, J.H., and Webb, W.W. (1990). Two-photon laser scanning fluorescence microscopy. Science 248, 73-76.

Derkach, V., Surprenant, A., North, R. A. (1989). "5-HT3 receptors are membrane ion channels." Nature 339(6227): 706-9.

Ehrlich, B. E., Kaftan, E., Bezprozvannaya, S., Bezprozvanny, I. (1994). "The pharmacology of intracellular Ca(2+)-release channels." Trends Pharmacol Sci 15: 145-9.

Fierro, L., DiPolo, R., and Llano, I. (1998). Intracellular calcium clearance in Purkinje cell somata from rat cerebellar slices [In Process Citation]. J Physiol (Lond) 510, 499-512.

Finch, E. A., Turner, T. J., and Goldin, S. M. (1991). Calcium as a coagonist of inositol 1,4,5-trisphosphate-induced calcium release. Science 252, 443-6.

Fine, A., Amos, W.B., Durbin, R.M., and McNaughton, P.A. (1988). Confocal microscopy: applications in neurobiology. Trends Neurosci. 11, 345-351.

Foehring, R. C. (1996). "Serotonin modulates N- and P-type calcium currents in neocortical pyramidal neurons via a membrane-delimited pathway." J Neurophysiol 75(2): 648-59.

Cohen, A. S., Moore, K. A., Bangalore, R., Jafri, M. S., Weinreich, D., Kao, J. P. (1997). "Ca(2+)-induced Ca2+ release mediates Ca2+ transients evoked by single action potentials in rabbit vagal afferent neurones." J Physiol (Lond) 499(Pt 2): 315-28.

Colbert, C. M. and D. Johnston (1996). "Axonal action-potential initiation and Na+ channel densities in the soma and axon initial segment of subicular pyramidal neurons." J Neurosci 16(21): 6676-86.

Colino, A. and J. V. Halliwell (1987). "Differential modulation of three separate K-conductances in hippocampal CA1 neurons by serotonin." Nature 328(6125): 73-7.

Cook, E. P. and D. Johnston (1997). "Active dendrites reduce location-dependent variability of synaptic input trains." J Neurophysiol 78(4): 2116-28.

Coronado, R., Morrissette, J., Sukhareva, M., Vaughan, D. M. (1994). "Structure and function of ryanodine receptors." Am J Physiol 266: C1485-504.

Corradetti, R., Ballerini, L., Pugliese, A. M., Pepeu, G. (1992). "Serotonin blocks the long-term potentiation induced by primed burst stimulation in the CA1 region of rat hippocampal slices." Neuroscience 46(3): 511-8.

Denk, W., Strickler, J.H., and Webb, W.W. (1990). Two-photon laser scanning fluorescence microscopy. Science 248, 73-76.

Derkach, V., Surprenant, A., North, R. A. (1989). "5-HT3 receptors are membrane ion channels." Nature 339(6227): 706-9.

Ehrlich, B. E., Kaftan, E., Bezprozvannaya, S., Bezprozvanny, I. (1994). "The pharmacology of intracellular Ca(2+)-release channels." Trends Pharmacol Sci 15: 145-9.

Fierro, L., DiPolo, R., and Llano, I. (1998). Intracellular calcium clearance in Purkinje cell somata from rat cerebellar slices [In Process Citation]. J Physiol (Lond) 510, 499-512.

Finch, E. A., Turner, T. J., and Goldin, S. M. (1991). Calcium as a coagonist of inositol 1,4,5-trisphosphate-induced calcium release. Science 252, 443-6.

Fine, A., Amos, W.B., Durbin, R.M., and McNaughton, P.A. (1988). Confocal microscopy: applications in neurobiology. Trends Neurosci. 11, 345-351.

Foehring, R. C. (1996). "Serotonin modulates N- and P-type calcium currents in neocortical pyramidal neurons via a membrane-delimited pathway." J Neurophysiol 75(2): 648-59.

Friel, D. D. and R. W. Tsien (1992). "A caffeine- and ryanodine-sensitive Ca2+ store in bullfrog sympathetic neurones modulates effects of Ca2+ entry on [Ca2+]i." J Physiol (Lond) 450: 217-46.

Furuichi, T., Furutama, D., Hakamata, Y., Nakai, J., Takeshima, H., and Mikoshiba, K. (1994). Multiple types of ryanodine receptor/Ca2+ release channels are differentially expressed in rabbit brain. J Neurosci 14, 4794-805.

Galione, A. (1994). "Cyclic ADP-ribose, the ADP-ribosyl cyclase pathway and calcium signalling." Mol Cell Endocrinol 98(2): 125-31.

Garaschuk, O., Yaari, Y., and Konnerth, A. (1997). Release and sequestration of calcium by ryanodine-sensitive stores in rat hippocampal neurones. J Physiol (Lond) 502, 13-30.

Golovina, V. A. and M. P. Blaustein (1997). "Spatially and functionally distinct Ca2+ stores in sarcoplasmic and endoplasmic reticulum." Science 275(5306): 1643-8.

Grynkiewicz, G., Poenie, M., and Tsien, R. Y. (1985). A new generation of Ca2+ indicators with greatly improved fluorescence properties. J Biol Chem 260, 3440-50.

Hardingham, G. E., Chawla, S., Johnson, C. M., and Bading, H. (1997). Distinct functions of nuclear and cytoplasmic calcium in the control of gene expression. Nature 385, 260-5.

Hasan, G. and M. Rosbash (1992). "Drosophila homologs of two mammalian intracellular Ca(2+)-release channels: identification and expression patterns of the inositol 1,4,5-triphosphate and the ryanodine receptor genes." Development 116: 967-75.

Hebb, D.O (1949) Organization of Behavior. New York: Wiley.

Helmchen, F., Imoto, K., and Sakmann, B. (1996). Ca2+ buffering and action potential-evoked Ca2+ signaling in dendrites of pyramidal neurons. Biophys J 70, 1069-81.

Hernandez-Cruz, A., Escobar, A. L., and Jimenez, N. (1997). Ca(2+)-induced Ca2+ release phenomena in mammalian sympathetic neurons are critically dependent on the rate of rise of trigger Ca2+. J Gen Physiol 109, 147-67.

Hille, B. (1994). "Modulation of ion-channel function by G-protein-coupled receptors." Trends Neurosci 17(12): 531-6.

Hoffman, D. A., Magee, J. C., Colbert, C. M., and Johnston, D. (1997). K+ channel regulation of signal propagation in dendrites of hippocampal pyramidal neurons [see comments]. Nature 387, 869-75.

Ishii, Y., Kawai, T., and Watanabe, M. (1992). Inhibitory effects of cyclopiazonic acid on the spike after- hyperpolarization in rat sympathetic neurons. Jpn J Pharmacol 58, 451-6.

Jacobs, J. M. and T. Meyer (1997). "Control of action potential-induced Ca2+ signaling in the soma of hippocampal neurons by Ca2+ release from intracellular stores." J Neurosci 17(11): 4129-35.

Jaffe, D. B., Johnston, D., Lasser-Ross, N., Lisman, J. E., Miyakawa, H., and Ross, W. N. (1992). The spread of Na+ spikes determines the pattern of dendritic Ca2+ entry into hippocampal neurons. Nature 357, 244-6.

Julius, D., MacDermott, A. B., Axel, R., and Jessell, T. M. (1988). Molecular characterization of a functional cDNA encoding the serotonin 1c receptor. Science 241, 558-64.

Kano, M., Garaschuk, O., Verkhratsky, A., and Konnerth, A. (1995). Ryanodine receptor-mediated intracellular calcium release in rat cerebellar Purkinje neurones. J Physiol (Lond) 487, 1-16.

Kavalali, E. T., Zhuo, M., Bito, H., and Tsien, R. W. (1997). Dendritic Ca2+ channels characterized by recordings from isolated hippocampal dendritic segments. Neuron 18, 651-63.

Kia, H. K., Miquel, M. C., Brisorgueil, M. J., Daval, G., Riad, M., El Mestikawy, S., and Hamon, M. V. D. (1996). Immunocytochemical localization of serotonin1A receptors in the rat central nervous system. J Comp Neurol 365, 289-305.

Klingauf, J. and E. Neher (1997). "Modeling buffered Ca2+ diffusion near the membrane: implications for secretion in neuroendocrine cells." Biophys J 72(2 Pt 1): 674-90.

Kramer, R. H., Kaczmarek, L. K., and Levitan, E. S. (1991). Neuropeptide inhibition of voltage-gated calcium channels mediated by mobilization of intracellular calcium. Neuron 6, 557-63.

Lasser-Ross, N., Miyakawa, H., Lev-Ram, V., Young, S. R., and Ross, W. N. (1991). High time resolution fluorescence imaging with a CCD camera. J Neurosci Methods 36, 253-61.

Lee, H. C. (1997). "Mechanisms of calcium signaling by cyclic ADP-ribose and NAADP." Physiol Rev 77(4): 1133-64.

Lee, H. C. (1998). "Calcium signaling by cyclic ADP-ribose and NAADP. A decade of exploration." Cell Biochem Biophys 28(1): 1-17.

Llano, I., DiPolo, R., and Marty, A. (1994). Calcium-induced calcium release in cerebellar Purkinje cells. Neuron 12, 663-73.

Lopez-Lopez, J. R., Shacklock, P. S., Balke, C. W., and Wier, W. G. (1995). Local calcium transients triggered by single L-type calcium channel currents in cardiac cells. Science 268, 1042-5.

Lubbert, H., Hoffman, B. J., Snutch, T. P., van Dyke, T., Levine, A. J., Hartig, P. R., Lester, H. A., and Davidson, N. (1987). cDna cloning of a serotonin 5-Ht1c receptor by electrophysiological assays of mRna-injected Xenopus oocytes. Proc Natl Acad Sci U S A 84, 4332-6.

Lubbert, H., Snutch, T. P., Dascal, N., Lester, H. A., and Davidson, N. (1987). Rat brain 5-HT1C receptors are encoded by a 5-6 kbase mRNA size class and are functionally expressed in injected Xenopus oocytes. J Neurosci 7, 1159-65.

Lytton, J., Westlin, M., Burk, S. E., Shull, G. E., and MacLennan, D. H. (1992). Functional comparisons between isoforms of the sarcoplasmic or endoplasmic reticulum family of calcium pumps. J Biol Chem 267, 14483-9.

Lytton, J., Westlin, M., and Hanley, M. R. (1991). Thapsigargin inhibits the sarcoplasmic or endoplasmic reticulum Ca-ATPase family of calcium pumps. J Biol Chem 266, 17067-71.

MacLennan, D. H. (1990). "Molecular tools to elucidate problems in excitation-contraction coupling." Biophys J 58: 1355-65.

MacLennan, D. H., Brandl, C. J., Korczak, B., and Green, N. M. (1985). Amino-acid sequence of a Ca2+ + Mg2+-dependent ATPase from rabbit muscle sarcoplasmic reticulum, deduced from its complementary DNA sequence. Nature 316, 696-700.

Magee, J. C. and D. Johnston (1995). "Characterization of single voltage-gated Na+ and Ca2+ channels in apical dendrites of rat CA1 pyramidal neurons." J Physiol (Lond) 487(Pt 1): 67-90.

Magee, J. C. and D. Johnston (1997). "A synaptically controlled, associative signal for Hebbian plasticity in hippocampal neurons [see comments]." Science 275(5297): 209-13.

Magee, J. C. and D. Johnston (1997). "A synaptically controlled, associative signal for Hebbian plasticity in hippocampal neurons [see comments]." Science 275(5297): 209-13.

Malenka, R. C. (1994). "Synaptic plasticity in the hippocampus: LTP and LTD." Cell 78(4): 535-8.

Malinow, R. (1991). "Transmission between pairs of hippocampal slice neurons: quantal levels, oscillations, and LTP." Science 252(5006): 722-4.

Markram, H., Helm, P. J., and Sakmann, B. (1995). Dendritic calcium transients evoked by single back-propagating action potentials in rat neocortical pyramidal neurons. J Physiol (Lond) 485, 1-20.

Markram, H., Lubke, J., Frotscher, M., and Sakmann, B. (1997). Regulation of synaptic efficacy by coincidence of postsynaptic APs and EPSPs [see comments]. Science 275, 213-5.

McCormick, D. A. and H. C. Pape (1990). "Noradrenergic and serotonergic modulation of a hyperpolarization- activated cation current in thalamic relay neurones." J Physiol (Lond) 431: 319-42.

McCormick, D. A. and H. C. Pape (1990). "Noradrenergic and serotonergic modulation of a hyperpolarization- activated cation current in thalamic relay neurones." J Physiol (Lond) 431: 319-42.

Miller, K. K., Verma, A., Snyder, S. H., and Ross, C. A. (1991). Localization of an endoplasmic reticulum calcium ATPase mRNA in rat brain by in situ hybridization. Neuroscience 43, 1-9.

Moore, K. A., Cohen, A. S., Kao, J. P. Y., and Weinreich, D. (1998). Ca2+-induced Ca2+ release mediates a slow post-spike hyperpolarization in rabbit vagal afferent neurons. J Neurophysiol 79, 688-94.

Mulkey, R. M. and R. S. Zucker (1991). "Action potentials must admit calcium to evoke transmitter release [published erratum appears in Nature 1991 May 30;351(6325):419]." Nature 350(6314): 153-5.

Nabauer, M., Callewaert, G., Cleemann, L., and Morad, M. (1989). Regulation of calcium release is gated by calcium current, not gating charge, in cardiac myocytes [see comments]. Science 244, 800-3.

Neher, E. (1992). "Correction for liquid junction potentials in patch clamp experiments." Methods Enzymol 207: 123-31.

Neher, E. (1998). "Vesicle pools and Ca2+ microdomains: new tools for understanding their roles in neurotransmitter release." Neuron 20(3): 389-99.

Nelson, E. J., Li, C. C., Bangalore, R., Benson, T., Kass, R. S., and Hinkle, P. M. (1994). Inhibition of L-type calcium-channel activity by thapsigargin and 2,5-t-butylhydroquinone, but not by cyclopiazonic acid. Biochem J 302, 147-54.

Nicoll, R. A. (1988). "The coupling of neurotransmitter receptors to ion channels in the brain." Science 241(4865): 545-51.

Nicoll, R. A., Malenka, R. C., and Kauer, J. A. (1990). Functional comparison of neurotransmitter receptor subtypes in mammalian central nervous system. Physiol Rev 70, 513-65.

Pape, H. C. and D. A. McCormick (1989). "Noradrenaline and serotonin selectively modulate thalamic burst firing by enhancing a hyperpolarization-activated cation current." Nature 340(6236): 715-8.

Prentki, M., Biden, T. J., Janjic, D., Irvine, R. F., Berridge, M. J., and Wollheim, C. B. (1984). Rapid mobilization of Ca2+ from rat insulinoma microsomes by inositol-1,4,5-trisphosphate. Nature 309, 562-4.

Pritchett, D. B., Bach, A. W., Wozny, M., Taleb, O., Dal Toso, R., Shih, J. C., and Seeburg, P. H. (1988). Structure and functional expression of cloned rat serotonin 5HT-2 receptor. Embo J 7, 4135-40.

Regehr, W. G. and D. W. Tank (1992). "Calcium concentration dynamics produced by synaptic activation of CA1 hippocampal pyramidal cells." J Neurosci 12(11): 4202-23.

Ross, W. N. and V. M. Sandler (1998) "Serotonin and spikes synergisticly release calcium in dendrites of hippocampal pyramidal cells." Society for Neuroscience 28th Annual Meeting, Los Angeles, CA, 1998.

Rossier, M. F., Python, C. P., Burnay, M. M., Schlegel, W., Vallotton, M. B., and Capponi, A. M. (1993). Thapsigargin inhibits voltage-activated calcium channels in adrenal glomerulosa cells. Biochem J 296, 309-12.

Rousseau, E. and G. Meissner (1989). "Single cardiac sarcoplasmic reticulum Ca2+-release channel: activation by caffeine." Am J Physiol 256(2 Pt 2): H328-33.

Sachs, G. and K. Munson (1991). "Mammalian phosphorylating ion-motive ATPases." Curr Opin Cell Biol 3: 685-94.

Sah, P., Francis, K., McLachlan, E. M., and Junankar, P. (1993). Distribution of ryanodine receptor-like immunoreactivity in mammalian central nervous system is consistent with its role in calcium-induced calcium release. Neuroscience 54, 157-65.

Sah, P. and E. M. McLachlan (1991). "Ca(2+)-activated K+ currents underlying the afterhyperpolarization in guinea pig vagal neurons: a role for Ca(2+)-activated Ca2+ release." Neuron 7(2): 257-64.

Sakai, N. and C. Tanaka (1993). "Inhibitory modulation of long-term potentiation via the 5-HT1A receptor in slices of the rat hippocampal dentate gyrus." Brain Res 613(2): 326-30.

Sandler, V. M., Puil, E., and D. W. Schwarz (1998). "Intrinsic response properties of bursting neurons in the nucleus principalis trigemini of the gerbil. " Neuroscience 83, 891-904.

Sandler, V.M. and W.N. Ross "Serotonin Modulates Spike Backpropagation and Associated [Ca^{2+}] Changes in the Apical Dendrites of Hipocampal CA1 Pyramidal Neurons. " J. Neurophysiology (in press)

Sandler, V.M. and W.N. Ross (1997) "Serotonin reduces the amplitude of backpropagating spikes in the apical dendrites of hippocampal pyramidal neurons. " Society for Neuroscience 27th Annual Meeting, New Orleans, DC, 1997.

Sandler, V.M., E. Puil, and D.W.F. Schwarz. (1996) "Na^+-dependent plateau potentials and Na^+-dependent K^+ conductance in the nucleus principalis trigemini neurons." Society for Neuroscience 26th Annual Meeting, Washington, DC, 1996, pp. 1214, #483.4

Saudou, F. and R. Hen (1994). "5-Hydroxytryptamine receptor subtypes: molecular and functional diversity." Adv Pharmacol 30: 327-80.

Schiller, J., Helmchen, F., and Sakmann, B. (1995). Spatial profile of dendritic calcium transients evoked by action potentials in rat neocortical pyramidal neurones. J Physiol (Lond) 487, 583-600.

Seamon, K. B., Vaillancourt, R., and Daly, J. W. (1985). Modulation of forskolin binding to rat brain membranes. J Cyclic Nucleotide Protein Phosphor Res 10, 535-49.

Shmigol, A., Kostyuk, P., and Verkhratsky, A. (1995). Dual action of thapsigargin on calcium mobilization in sensory neurons: inhibition of Ca2+ uptake by caffeine-sensitive pools and blockade of plasmalemmal Ca2+ channels. Neuroscience 65, 1109-18.

Shmigol, A., Kostyuk, P., and Verkhratsky, A. (1995). Dual action of thapsigargin on calcium mobilization in sensory neurons: inhibition of Ca2+ uptake by caffeine-sensitive pools and blockade of plasmalemmal Ca2+ channels. Neuroscience 65, 1109-18.

Shmigol, A., Svichar, N., Kostyuk, P., and Verkhratsky, A. (1996). Gradual caffeine-induced Ca2+ release in mouse dorsal root ganglion neurons is controlled by cytoplasmic and luminal Ca2+. Neuroscience 73, 1061-7.

Sitsapesan, R. and A. J. Williams (1990). "Mechanisms of caffeine activation of single calcium-release channels of sheep cardiac sarcoplasmic reticulum." J Physiol (Lond) 423: 425-39.

Smith, J. S., Imagawa, T., Ma, J., Fill, M., Campbell, K. P., and Coronado, R. (1988). Purified ryanodine receptor from rabbit skeletal muscle is the calcium- release channel of sarcoplasmic reticulum. J Gen Physiol 92, 1-26.

Soeller, C. and M. B. Cannell (1997). "Numerical simulation of local calcium movements during L-type calcium channel gating in the cardiac diad." Biophys J 73: 97-111.

Spruston, N., Schiller, Y., Stuart, G., and Sakmann, B. (1995). Activity-dependent action potential invasion and calcium influx into hippocampal CA1 dendrites [see comments]. Science 268, 297-300.

Spruston, N., Schiller, Y., Stuart, G., and Sakmann, B. (1995). Activity-dependent action potential invasion and calcium influx into hippocampal CA1 dendrites [see comments]. Science 268, 297-300.

Streb, H., Irvine, R. F., Berridge, M. J., and Schulz, I. (1983). Release of Ca2+ from a nonmitochondrial intracellular store in pancreatic acinar cells by inositol-1,4,5-trisphosphate. Nature 306, 67-9.

Stehno-Bittel, L., Lückhoff, A., Clapham, D. E. (1995). "Calcium release from the nucleus by $InsP_3$ receptor channels." Neuron 14: 163-167.

Stuart, G. and N. Spruston (1998). "Determinants of voltage attenuation in neocortical pyramidal neuron dendrites." J Neurosci 18(10): 3501-10.

Stuart, G. J. and B. Sakmann (1994). "Active propagation of somatic action potentials into neocortical pyramidal cell dendrites." Nature 367(6458): 69-72.

Svoboda, K., Denk, W., Kleinfeld, D., and Tank, D. W. (1997). In vivo dendritic calcium dynamics in neocortical pyramidal neurons. Nature 385, 161-5.

Svoboda, K., Tank, D. W., and Denk, W. (1996). Direct measurement of coupling between dendritic spines and shafts. Science 272, 716-9.

Takeshima, H., Nishimura, S., Nishi, M., Ikeda, M., and Sugimoto, T. (1993). A brain-specific transcript from the 3'-terminal region of the skeletal muscle ryanodine receptor gene. FEBS Lett 322, 105-10.

Thastrup, O. (1990). "Role of Ca2(+)-ATPases in regulation of cellular Ca2+ signalling, as studied with the selective microsomal Ca2(+)-ATPase inhibitor, thapsigargin." Agents Actions 29: 8-15.

Thastrup, O., Cullen, P. J., Drobak, B. K., Hanley, M. R., and Dawson, A. P. (1990). Thapsigargin, a tumor promoter, discharges intracellular Ca2+ stores by specific inhibition of the endoplasmic reticulum Ca2(+)-ATPase. Proc Natl Acad Sci U S A 87, 2466-70.

Toescu, E. C., SC, O. N., Petersen, O. H., and Eisner, D. A. (1992). Caffeine inhibits the agonist-evoked cytosolic Ca2+ signal in mouse pancreatic acinar cells by blocking inositol trisphosphate production. J Biol Chem 267, 23467-70.

Tombaugh, G. C. and G. G. Somjen (1997). "Differential sensitivity to intracellular pH among high- and low- threshold Ca2+ currents in isolated rat CA1 neurons [published errata appear in J Neurophysiol 1997 May;77(5):following table of contents and 1997 Jun;77(6):2856]." J Neurophysiol 77(2): 639-53.

Torres, G. E., Arfken, C. L., and Andrade, R. (1996). 5-Hydroxytryptamine4 receptors reduce afterhyperpolarization in hippocampus by inhibiting calcium-induced calcium release. Mol Pharmacol 50, 1316-22.

Tsubokawa, H. and W. N. Ross (1996). "IPSPs modulate spike backpropagation and associated [Ca2+]i changes in the dendrites of hippocampal CA1 pyramidal neurons." J Neurophysiol 76(5): 2896-906.

Tsubokawa, H. and W. N. Ross (1997). "Muscarinic modulation of spike backpropagation in the apical dendrites of hippocampal CA1 pyramidal neurons." J Neurosci 17(15): 5782-91.

Turner, R. W., Meyers, D. E., Richardson, T. L., and Barker, J. L. (1991). The site for initiation of action potential discharge over the somatodendritic axis of rat hippocampal CA1 pyramidal neurons. J Neurosci 11, 2270-80.

Usachev, Y., Shmigol, A., Pronchuk, N., Kostyuk, P., and Verkhratsky, A. (1993). Caffeine-induced calcium release from internal stores in cultured rat sensory neurons. Neuroscience 57, 845-59.

Usachev, Y. M. and S. A. Thayer (1997). "All-or-none Ca2+ release from intracellular stores triggered by Ca2+ influx through voltage-gated Ca2+ channels in rat sensory neurons." J Neurosci 17(19): 7404-14.

van Breemen, C. and K. Saida (1989). "Cellular mechanisms regulating [Ca2+]i smooth muscle." Annu Rev Physiol 51: 315-29.

Verkhratsky, A. and A. Shmigol (1996). "Calcium-induced calcium release in neurones." Cell Calcium 19(1): 1-14.

Villani, F. and D. Johnston (1993). "Serotonin inhibits induction of long-term potentiation at commissural synapses in hippocampus." Brain Res 606(2): 304-8.

Wells, J. N., Wu, Y. J., Baird, C. E., and Hardman, J. G. (1975). Phosphodiesterases from porcine coronary arteries: inhibition of separated forms by xanthines, papaverine, and cyclic nucleotides. Mol Pharmacol 11, 775-83.

Westenbroek, R. E., Ahlijanian, M. K., and Catterall, W. A. (1990). Clustering of L-type Ca2+ channels at the base of major dendrites in hippocampal pyramidal neurons. Nature 347, 281-4.

Zorzato, F., Fujii, J., Otsu, K., Phillips, M., Green, N. M., Lai, F. A., Meissner, G., and MacLennan, D. H. (1990). Molecular cloning of cDNA encoding human and rabbit forms of the Ca2+ release channel (ryanodine receptor) of skeletal muscle sarcoplasmic reticulum. J Biol Chem 265, 2244-56.